METROPLEX IDENTIFICATION, EVALUATION, AND OPTIMIZATION

A Thesis
Presented to
The Academic Faculty

by

Evan McClain

In Partial Fulfillment
of the Requirements for the Degree
Doctor of Philosophy in the
School of Aerospace Engineering

Georgia Institute of Technology
May 2013

METROPLEX IDENTIFICATION, EVALUATION, AND OPTIMIZATION

Approved by:

Dr. John-Paul Clarke, Committee Chair
School of Aerospace Engineering
Georgia Institute of Technology

Dr. Ellis Johnson
School of Industrial and Systems Engineering
Georgia Institute of Technology

Dr. Eric Feron
School of Aerospace Engineering
Georgia Institute of Technology

Dr. Vitali Volovoi
School of Aerospace Engineering
Georgia Institute of Technology

Dr. Panagiotis Tsiotras
School of Aerospace Engineering
Georgia Institute of Technology

Date Approved: March 11, 2013

DEDICATION

To my wife

ACKNOWLEDGEMENTS

I would like to thank my advisor, Dr. John-Paul Clarke. Without his encouragement I would have never pursued a graduate degree. With his guidance I have been able to study fun and interesting problems. He has introduced me to his grand unified theory of air transportation and I have learned from his vision.

I would also like to thank NASA for sponsoring much of the work presented in this thesis

Finally, I would like to thank all of my friends and family who have been nothing but supportive in my endeavor and especially my wife who has put up with my somewhat crazy work schedule.

TABLE OF CONTENTS

LIST OF TABLES

LIST OF FIGURES

SUMMARY

As airspace congestion becomes increasingly more common, one of the primary places airspace congestion is felt today, and will only continue to increase, is in areas where more than one major airport interact. We will call these groups of interdependent airports a metroplex; a term originally coined to describe large metropolitan areas where more than one city of equal (or near equal) size or importance. These metroplex areas are of particular importance in understanding future capacity demands because many of these areas are currently experiencing problems with meeting the current demand, and demand is only projected to increase as air travel becomes more popular. Many of these capacity issues have been identified in the FAA's Future Airport Capacity Task (FACT). From the second FACT report, it is stated that "the FACT 1 analysis revealed that many of our hub airports and their associated metropolitan areas could be expected to experience capacity constraints (i.e. unacceptable levels of delay) by 2013 and 2020, even if the planned improvements envisioned at that time were completed."[17] This analysis shows that the current methods of expanding airports will not scale with the growing demand. To address this growing demand, a three part solution is proposed.

The first step is to properly identify the metroplex areas to be evaluated. While the FACT reports serve to identify areas where capacity growth does not meet demand, these areas are not grouped into metroplexes. To do this grouping, an interaction metric was developed based on airport distance and traffic volume. This interaction metric serves as a proxy for how the existence of a second airport impacts the operation of the first. This pairwise metric was then computed for all commercial airports in the US and were grouped into metroplexes using a clustering algorithm.

The second obstacle was to develop a tool to evaluate each metroplex as new algorithms were tested. A discrete event based simulation was developed to model each link in the airspace structure for each aircraft that enters the TRACON. This program tracks the

delay each aircraft is required to accumulate in holding patterns or traffic trombones.

A third and final method discussed here was an optimization program that can be used to schedule aircraft that are entering the TRACON to perform small modifications in their speed while en route to reduce the overall delay (both en route and in the TRACON). While formal optimization methods for scheduling aircraft arrivals have been presented before, the computational complexity has greatly prevented such algorithms from being used to schedule many aircraft in a dense schedule. This is because mixed integer programming (MIP) is a NP-hard problem. Practically, this means that the solution time can grow exponentially as the problem size (number of aircraft) increases. To address this issue, a Benders' decomposition scheme was introduced that allows solutions to be computed in near real-time on commodity hardware. These solutions can be evaluated and compared against the currently used TMA algorithm to show surprising gains in high density traffic.

CHAPTER I

INTRODUCTION

Airspace congestion has become increasingly common in metroplexes – a term originally coined to describe large metropolitan areas with more than one city of equal (or near equal) size or importance, that is now used in the aviation community to describe terminal areas with more than one major airport of equivalent size and interacting traffic flows. The Joint Planning and Development Office (JPD) NextGen Concepts of Operations [37] defines a metroplex as "a group of two or more adjacent airports whose arrival and departure operations are highly interdependent." These metroplexes are of particular importance in understanding and addressing future capacity issues because many of them are already experiencing significant congestion and delays due the current demand being at or near their capacity, and will likely be the primary source of congestion and delay in the airspace system as demand grows. The Federal Aviation Administration's (FAA) Operational Evolution Plan (OEP) initiative [17]. This congestion is very costly, and has been projected to cost over $30 billion in 2007 [4] and is only expected to increase. To reduce this yearly waste, a next generation air transportation system (NextGen) is being proposed to handle such changes in demand and throughput [21].

Many of these capacity issues were identified during the FAA's Future Airport Capacity Task (FACT). In fact, the authors of the second FACT report observed that "the FACT 1 analysis revealed that many of our hub airports and their associated metropolitan areas could be expected to experience capacity constraints (i.e. unacceptable levels of delay) by 2013 and 2020, even if the planned improvements envisioned at that time were completed."[17] Further, this analysis showed that it is not possible to meet the growing demand by simply expanding airports. The interactions between traffic flows to neighboring airports of similar size are a significant issue at high traffic levels. This need for expanding air traffic control methods is nothing new and the growth of air traffic has long been a topic of research and discussion [46].

A solution to the metroplex congestion and delay problem has been developed via the three steps described below:

The first step was to properly identify the metroplex areas to be evaluated. While the FACT reports identify areas where capacity growth does not meet demand, these areas are not grouped into metroplexes. To do this end, an interaction metric was developed based on airport distance and traffic volume. This interaction metric serves as a proxy for how the existence of a second airport impacts the operation of the first, and vice versa. This pair-wise metric was computed for all pairs of commercial airports in the US, and then used

in a clustering algorithm to group airports into metroplexes.

The second step was to develop a tool to evaluate, for each metroplex, the performance of any algorithms that were developed. A discrete event based simulation was developed to model each link in the airspace structure for each aircraft that enters the TRACON. This program tracks the delay each aircraft is required to accumulate in holding patterns or traffic trombones.

A third and final step was the development of an optimization program that can be used to schedule aircraft that are entering the TRACON to perform small modifications in their speed while en route to reduce the overall delay (both en route and in the TRACON). While formal optimization methods for scheduling aircraft arrivals have been presented before, the computational complexity has greatly prevented such algorithms from being used to schedule many aircraft in a dense schedule. This is because mixed integer programming (MIP) is a NP-hard problem. Practically, this means that the solution time can grow exponentially as the problem size (number of aircraft) increases. To address this issue, a Benders' decomposition scheme was introduced that allows solutions to be computed in near real-time on commodity hardware. These solutions can be evaluated and compared against the currently used TMA algorithm to show surprising gains in high-density traffic. Decision support tools that utilize data link [63] could be connected to such optimization programs to assist controllers to reduce the lost capacity in the system.

To properly formulate the problems and to reduce our models to computational feasibility, several site visits were performed at some of the largest TRACONS in the US [1] to understand the unique problems that air traffic controllers face when handling such complex airspace.

1.1 Review of Relevant Literature

Because the metroplex as a whole is such a large problem, typically only the individual aspects of metroplex operations are studied. Runway scheduling is the most common research topic, but

The problem of airport runway scheduling has been significant study on the topic. These methods and papers usually fall within two major areas of provable optimality and heuristic methods. Generally, Dear's work on "The dynamic scheduling of aircraft in the near terminal area" [18] is cited as the first complete work on this subject and used constrained position shifting to limit the number of swaps when compared to a simple FCFS method. Many other authors have added to the literature in this area, but arrival scheduling is a much more completely studied topic due to the possible gains found in the usual IFR wake vortex separation requirements.

The single runway arrival problem is addressed in Soomer and Franx's "Scheduling

[1] A80, N90, SCT, and Miami

Aircraft Landings using Airlines' Preferences" paper [58]. This paper presents a model that determines arrival sequence and time for a single runway while maintaining separation. In the model, each aircraft can have a different cost function, which would be provided by the airlines, and this cost between airlines is scaled to ensure equity between airlines. A heuristic is used to evaluate swapping within a neighborhood of FCFS order and the shifting is limited by a number of positions. This heuristic is used to minimize unused capacity by building a compressed schedule.

In Eun, Hwang, and Bang's "Optimal Arrival Flight Sequencing and Scheduling Using Discrete Airborne Delays" a formal optimization method is introduced to schedule and space an arrival stream [22]. The algorithm presented in this paper considered discrete delay times as decision variables, and the objective is to minimize the sum of the delays. Lagrangian relaxation is used to provide a lower bound for the branch-and-bound algorithm that is implemented, and the results show that the delay times are significantly smaller using the proposed formal optimization algorithm.

Due to the similarities to machine scheduling, several parallels have been drawn. Bianco, Rinaldi, and Sassano in their "A combinatorial optimization approach to aircraft sequencing problem" [9] introduced a combinatorial model for this arrival scheduling problem where it is formulated as a scheduling problem of a single machine treating the aircraft to be scheduled as n jobs to optimally utilize the resource. This approach was also used in [8]. This demonstrated that this problem can be reduced to an asymmetric traveling salesman problem for a special case, showing that the problem is NP-complete [31] as would be expected by any such scheduling problem.

Beasley, Krishnamoorthy, Sharaiha, and Abramson in their "Scheduling aircraft landings-the static case" [6] present a mixed integer program that has served as a standard method for describing the runway scheduling problem in many other papers. In addition to providing the base formulation, they presented computational results showing that their formulation works well for small cases but that it is not capable of handling all real world instances within reasonable time limits. The main reason for this limitation is that the "big-M" construction to model non-convexities results in a weak LP-relaxation, an undesirable property in most solution methods for integer programs. Therefore, in the literature, the exact formulation has been used as a reference to compare the performance of heuristic methods rather than as a practical method to solve the scheduling problem in real-time. Here we will use a similar big-M construction method but will use a decomposition scheme to relax some of the problem size constraints.

A paper titled "Combinatorial Benders' Cuts for Mixed-Integer Linear Programming" [15] by Gianni Codato and Matteo Fischetti discuss a method for using a Benders' decomposition to provide much tighter LP relaxations for the master MIP. Their model builds a master problem that is entirely integer and contains combinatorial information on the set

of feasible integer solutions gained from the original mixed integer program.

The most common objective is to simply minimize delay or to maximize throughput, but other objectives have been studied. Sölveling in his "Scheduling of runway operations for reduced environmental impact" [57] looked at objectives to minimize the environmental impact. Environmentally optimal schedules were compared against simple FCFS schedules. Due to the linkages between environmental metrics and fuel burn, the environmantally optimal and fuel optimal schedules were shown to not differ significantly from a fuel-optimal schedule. This linkage also helped show that any increase in operational costs to the airlines would be minimal.

1.2 Thesis Outline

There are 6 chapters in this thesis. The second chapter summarizes the findings of several site visit reports and goes into the specific metroplex operations. The objective of these surveys was to develop a more complete understanding of the parameters and issues that are intrinsic to the core metroplex problem. This was done through examining the current day operations in these large metroplexes. While a qualitative understanding of metroplex operations is useful for framing the problem, a more concrete numeric metric for estimating metroplex interdependencies is presented in chapter 3. In this chapter a quantitative metric is presented which allows for a clustering algorithm to be performed giving a quantitative understanding of the scope (number of airports) and size (total "interaction") of each metroplex. This quantitative understanding allows us to study how these metroplexes will evolve given FAA's Terminal Area Forecast (TAF). Once the metroplex has been identified, we can evaluate the delay and other metrics of interest using the simulation tool developed in chapter 4. This tool can be used to understand throughput, sensitivity to uncertainty, etc. Chapter 5 presents an optimization framework that, when given an input demand and metroplex model, can optimize the schedule to minimize total delay, fuel burn, or some other metric. Finally, chapter 6 summarizes the findings and outlines possible areas for future research.

CHAPTER II

CHARACTERIZATION AND UNDERSTANDING OF METROPLEX OPERATIONS

While there exists much literature related to metroplex operations, the metroplex problem has not been systematically studied before. As discussed earlier, the predicted future traffic growth will increase the coupling of operations in exiting metroplex airspace, and will potentially create new metroplex areas. The natural first step in exploring the metroplex problem is to investigate existing metroplex sites in the NAS to obtain a deeper understanding of the metroplex problem in real world operations. Given the limited resources and time available, only a small number of metroplex sites could be studied. Candidate metroplex sites were selected by reviewing on the list of metroplexes identified in the literature and comparing their basic characteristics. The FAA's OEP initiative [25] has identified that over the next 20 years, U.S. population and economic growth are expected to be concentrated in 15 metropolitan areas. These metropolitan areas are listed in Table 1.

Table 1: OEP 15 Metropolitan Areas with Projected Fast Growth

Metro Area (TRACON)	Associated Airports	
OEP Airport, Name	ID	Name
Atlanta (A80)	PDK	Dekalb-Peachtree
ATL, Atlanta Hartsfield Intl.	RYY	Cobb County-McCollum Field
	FTY	Fulton County Airport-Brown Field
Charlotte (CLT)	JQF	Concord Regional
CLT, Charlotte/Douglas Intl.	UZA	Rock Hill/York County/Bryant Field
Chicago (C90)	ARR	Aurora Municipal
MDW, Chicago Midway	UGN	Waukegan Regional Airport
ORD, Chicago O'Hare Intl.	LOT	Lewis University Airport
	IGQ	Lansing Municipal Airport
	DPA	Dupage
	PWK	Chicago Executive
	RFD	Chicago/Rockford Intl.
	MKE	General Mitchell Intl.
	ENW	Kenosha Regional

Continued on next page

Table 1 – *Continued from previous page*

	GYY	Gary/Chicago Intl.
Houston (I90)	HOU	Houston Hobby
IAH, George Bush Intl.	EFD	Ellington Field
	CXO	Lone Star Executive
	DWH	David Wayne Hooks
	IWS	West Houston
	SGR	Sugar Land
	LVJ	Pearland Regional
	AXH	Houston Southwest
Las Vegas (L30)	VGT	North Las Vegas
LAS, Las Vegas McCarran Intl.	HND	Henderson Executive
Los Angeles (SCT)	VNY	Van Nuys
LAX, Los Angeles Intl.	WHP	Whiteman
	POC	Brackett Field
	CNO	Chino
	BUR	Bob Hope
	SNA	John Wayne Airport-Orange County
	ONT	Ontario Intl.
	LGB	Long Beach /Daugherty Field
Minneapolis (M98)	ANE	Anoka County
MSP, Minneapolis-St Paul Intl.	21D	Lake Elmo
	STP	St. Paul Downtown
	SGS	South St. Paul
	MIC	Crystal
	FCM	Flying Cloud
	LVN	Airlake
New York (N90)	CDW	Essex County
JFK, New York John F. Kennedy Intl.	TEB	Teterboro
LGA, New York LaGuardia	MMU	Morristown Municipal
EWR, Newark Intl.	FRG	Republic
	SWF	Stewart Intl.
	ISP	Long Island-MacArthur
	ABE	Lehigh Valley Intl.
	HPN	Westchester County
Philadelphia (PHL)	PNE	Northeast Philadelphia
PHL, Philadelphia Intl.	ACY	Atlantic City Intl.

Continued on next page

Table 1 – *Continued from previous page*

	LOM	Wings Field
	ILG	New Castle
Phoenix (P50)	FFZ	Falcon Field
PHX, Phoenix Sky Harbor Intl.	DVT	Phoenix Deer Valley
	SDL	Scottsdale
	CHD	Chandler Municipal
	GEU	Glendale Municipal
	IWA	Williams Gateway
San Diego (SCT)	SEE	Gillespie Field
SAN, San Diego Intl. Lindbergh	CRQ	McClellan-Palomar
	SDM	Brown Field Municipal
	MYF	Montgomery Field
San Francisco (NCT)	RHV	Reid-Hillview of Santa Clara County
SFO, San Francisco Intl.	LVK	Livermore Municipal
	CCR	Buchanan Field
	PAO	Palo Alto Airport
	SQL	San Carlos
	HWD	Hayward Executive
	OAK	Metropolitan Oakland Intl.
	SJC	Norman Y. Mineta San Jose
Seattle (S46)	BFI	Boeing Field
SEA, Seattle-Tacoma Intl.	RNT	Renton Municipal
	S50	Auburn Municipal
	PAE	Snohomish Co (Paine Fld)
	S43	Harvey Field
South Florida (MIA, PBI)	FXE	Fort Lauderdale Executive
MIA, Miami Intl.	TMB	Kendall-Tamiami Executive
FLL, Fort Lauderdale-Hollywood Intl.	LNA	Palm Beach County Park
	OPF	Opa Locka
	PBI	Palm Beach Intl.
Washinton Baltimore (PCT)	JYO	Leesburg Executive
IAD, Washington Dulles Intl.	HEF	Manassas Regional/Harry P. Davis Field
DCA, Ronald Reagan National	DMW	Carroll County Regional
BWI, Baltimore-Washington Intl.	W66	Warrenton-Fauquier County
	MTN	Martin State
	FDK	Frederick Municipal

To identify the issues and constraints that dictate current practices (dependencies and interactions between metroplex airports) and to determine the state of the art for managing interdependent airport operations, a list of candidate metroplex sites needed to be determined for further investigation. The FAA's list of OEP 15 metropolitan areas was used as the starting point. Figure 1 shows the location of candidate metroplex sites identified in previous studies. Figure 1(a) is borrowed from Bonnefoy and Hansman [10], and lists metroplexes identified in a study of the emergence of secondary airports. Figure 1(b) is quoted from Sensis' work for the NASA NextGen Airspace Project [30]). Note the existence of two 3-OEP-airport metroplexes (New York – EWR/JFK/LGA and Washington DC – BWI/IAD/DCA), and two 2-OEP-airport metroplexes (Chicago – ORD/MDW and Miami – MIA/FLL), all of which were included as candidate metroplexes for further study. A list of major airports was also developed according to their projected demand/capacity ratio based on 3X demand and the 2015 OEP baseline capacity [56] for identifying candidate metroplexes. This list is shown in Table 2 along with identified capacity needs in Capacity Needs in the National Airspace System (FACT-2)[17]. The number of candidate sites to be surveyed was limited to a subset of existing metroplexes, and sites were selected to represent the breadth of metroplex definitions and operational concepts across the ATC community today. The metroplexes described below are but a representative sample of the wide range of operations that can be observed in the NAS today. The descriptions of interactions and dependencies are not intended to be complete. Rather, the descriptions are intended to illustrate the breadth of issues that can be encountered. In-depth analyses are of the surveyed sites are presented in site survey reports [48, 54, 60, 55] and the contrast and comparison report [49].

2.1 The New York Metroplex

The airspace around the New York metropolitan area is arguably the most complicated in the U.S.. The New York metroplex contains three OEP airports – EWR, JFK, and LGA – as well as another major general aviation airport – TEB – within a circle of radius 10 NM. These four airports averaged almost 4000 operations per day in 2006 (Statistics from FAA OPSNET online database, available at `http://www.apo.data.faa.gov/`). There are also 15 secondary airports in the vicinity, four of which are among the 100 busiest U.S. airports. Although the New York airspace has been carefully designed to minimize the need for coordination between airports under typical operating conditions, the configuration and operations of the airspace does in part depend on the runway configurations at the various airports within the metroplex. In severe weather, many ATC facilities in the NY area use the DSP developed by the FAA to schedule departure releases at adapted airports so that the resulting demand at departure flow fixes does not surpass prevailing flow rates at the

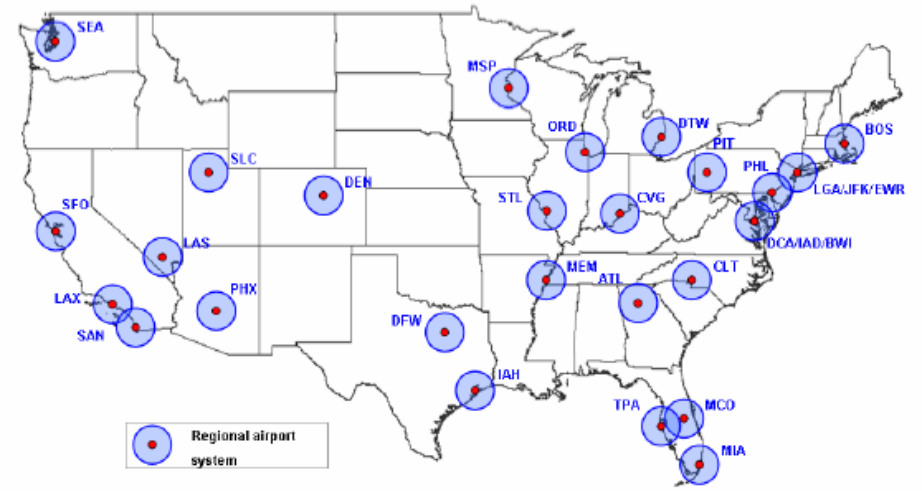

(a) Bonnefoy and Hansman

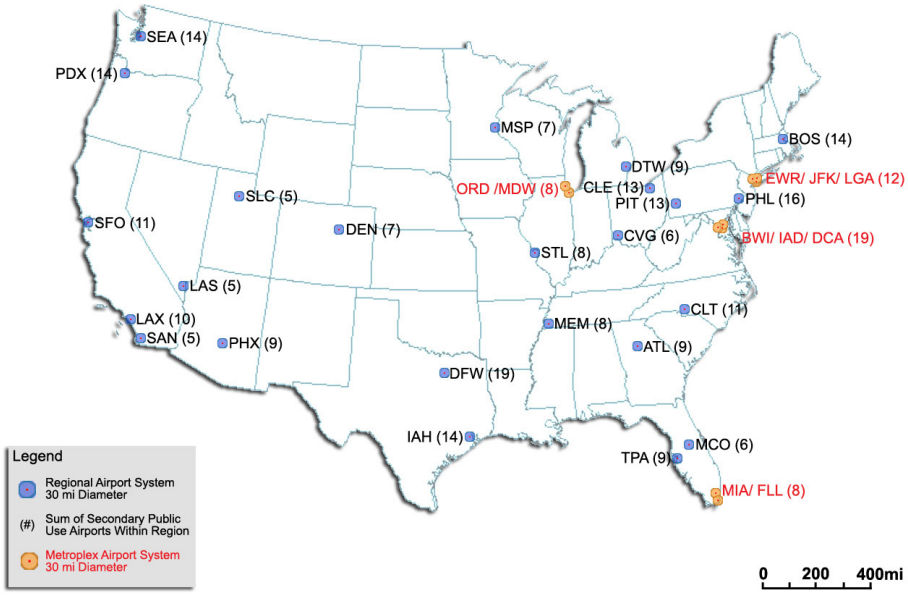

(b) Sensis

Figure 1: Location of candidate metroplex sites and metroplexes in the NAS

fixes. Operations in the New York Metroplex are supported by the New York TRACON (N90) and the New York Air Route Traffic Control Center (New York ARTCC, New York Center, or ZNY).

2.2 The Los Angeles Basin Metroplex

LAX is the fourth busiest airport in the U.S., averaging 1800 operations per day in 2006. Within 30 NM of LAX in the Los Angeles metropolitan area, there are seven other airports among the 150 busiest U.S. airports. Furthermore, three of these airports – VNY, LGB, and SNA – rank in the top 25, with an average total of 3100 operations per day, and are within 20 NM of LAX; but the vast majority of their flights are general aviation (GA). The close proximity of these airports causes their arrival and departure paths to cross over and under each other, and some of the airports also compete for arrival and departure fixes. Because LAX has the majority of the commercial traffic, it generally is given the priority, and the other airports alter their operations as required. To minimize the coordination required for runway configuration changes and to maximize the use of the preferred runway configurations and terminal area paths, the threshold for calm-wind runways tends to be 10 knots rather than the usual 5 knots. Operations in the Los Angeles Basin Metroplex are supported by the Southern California TRACON (SCT) and the Los Angeles ARTCC (ZLA).

2.3 The San Francisco Bay Metroplex

The San Francisco Bay metropolitan area includes only one OEP airport – SFO – but it also includes two other major airports – OAK and SJC. These three airports are within a circle of radius 15 NM. SFO and OAK are about 10 NM apart, but SJC is about 25 NM away from both of them. The average daily total number of operations for these three airports in 2006 was 2500. In comparing this figure to other metroplexes, however, one must keep in mind that much of the traffic at OAK is air cargo, which tends to occur in the late evening or early morning. There are also four other airports in the area that are in the 150 busiest U.S. airports. The runway configurations at the major airports in this metroplex are closely coordinated. Typically, SFO chooses its configuration, and the other two major airports use their configurations that are most aligned with SFO. If doing so would be unsafe, then they contact SFO, which will change its configuration if possible. Even when the runway configurations are properly aligned, east operations are complex because the arrival path to SFO runway 19 twice crosses over the arrival path to OAK Runway 11, which generally causes a restriction on the OAK arrival flow rate. Operations in the San Francisco Bay Metroplex are supported by the North California TRACON (NCT) and the Oakland ARTCC (ZOA).

2.4 The Washington DC Metroplex

The Washington, DC metropolitan area contains three OEP airports BWI, DCA, and IAD within a circle of 30-mile radius. IAD and DCA are about 20 NM apart, and BWI is less than 30 NM from DCA. IAD averaged 1200 operations per day in 2006, but BWI and DCA each had only 800, which gives a total of 2800 daily operations. The runway configurations of these three airports are independent. They do share departure fixes, however, and there are altitude restrictions on some arrival and departure paths to avoid conflicts. Operations in the Washington DC Metroplex are supported by the Potomac TRACON (PCT) and the Washington ARTCC (ZDC).

2.5 The Chicago Metroplex

The Chicago metropolitan area includes two OEP airports ORD and MDW less than 15 NM from each other. There are no other airports in the TRACON that are among the 150 busiest in the U.S. For the most part, ORD, which is the second busiest airport in the U.S. with 2600 daily operations in 2006, operates independently; and MDW, with 800 daily operations, changes its arrival and departure procedures to avoid conflicts. Typically, this only requires changing the flight paths; but, when ORD is departing off Runway 22L, MDW departures off Runway 31C must be cleared by the departure controller to avoid conflicts. The most extreme interdependence in this metroplex is the interference of MDW arrivals on Runway 13C with both departures from Runway 22L and arrivals to Runway 14L at ORD. In fact, departures off Runway 22L must be stopped because aircraft turning onto the 13C final are only 7 NM south of ORD. Operations in the Chicago Metroplex are supported by the Chicago TRACON (C90) and the Chicago ARTCC (ZAU).

2.6 Dallas-Fort Worth Metroplex

DFW, the third busiest airport in the U.S. with 1900 daily operations in 2006, is about 10 NM west northwest of DAL, which averaged 700 daily operations. The Dallas-Fort Worth metropolitan area is similar to the Chicago metroplex in terms of the number of major airports and the distance between them, but DFW and DAL have significantly fewer operations than ORD and MDW. Additionally, the DFW metroplex has approximately twice as many secondary airports in the top 500, with over twice as many operations as the secondary airports in the Chicago metroplex. The runway configurations at DFW and DAL are typically aligned. Simultaneous visual departures from DAL are not allowed in north flow because their departure paths head toward the DFW departure paths. When using Instrument Landing System (ILS) approaches in south flow, only a single stream of arrivals to DAL is allowed in order to avoid dependency with DFW arrivals because the extended final approach courses of the two airports converge. Operations in the Dallas-Fort Worth

Table 2: Characteristics of metroplex examples

Number of Airports	NY	LA	SF	DC	Chicago	DFW	Miami	Atlanta
OEP Airports	3	1	1	3	2	1	2	1
Top 50 airports	3	4	2	3	2	2	2	1
Top 100 airports	8	5	6	3	2	2	4	2
Top 200 airports	13	10	12	4	3	5	5	3

Metroplex are supported by the Dallas-Fort Worth TRACON (D10) and the Fort Worth ARTCC (ZFW).

2.7 The Miami Metroplex

The Miami metroplex is the only other occurrence of two OEP airports (i.e., MIA and FLL) within 20 NM of each other. Dependencies within this metroplex are expected due to the proximity of the airports. However, traffic volume at airports in this metroplex is relatively moderate as compared with many other metroplexes; the dependencies are likely less severe. An unique characteristics of the Miami metroplex is that MIA, FLL, and major secondary airports in this metroplex have similar runway orientation and runway configurations. Thus, this metroplex seems to provide an example of unique practices for handling dependencies between airports with similar runway configurations. Operations in the Miami Metroplex are supported by the Miami TRACON (MIA), the Palm Beach TRACON (PBI), and the Miami ARTCC (ZMA).

2.8 The Atlanta Metroplex

The Atlanta metroplex contains the busiest airport in the U.S. at 2700 daily operations in 2006. Operations in this metroplex are dominated by the traffic to and from ATL. Traffic to and from other smaller airports are normally routed around the ATL traffic pattern. A corridor over airport ATL exists to allow departure traffic from smaller airports to fly direct to their destinations. Atlanta thus represents another type of metroplex operation. Operations in the Atlanta Metroplex are supported by the Atlanta Large TRACON (A80) and the Atlanta ARTCC (ZTL).

Some characteristics of these metroplexes are summarized in Table 2. This table, in conjunction with the descriptions of dependencies in this section also indicates that these examples provide a good breadth of metroplex operations.

2.9 Metroplex Site Surveys

The objective of the metroplex site surveys was to develop a deeper understanding of these parameters and issues that are intrinsic to the metroplex problem through examining the current operations at representative metroplexes in the NAS. Within the resource limit and

time frame of this project, the research team, of which I was a part, visited Atlanta, Los Angeles, New York, and Miami.

Among the sites visited, Atlanta represents a metroplex with a single dominant large hub [24] airport and much smaller satellite airports [48]. The Los Angeles (LA) Basin represents a metroplex with multiple medium-to-large hub airports that are heavily affected by terrain and FAA Warning Areas/SUA [54]. New York Metro represents a metroplex with multiple, tightly spaced, large hub airports. Thus, operations are confined in limited airspace [60]. Miami represents a metroplex with two large hub airports and relatively small satellite airports such that interactions between two airports with similar configuration can be investigated [55].

2.9.1 Site Survey Procedure

The steps employed to collect, review, analyze, and disseminate information on operations at the specific metroplex sites studied are discussed in the following sub-sections.

2.9.1.1 Site Visit

Prior to each site visit a detailed questionnaire was prepared and sent to the ATC facility, and later used as a guideline during the visit. The questionnaire, developed with the assistance of experienced controllers, covers both generic aspects of metroplex operations and unique operational and environmental conditions specific to the site. Questions were normally related to hub airport configurations, arrival/departure routes, TFM, terrain, SUA, weather, noise restrictions, and most importantly, interaction and coordination with adjacent facilities. These facilities may include ARTCC, TRACON, Air Traffic Control Tower (ATCT, or Tower), airport ramp tower, and military ATC.

The site visit typically consisted of a briefing on facility operations and traffic management procedures, followed by a round-table interview with a facility manager, a representative from the Traffic Management Unit (TMU), and sometimes controllers. Major discussion focus was given to specific traffic flow interactions and coordination procedures, as well as to system automation and TFM tools that might have been used to assist the coordination procedures. Each facility provided an overview on how dependent or independent adjacent airport flows either conflicted or operated as single airports. Within the metroplex facilities, primary airports were identified and examined as to their interaction and control of adjacent facility configurations and/or traffic flows. Traffic flow and departure spacing were also discussed and determined if selective airports received priority flows or releases. Often, a tour of the control room or tower cab provided opportunities for reviewing procedures and tools working with live traffic. Training materials were also collected during these visits.

Facilities visited included, in chronological order: Atlanta Large TRACON (A80), Southern California TRACON (SCT), New York TRACON (N90) and Center (ZNY), and Miami

Tower/TRACON (MIA). The New York site visit also included visits to the Towers at John F Kennedy (JFK), LaGuardia (LGA), the Newark (EWR), and to the Continental Airlines ramp tower at EWR and Delta ramp tower at JFK.

2.9.1.2 Data Analysis

Airport statistics, traffic flows, Standard Terminal Arrival Route (STAR) and Standard Instrument Departure (SID) procedures, facility SOP, Letters of Agreement (LOAs), navigation charts, and relevant literature were reviewed prior to the site visits. Also reviewed were SOPs of adjacent facilities not visited to determine interactive flows. After the visit, detailed analyses were conducted. These analyses fell into four categories described blow.

Airport Data and Traffic Statistics For each metroplex, a list of airports was generated based on the distance from the "core" hub (the largest airport, or the airport that is given highest operational priority), runway length, traffic statistics, FAA's airport categorization [24] and supporting architecture [28]. The airport list provided a basis for data analysis efforts. Detailed traffic demand versus capacity analysis was performed for large hub airports in the metroplex. Capacity and operational constraints, and issues that have implications on metroplex operations, were identified through analyzing data collected during the site visit, from the airport owner and operator, and from government databases.

Traffic Flow Analysis Traffic flow analysis was performed utilizing PDARS, which processes both en route and terminal flight data and radar data (including every radar hit). Sample data were filtered by aircraft category (jet, or tubo-prop, and props), airport, and operation (arrival, departure or over flight) to reveal traffic patterns and flow interactions. Shared arrival and departure fixes were identified and viewed using PDARS in order to identify possible choke points or congestive flows. Different meteorological conditions, such as visual meteorological conditions (VMC), instrument meteorological conditions (IMC), and storm events, as well as runway configuration changes, were analyzed. Results were represented both in static and replay format indicating proximity of airports, airspace boundaries, crossing points and altitude assignments, arrival and departure transition areas (ATA and DTA), SUA and terrain, etc. Sample data were also provided to the team for quantitative analysis.

Air Traffic Control Procedures ATC procedures are defined by published STARs and SIDs, facility SOP, and LOAs with interacting ATC facilities or military regarding the use of SUA. These procedures also cover the use of special ATC automation tools and programs across facilities such as the Severe Weather Avoidance Plan (SWAP) [26]. In-depth analysis focused on detailed traffic flow interactions and coordination procedures.

An interaction is defined as an extra spatial or temporal restriction imposed on one ATC facility due to the proximity of another. Interactions include airspace delegation, arrival and departure routes and altitudes, coordination of departure release, restrictions on runway use, interdependencies between runway configurations at different airports, and initiation and use of special programs. A scheme was developed to use a tree structure to present individual interactions as leaves. Analysis results are presented with details as an appendix to each of the site survey reports, and as sections in the main body of those reports highlighting key points.

Analysis of Environmental Constraints For each metroplex site, available noise studies and Environmental Protection Agency (EPA) regional air quality classification standards [20] were reviewed to determine noise and air quality impacts and constraints affecting future metroplex design. Water-quality impacts at airports originate primarily from the use of deicing and anti-icing chemicals and specific operational practices. Greenhouse gases were not addressed. It is important to note that increased aviation activity will contribute to greenhouse gases [23] and that inventory and control of these contributions [16] is likely to be a factor in some aspects of metroplex design.

2.9.1.3 Facility Comparison

The metroplexes were contrasted and compared based on the data documented in metroplex site survey reports [48, 54, 60, 55]. The TRACON, as the primary ATC facility managing terminal area operations, is the primary focus in the following discussion. Because a TRACON may serve more than one metroplex (e.g., SCT serves LA Basin and San Diego), when focus is given to specific metroplexes, metroplex names may be used. It should be noted that TRACON IDs are sometimes used loosely to reference both the TRACONs and the relevant metroplexes in context (e.g., SCT may also be used when referencing LA Basin). Airport codes are given in the list of facility identifications at the beginning of this report thus are used directly without spelling out their full names in the text for the sake of simplicity. Because of its complexity and its importance in this research, the comparison of metroplex operations is discussed in a separate subsection. Airspace complexity is a topic of study in and of itself, and several methods for understanding airspace complexity have been studied [13, 47, 66] mostly related to controller actions. However, air traffic is a second source of measure for complexity [42] and metroplex operation exhibit both characteristics.

2.9.1.4 Facility Overview

The geographic location and the airspace boundaries for the A80 TRACON is shown in Figure 2, N90 is shown in Figure 3, SCT is shown in Figure 4, and MIA is shown in Figure 5. The relative size of these airspace boundaries reflects the geographic scope of responsibility

for each entity, however this may not be a good measure for operational complexity since the traffic volume and shape has to be taken into account.

Among the four, MIA is the smallest and only has a single operating area, thus it could be expected to be least complex. SCT has 6 areas, however it should be noted that PSP (serving Palm Springs) and NKX (serving San Diego) are some distance away from the other 4 areas. N90 has 5 areas and they all have overlaps, thus it could be expected to be the most complex. A80 has the largest coverage and operational areas. The complexity of A80 could be expected to be somewhere between MIA and SCT. A comparison of other facility characteristics is shown in Table 3.

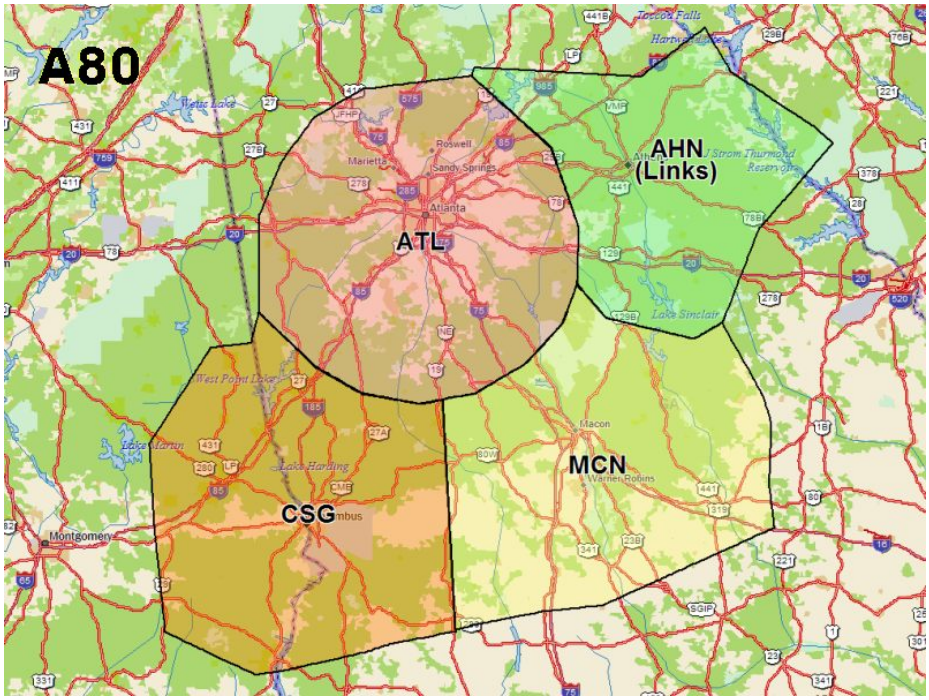

Figure 2: A80 TRACON

In Table 3, the usable airspace is defined as the percentage of the volume of TRACON airspace above minimum vectoring altitude with respect to the total airspace above mean sea level, thus it should be an indication of terrain constraints. Other items should be self-explanatory. From the table, one can conclude that A80 hosts a metroplex with a single dominant large hub airport. SCT hosts two metroplex operations with LA Basin representing a metroplex with multiple medium-to-large hub airports (six air carrier airports), that is significantly affected by terrain and SUA. N90 hosts a metroplex with multiple, tightly-spaced, large hub airports (three major airports within 10 NM radius), thus operations near the airport are severely confined by airspace. MIA hosts a metroplex with two large hub airports and relatively small satellite airports such that interactions between two airports

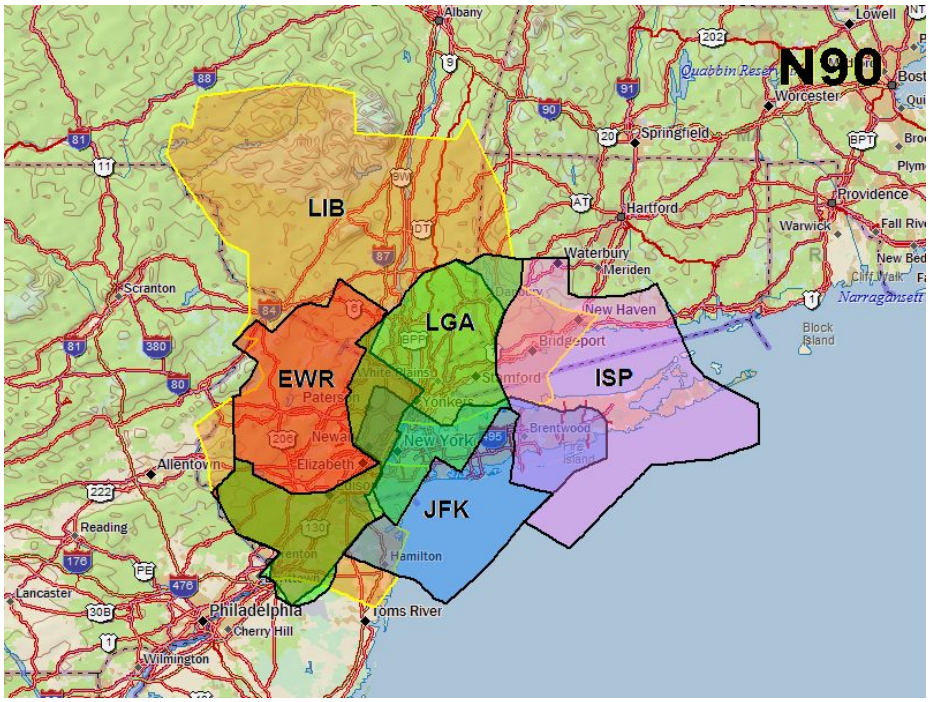

Figure 3: N90 TRACON

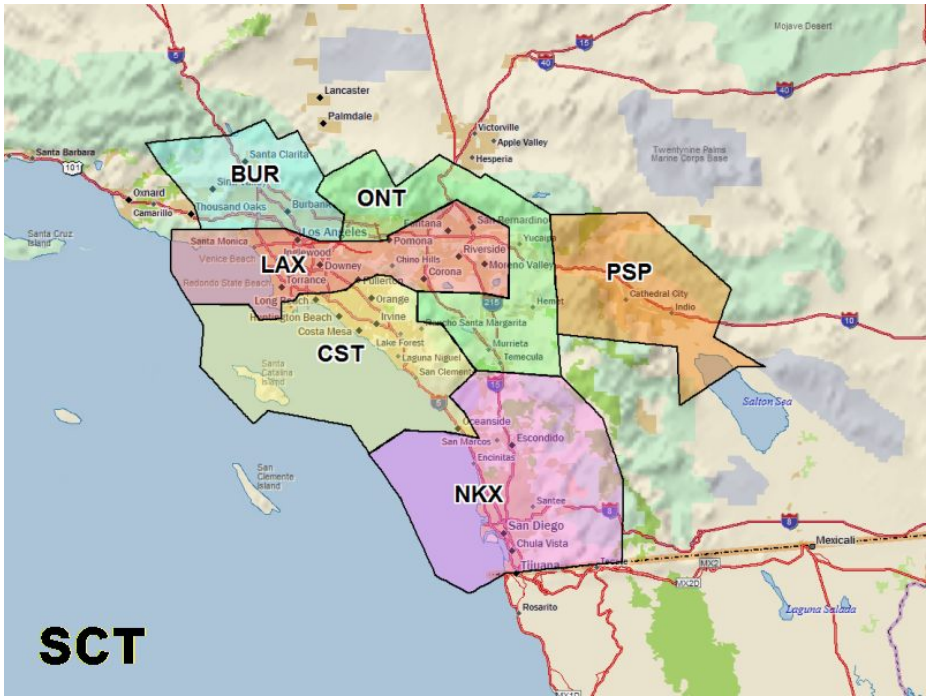

Figure 4: SCT TRACON

Table 3: Metroplex Facility Comparison

Item	A80	SCT	N90	MIA
Overview	Serves worlds busiest airport - ATL	Worlds busiest TRACON	Four busy airports (3 OEP + TEB) within 10 NM radius	All major airports aligned north- south along coast
Coverage (nmi^2/ft)	25,100/up to 14,000	14,920/up to 17,000	17,246/up to 17,000	5,817/up to 16,000
Usable Airspace	76%	45%	82%	99%
Airports	25	49	50	10
OEP Airports	ATL	LAX, SAN	JFK, LGA, EWR	MIA, FLL
FAA Towers	3	17	11	4
Federal Contract Towers	4	7	5	2
Military Towers	3	6	1	1
Class B Airspace	ATL	LAX, SAN	JFK, LGA, EWR	MIA
Class C Airspace	CSG	Bur, Ont, SNA, RIV (SAN)	ISP	FLL
Terminal Radar Service Area	MCN	PSP	None	None
Military Restricted Area	1 cluster inside; 2 clusters surrounding	1 cluster inside; 5 clusters surrounding	1 cluster inside; 2 clusters surrounding	None inside; 1 clusters surrounding
ADIZ & Warning Areas	1 cluster inside 4 clusters surrounding	None inside 6 clusters surrounding	None inside 2 clusters surrounding	None inside 4 clusters surrounding
Interacting ARTCC	ZTL	ZLA	ZNY, ZBW, ZDC	ZMA

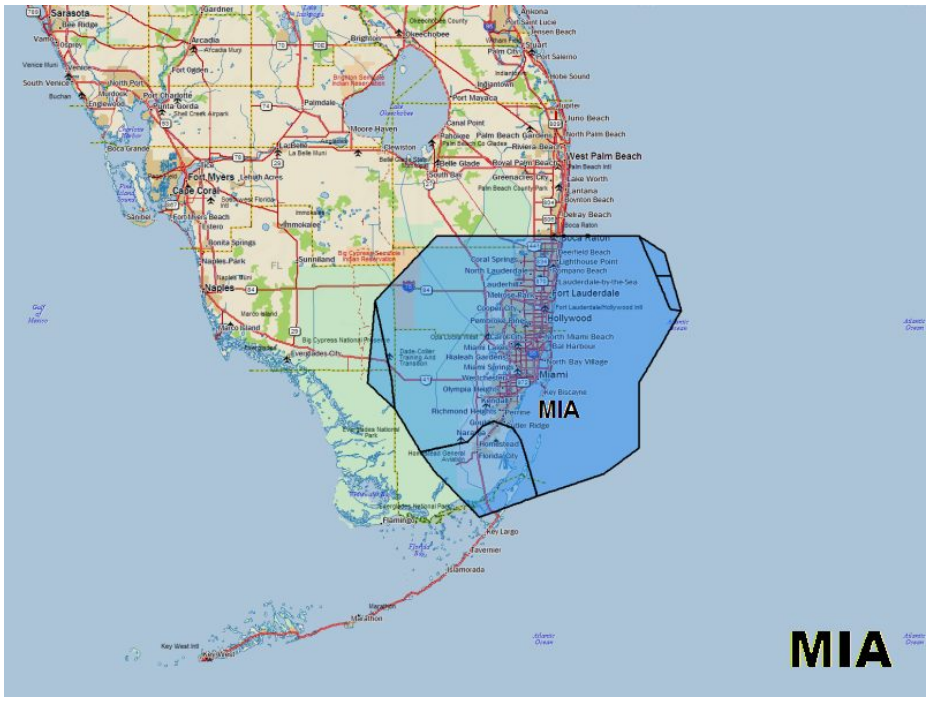

Figure 5: MIA TRACON

Table 4: Annual TRACON Instrument Operations (2007 Data)

Item	A80	SCT	N90	MIA
FAA Rank	5	1	2	9
Operations (1,000)	1,433,000	2,243,000	2,066,000	943,000
Loading (1,000/nmi^2)	57.07	150.34	119.80	162.11

may be studied relatively easily.

2.9.1.5 Traffic Statistics

The number of annual instrument operations for 2007 for the four TRACONs are listed in Table 4. Also listed is the FAA rank of each TRACON and a loading derived by dividing the annual operations by the coverage area from Table 3. Of interest is MIA, which has the smallest number of annual instrument operations yet the highest traffic loading per unit of surface area covered. Given the much lower percentage of *usable* airspace, SCT still qualifies as the busiest TRACON in the world.

Table 5 lists the annual 2007 itinerant (traveling from one airport to another) air carrier operations, and total operations at metroplex airports whose annual total itinerant operations are 100,000 or more. Total itinerant operations include air taxi, general aviation, and military operations that are not listed in the table. The Metroplex Total is the sum total for listed airports in the metroplex. Weight is the percentage of metroplex traffic to/from a

Table 5: Annual Itinerant Operations at Major Metroplex Airports

Metroplex	Airport Annual Statistics					Metroplex
	ID	Air Carrier	Total	Growth	Weight	Total
Atlanta	ATL	713,815	989,295	2.45%	86%	1,152,467
	PDK	24	163,172	0.40%	14%	
LA Basin	LAX	467,071	672,095	1.58%	39%	1,714,664
	SNA	92,450	252,624	0.46%	15%	
	ONT	89,970	142,666	-1.72%	8%	
	BUR	58,970	183,930	-1.85%	11%	
	LGB	26,668	195,303	0.73%	11%	
	VNY	0	268,046	0.68%	16%	
NY Metro	JFK	350,421	453,258	0.41%	23%	2,011,295
	EWR	273,752	444,881	0.38%	22%	
	LGA	201,374	401,410	-0.15%	20%	
	ISP	27,558	111,934	0.41%	6%	
	HPN	11,116	184,975	0.82%	9%	
	FRG	201	106,961	0.26%	5%	
	TEB	6	202,128	0.41%	10%	
	MMU	0	105,748	-0.18%	5%	
Miami	MIA	294,068	386,645	1.52%	39%	979,445
	FLL	189,310	304,595	1.99%	31%	
	TMB	32	122,165	2.72%	12%	
	FXE	0	166,040	0.54%	17%	

given airport indicating traffic distributions among metroplex airports. The data show that the Atlanta metroplex has the busiest hub airport and fewest heavily trafficked airports. The New York metroplex has the highest number of heavily trafficked airports.

2.9.1.6 Core Airports

A core hub airport is the airport with highest traffic volume or highest overall operational priority, within the metroplex; often these two aspects are aligned. A comparison of core hub airports would thus reveal the most critical issues related to hub airports that may be of significance at the metroplex level.

All sites have ground transportation congestion issues with, Los Angeles and New York facing the most serious problem. Atlanta currently has only one commercial airport, but that may change as demand grows. Ground connection between JFK and LGA is relatively short but connections with other airports are almost unacceptable for connecting a flight. The situation is similar for Los Angeles metroplex airports. The connection between MIA and FLL, however, is improving with a new multimodal transit center under construction.

Airport demand and capacity are represented by a typical VMC weekday in 2007. The demand was divided into quarter-hour slots, and then compared with VMC and IMC capacities from the FAA 2004 capacity benchmark [29]. A total daily demand/capacity ratio [64]

was calculated by dividing the total daily operations with 16 hours worth of VMC capacity. It is seen that, with the exception of MIA, the core hub airports are very congested, with the worst situation at JFK. However, the capacity constraints at ATL and LAX are currently surface limitations (LAX has 1/10th of the acres of Dallas) while at JFK it is more an airspace problem, although limited arrival gates and construction causes gridlock during peak periods.

Three of the core airports have east or west operations with one direction used more often. JFK has many different configurations due to the crossing runway layout. At N90 the JFK/LGA and EWR/TEB airports require close coordination procedures to maximize traffic flows. This is primarily due to airspace congestion and the little airspace available to vector aircraft for additional spacing. The comparison of metroplex core hubs, namely ATL, LAX, JFK, and MIA, are summarized below.

A80: ATL

- Airport Layout: The airport layout is shown in Figure 6.
- Location: 11 statute miles south of Atlanta downtown.
- Inter-Airport Ground Connection: No secondary commercial airport
- Demand and Capacity
  - $>$ IMC capacity for 21 slots.
  - $>$ VMC capacity for 8 slots.
  - Total daily ratio: 0.77; very congested.
- Surface Limitation
  - Limited gates for the volume of traffic.
  - Lack of a "penalty box" or overflow areas.
  - Surface limitation may become a factor for arrival rates during busy periods when three runway landings are in effect.
- Airport Configuration: East and West, with West configuration more common.

SCT: LAX

- Airport Layout: The airport layout is shown in Figure 7.
- Location: 15 statute miles southwest of downtown Los Angeles.
- Inter-Airport Ground Connection:

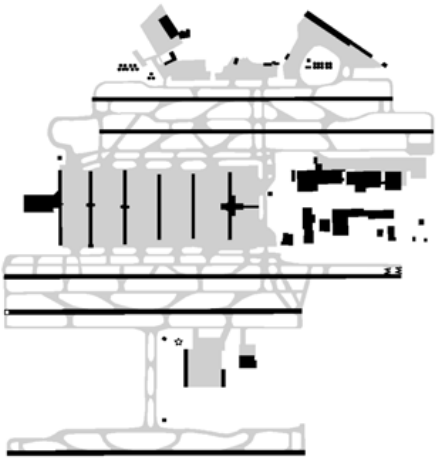

Figure 6: A80: ATL

  - Flyaway bus to VNY (60 min.).
  - Congestion is a problem.
  - No rail connection

- Demand and Capacity
  - > IMC capacity for 7 slots.
  - > VMC capacity for 1 slots.
  - Total daily ratio: 0.72; very congested.

- Surface Limitation
  - Limited airport real estate: limited taxi areas and gates.
  - Limited holding space between closely-spaced runway pairs.
  - Endangered species habitat limit feasibility of western end-around taxiways.
  - Runway incursion problems.

- Airport Configuration: East and West, with West configuration more common.

N90: JFK

- Airport Layout: The airport layout is shown in Figure 8.
- Location: 12 statute miles east of Lower Manhattan.
- Inter-Airport Ground Connection:

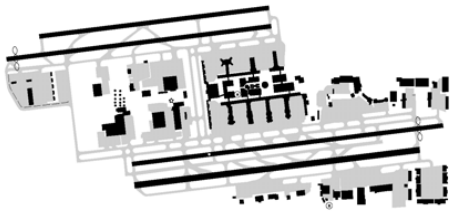

Figure 7: SCT: LAX

  - Van/express bus to LGA (30 min.), to EWR (90 min).
  - No direct rail connection

- Demand and Capacity
  - > IMC capacity for 33 slots.
  - > VMC capacity for 21 slots.
  - Total daily ratio: 0.88; *very* congested.

- Surface Limitation
  - Limited airport real estate at hub airports: limited taxi areas layout design.
  - Surface limitations less an issue.
  - Runway capacity mostly driven by airspace.

- Airport Configuration: many, 31L/R used most often.

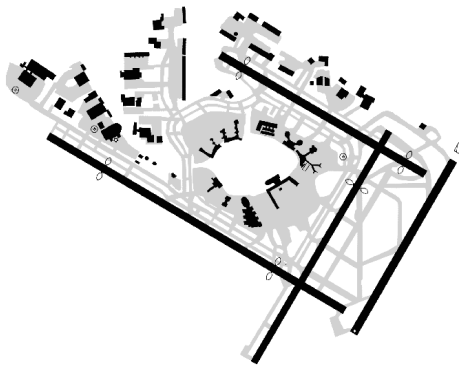

Figure 8: N90: JFK

MIA: MIA

- Airport Layout: The airport layout is shown in Figure 9.

- Location: 5 statute miles west of downtown Miami.
- Inter-Airport Ground Connection:
  - Shuttle to FLL (45 min.).
  - Tri-Rail connects MIA and FLL (and PBI).
- Demand and Capacity
  - < VMC/IMC capacity.
  - Total daily ratio: 0.44; not congested.
- Surface Limitation
  - Surface congestion is generally not considered a major problem at MIA or FLL.
- Airport Configuration: East and West, East is used most often.

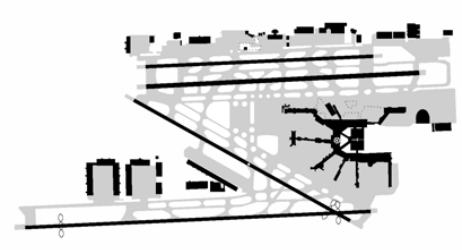

Figure 9: MIA: MIA

2.10 Comparison Between Metroplex Operations

VMC nominal traffic flows for A80 is depicted in Figure 10, N90 is presented in Figure 11, SCT is shown in Figure 12, and MIA is also shown in Figure 13. These traffic flows depict how ATC handles the complexities of each metroplex's operations in today's environment. These figures also show some of the differences between these four metroplexes.

ATL's 4-corner post arrival operation is clearly seen in Figure 10. Due to high traffic volume at the northeast corner, two independent entry flows may be used at times. Traffic flows from the other feeds may be adjusted based on the demand from the northeast corner. Where departure flows cross arrival flows, altitude restrictions are enforced. Satellite flows are normally routed around and below ATL traffic (not shown). Turbo-prop and jet departures of secondary airports can be stacked (11,000 ft & 13,000 ft) with the ATL traffic in the feed to ZTL.

In Miami, although MIA and FLL do not have traditional standard 4-corner post operations, the existing arrival corridors serve the same purposes. Due to their distance (18

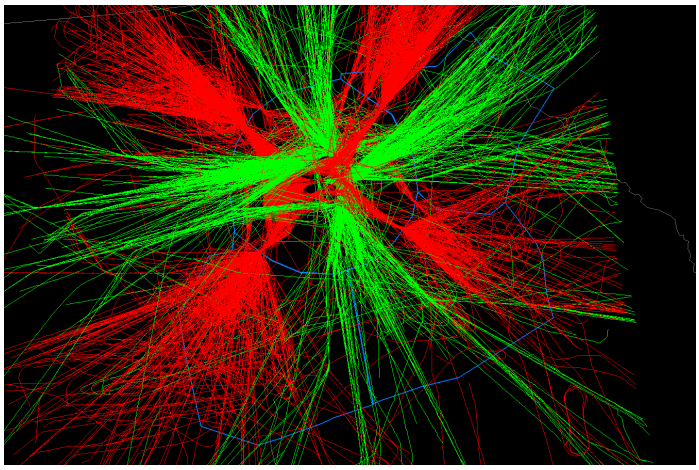

Figure 10: A80 nominal traffic flows. Arrivals in Red, Departures in Green.

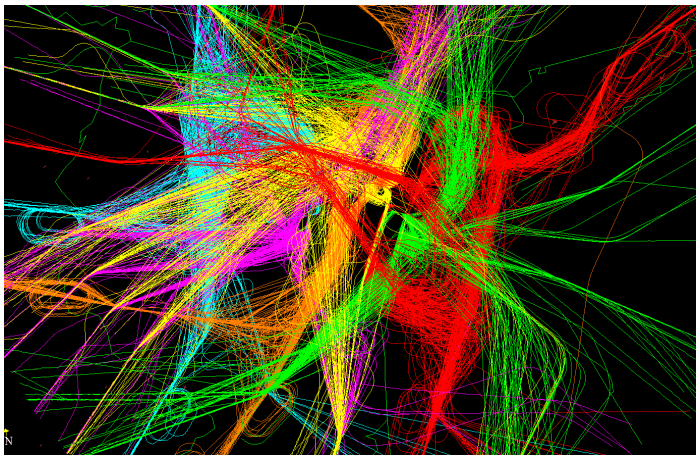

Figure 11: N90 nominal traffic flows. EWR Arrivals in Light Blue, EWR Departures in Magenta, LGA Arrivals in Orange, LGA Departures in Yellow, JFK Arrivals in Red, and JFK Departures in Green

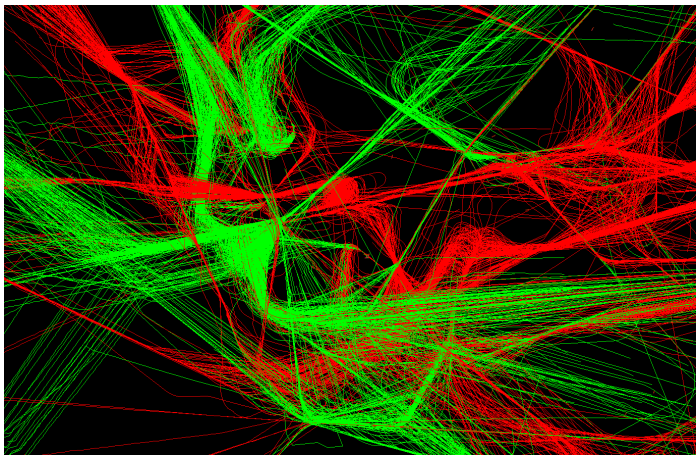

Figure 12: SCT nominal traffic flows. Arrivals in Red, departures in Green.

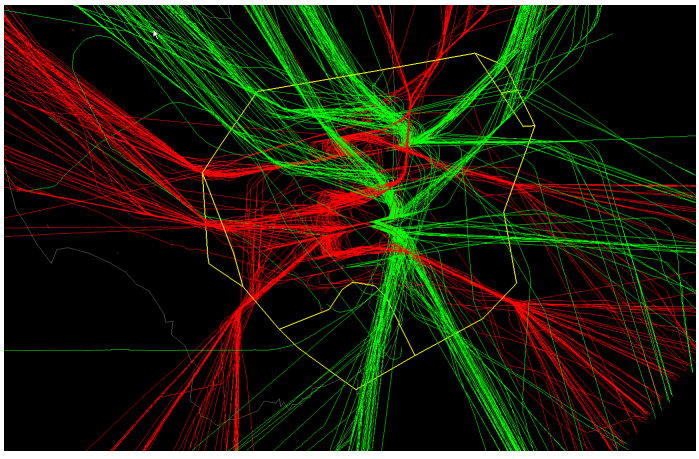

Figure 13: MIA nominal traffic flows. Arrivals in Red, departures in Green.

NM), traffic flows from these two airports, especially the high volume traffic to and from the north, may cross with proper vertical separation and use different arrival and departure gates. Less congested airspace also allows for satellite traffic being mixed in with no problem. ZMA uses transition areas and often reroutes arrival and departure traffic during weather events. Since ZMA and MIA regularly operate with thunderstorm activity, the facilities utilize efficient SWAP procedures and maintain traffic flows. FLL and MIA can operate independently in different configuration without a decrease in capacity.

A four-corner post operation is not observed in LA Basin due to airspace constraints, terrain, and adjacent airport flows (6 air carrier airports). Sharing arrival and departure gates/fixes is common, although other airport flows (arrival and departures) from the east are pushed below the primary LAX flow. Traffic flows from different airports do merge and cross but that normally occurs some distance away from the airport. Flows seem to be confined; but gaps do exist (see north of ONT and south of CNO). Those gaps are actually terrain to be avoided – ONT airport sits in a valley east of LAX. SCT and N90 both have high business jet and turbo-prop traffic to adjacent airport (SNA, LGB, VNY, SMO).

Traffic flows in the New York metroplex are dense and very complex. If multiple colors were not used, the traffic pattern would not be discernible. Sharing arrival and departure gates is very common, although JFK traffic flows are less dependent due to the ocean arrivals. The crossing and merging of traffic flows occur much closer to the hub airports. Because the three large hub airports are so close to each other, there is not much airspace available for vectoring within the terminal area using an extended final to manage arrival traffic is not possible, since airspace is shared with other arrival and departure areas. LGA and JFK are closely related operations. EWR and TEB are closely dependant operations, especially when runway operations are set to EWR Runway 4 and TEB Runway 6 operations. Business jet/turbo prop airports HPN and TEB share arrival fixes and departure fixes. Holding is also frequent at multiple entry fixes.

2.10.1 Airspace Complexity, Operational Constraints and Procedures

For airport configuration changes, each airport in A80 is largely independent of each other. If ATL requires a change, the other airports may react to the change. But changes in operations for ATL during busy hours is avoided if at all possible due to the throughput loss. Changes in runway directions may be done significantly in advance to avoid delay. Airport configuration changes in SCT are fairly coupled. Each configuration change must be coordinated with ZLA and are done only when absolutely necessary. N90, on the other hand, demonstrates strongly coupled configuration changes. The TRACON and JFK drive the changes and are given higher priority. Due to the complexity of the airspace and difficulty involved in changing such a densely operated airspace, a flush and stop procedure may be needed to clear the airspace before such a change.

Each metroplex also faces issues with the airspace structure that they are forced to operate within. A80 lacks sufficient class B airspace in the north east corner of ATL, which has some of the busiest fixes in the NAS. Class B extensions are planned for the future. SCT faces issues with an uneven TRACON ceiling, with the top ranging from 6,000 ft. all the way up to 17,000 ft. N90 simply lacks enough airspace, which gives ATC little room to maneuver and to set up holding patterns. MIA currently only has FLL in Class C airspace, while they need to extend the Class B airspace to include FLL.

Weather is an issue for each of these TRACONS. A80 has significant convective weather. SCT has significant winds, issues with coastal fog, and convective weather as well. N90 has convective weather during the summer and winter storms and snow during the winter which requires significant de-icing. MIA also has significant summer thunderstorms.

Terrain and special use airspace (SUA) is only a significant factor for SCT due to several existing warning areas and mountains constraining the traffic flow into small corridors. N90's eastern seaboard SUA can now be used during large weather situations.

Due to the metroplex complexities, these TRACONS often have significant interactions between the traffic in the other airports. A80 contains the world's busiest airport, and so the other airports in the TRACON are forced to fly non-optimal routes. For example, jets departing from PDK are often released with altitude restricted climbs. For SCT, VNY may be shut down if BUR is unable to change to certain configurations. The shared arrival and departure fix and northbound departures out of SCT are extremely congested. Sharing the departure queue information would significantly help SCT's decision making capabilities. N90 mostly has issues with sharing airspace. There is little room for flights landing on 29/11 into EWR to perform missed approaches due to the close proximity of LGA. Competing and sharing arrival and departure routes require vertical or temporal separation. For MIA, arrivals into both MIA and FLL from the southwest and northeast share the same STARs. The traffic is often spatially separated. Operations into satellite airports may be mixed into the hub traffic and will call the TRACON for departure release.

2.11 Conclusions

While using these visits to help understand the complexities that are intrinsic to metroplex operations was a useful and necessary exercise, many simplifying assumptions need to be made before algorithms can be evaluated and compared. The core of the metroplex problem can be distilled to the case where multiple airports share airspace resources. This core problem will be the topic of the chapter dealing with metroplex evaluation.

CHAPTER III

METROPLEX IDENTIFICATION

3.1 Introduction

With the ever increasing growth of airborne traffic, many individual airports can no longer be viewed as individual entities, but rather as members of a larger, interdependent group. We call such a group of airports a metroplex. While we can qualitatively cluster nearby airports into metroplexes, creating a numerical metric is desirable for understanding the growth of each metroplex, determining when an airport enters a nearby metroplex, and studying the creation of new metroplexes as traffic increases.

In this chapter we will attempt to define several factors in our search for an interaction metric. While we believe that the derived metric is directly related to the notion of interaction between airports, the methods presented here could be used as a framework to build and test alternate metrics.

The notion of our metric is that each airport has an ideal arrival space (volume) surrounding it, and if the arrival space of two neighboring airports overlap, the aircraft flying through this shared space would cause interaction. This interaction is a measure of the added complexity due to the neighboring airport. This pairwise complexity would be handled through procedure design, additional controller workload, or any other method used to reduce this complexity. The metric presented here attempts to capture such interaction with the goal of clustering airports that share high values of this interaction into metroplexes algorithmically. This will allow for numerical sorting and analysis of metroplexes based on our interaction metric.

3.2 Optimal Approach for Truly Independent Airport

Before we consider how much one airport will impact its neighbor, we must first understand the operation of each airport with no restrictions. Several methods could be used to calculate this arrival space. A rather naïve definition of such a space would be to use the space defined by the three degree glide slope used by aircraft on their approach. We could assume that the three degree slope would be used uniformly around the airport to generate a cone. A thickness could be defined by using the uncertainty in the glide slope angle.

While that method would produce a reasonable approximation of the arrival space, it would not be accurate before the glide slope was acquired. To provide a more precise approximation to the arrival space, a simulation tool being developed at the Air Transportation Laboratory (ATL) at Georgia Tech was used to provide 4D trajectories for several aircraft

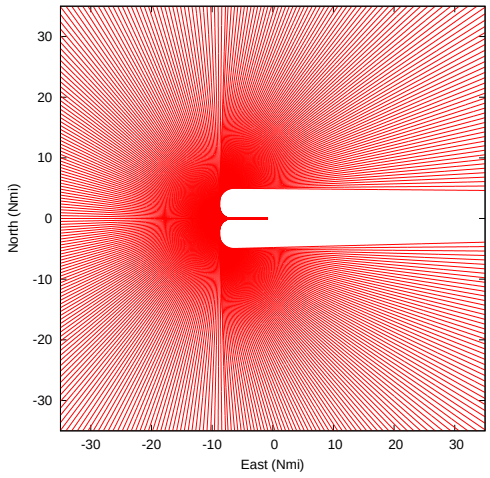

Figure 14: Lateral path as simulated.

types from each degree heading from top of decent down to the runway threshold. This was done using 360 unrestricted Continuous Descent Arrivals (CDAs), one for each degree heading. The lateral track has three defined waypoints:

1. Entry point
2. Turn onto final (10 nmi from runway threshold)
3. Runway threshold

These wayponts are entered into the flight management system (FMS) where they are then simulated using actual aircraft drag polars, flap schedules, etc. Figure 3.2 depicts the lateral path as simulated. While the lateral paths are depicted as flown, the simulation was based only on the points described.

These flight paths were used to define the region of "optimal" approaches into an independent airport. We believe the CDA is the optimal approach due to the measurable fuel and time savings that have been found both through simulation and during flight tests.

3.2.1 Continuous Descent Arrival

The development of CDAs was one of the first main projects of the ATL at the Georgia Institute of Technology. With increasing fuel prices and a heightened awareness for environmental and noise concerns, airlines and air traffic control are looking at various methods to improve an aircraft's performance during flight. One such opportunity presented itself during the descent phase of a flight. Currently, aircraft perform what may be termed a "step descent" to the runway. That is, aircraft do not descend constantly during the approach to the runway; instead, they descend from one altitude to another, continue in level flight

until a certain point, and then resume their descent to the runway or another altitude. This method is not fuel-efficient since an increase in thrust may be needed to maintain altitude during a level flight segment and by increasing thrust, more noise and pollutants are produced. Such a procedure is currently in place for many reasons, including airspace restrictions, traffic volume, and controller workload.

CDAs were developed with the goal of minimizing these level segments and allowing aircraft to descend "continuously" to the runway, without having to level out at a certain altitude. An analogy to such a procedure is driving down a hill in a car, with the foot off the accelerator and letting the car coast down the hill without driving over any flat regions of road. To design a CDA, a fast-time simulator has been created in Matlab and is used to simulate the trajectories that aircraft would take if they flew such a procedure. These trajectories are then provided to air traffic control, who then informs the ATL as to whether the designed procedure fits into current airspace restrictions. If so, the procedure is then flight tested in aircraft simulators, followed by a live demonstration before publication. If not, a redesign is conducted to ensure compliance with airspace restrictions [14].

Currently, CDAs designed by the Air Transportation Lab are in use at two airports in the US: Louisville International Airport and Los Angeles International Airport. Results from Louisville have shown that up to 1000 lbs of fuel can be saved per flight along with a substantial decrease in noise over a flight path flown by a B767-300. At Los Angeles International Airport, most flights flying in from the East Coast of the US utilize the designed procedure and along with air traffic control, are very happy with the arrival. Airports currently involved in CDA development include Atlanta's Hartsfield-Jackson International Airport and San Diego International Airport, with a CDA flight test conducted in Atlanta during spring of 2007 and with additional tests in August 2008. Delta Air Lines has been a key partner in the development of these procedures, participating in both the flight test portion, and allowing the ATL to use its flight simulators. Several other carriers have participated in these flight tests. The fuel saving potential at Hartsfield-Jackson International Airport is enormous due to the number of flights flown by the dominant carrier, Delta Air Lines.

CDAs are an important part of the Next Generation Air Transportation System (NextGen) of air traffic control. The goal by 2020 is to implement as many CDAs as possible at airports around the US, possibly providing a substantial fuel savings to airlines, as well as alleviating environmental and noise concerns for communities around airports.

3.2.2 Airport Cone

The CDAs were simulated for each of the lateral paths described above to produce the "cone" of arrivals descending into the airport. The flight paths of each simulated path is shown in figure 3.2.2.

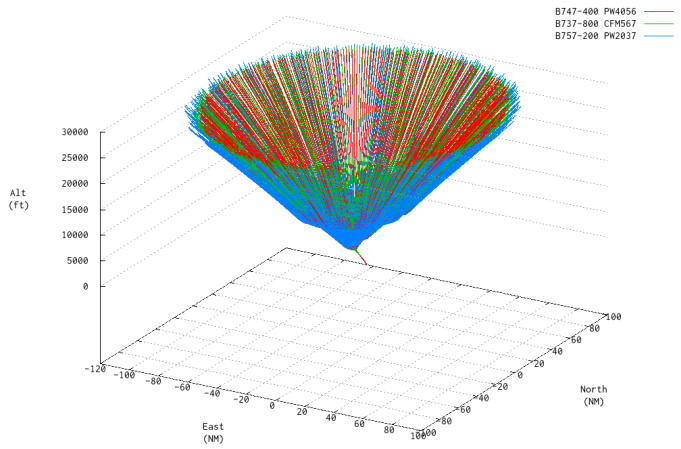

Figure 15: Cone of arrivals for B747-400, B737-800, and B757-200.

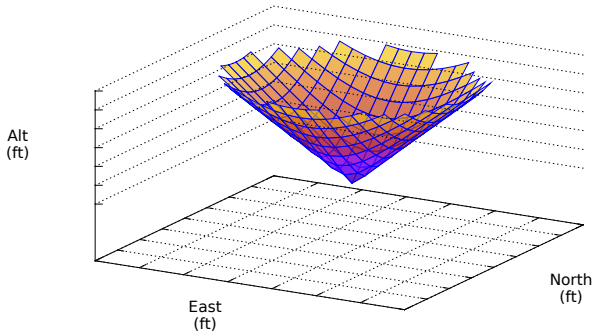

Figure 16: B737-800 Fit.

While the raw data is useful, it is not practical to do thousands of interpolations to determine the altitude of the cone. To speed up computation, a surface fit was performed on each of these "cones" is the form given in Equation 1.

$$h(x,y) = a\sqrt{(x+b)^2 + (y+c)^2} + dx + ey + f \tag{1}$$

Where h is the altitude, and a through f are fit parameters found through least squares fitting for each aircraft type. An example fit is shown in figure 3.2.2. A table of the fit parameters is given in table 6.

Using the surface fit, it is trivial to do many transformations to tailor the arrival space for each airport. This includes rotating the cone to accommodate arrivals from any direction, not just from the west. It also allows us to easily account for airports with different

Table 6: Fit parameters for various aircraft types.

Type	a	b	c	d	e	f
B737-800:	0.0516723	26539.1	126.131	0.00497552	-8.40873e-5	1222.53
B747-400:	0.052834	26083.7	152.484	0.0051573	-7.74693e-5	1080.29
B757-200:	0.0495742	26434.9	-52.6077	0.00468949	3.00018e-6	1206.07

elevations.

3.3 Metric

Now that we have defined an "optimal" airspace for a completely unrestricted airport, we will work towards a distance metric to determine how far from this ideal we will be forced to displace our airspace due to the proximity of other nearby airports. This metric will be used as a proxy for the complexity of the airspace due to the interference of nearby airports. To account for the added complexity, two factors will be incorporated into our metric: the amount of air traffic that must be moved away from the optimal and the distance the traffic must be moved.

The air traffic volume numbers used for this analysis was taken from the Federal Aviation Administration's (FAA) Terminal Area Forcast (TAF) database. However, the method presented here is applicable for any consistent volume numbers. We will also include analysis of past and predicted future demand scenarios to study the growth, and even the creation, of metroplexes.

The displacement from an optimal approach is a slightly more complicated matter. Here we use the maximum and minimum CDA flight paths for several aircraft types to define a "cone" with thickness as before. We then take two of these cones and overlay them on two separate airports, as depicted in figure 17.

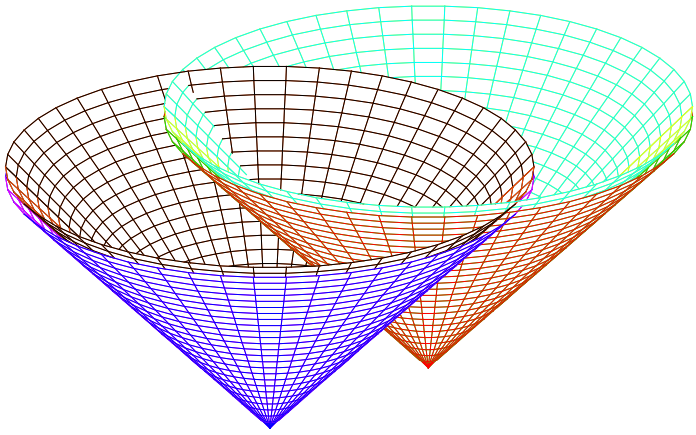

Figure 17: Cone Intersection.

For the sake of discussion, we will refer to these airports as airport$_i$ and airport$_j$. To

calculate the volume of intersection for airport$_i$, we integrate the volume of cone$_i$'s shell that lies within the convex hull of the truncated cone$_j$. This volume represents the space which, if an aircraft was descending through this space into airport$_i$, would require some effort to keep deconflicted from any aircraft arriving into airport$_j$. This effort is not necessarily effort exerted by an air traffic controller, but could be the work required to develop spatially deconflicted STARs, or even the cost in implementing an advanced time based metering system.

To ease computation the cones are truncated at FL300. This truncation was also applied to more closely represent the region of arrivals. While the top of descent for each aircraft will be different, the path should be similar to that of the simulation once the aircraft reaches FL300.

To account for the traffic and the volume interactions, the pairwise metric was used as shown in Equation 2.

$$\text{metric}_{i,j} = \frac{\text{volume}_i \cdot \text{volume}_j \cdot \text{traffic}_i \cdot \text{traffic}_j}{\text{full volume}^2} \tag{2}$$

Where traffic$_i$ is the air traffic numbers for airport$_i$ found using some database and volume$_i$ is the described volume of integration. The full volume term is the entire volume of one of these cones up to FL300. This normalization factor was used to introduce the notion of a fraction of displaced traffic. The fraction of volume$_i$ to the full volume corresponds to the fraction of displaced airspace, and, assuming a uniform density of air traffic around the cone, the product of this fraction with the total air traffic for this airport will give the same metric in a notional form as given in Equation 3.

$$\text{metric}_{i,j} = \text{displaced traffic}_i \cdot \text{displaced traffic}_j \tag{3}$$

Giving a unit of displaced air traffic squared per unit time (where the time is the period over which the data is aggregated for the given database of air traffic numbers). This assumption of uniform traffic density could be relaxed given operational data for the airports in question.

3.4 Quality Threshold Clustering

Once a metric has been defined, a useful exercise is to apply it to a sample problem to determine how well it applies to a real world example. Throughout the derivation of this metric, two goals were in mind: how do we quantify the interactions between airports, and what is a more rigorous definition of a metroplex. Since the quantification problem was addressed in the previous section, we will now focus on metroplex classification.

The problem of grouping data points together based on a distance is well defined and has been thoroughly studied in many fields. This is commonly described as clustering, and there are many clustering algorithms which will group data when given some logic to apply during the clustering process. Some of the most common clustering algorithms (such as

K-Means) require either a fixed or suggested number of clusters to group the points into to be known [32]. These algorithms present several benefits, including computation speed, but for the work here the downsides outweigh the benefits. The first downside is that these algorithms requires a number of clusters to be known a priori. This would correspond to knowing the number of metroplexes before the clustering is applied. Much research has been done to guestimate the proper number of clusters for a given dataset, and using several of these methods to suggest a more rigorous number of metroplexes is being looked into for future work. One issue that we would like to avoid is that most of these methods are stochastic in nature; we would prefer to use a deterministic method that provides the same metroplex clusters when given the same input data. A second, and more restrictive issue, is that because our metric is only defined for pairs of airports, and is not a true distance in the mathematical sense, generating random cluster centers and computing an actual center for each cluster is not feasible. While much work has gone into classifying airports into such metroplexes, one factor that is known is that as air traffic increases, the interaction between such airports will increase. Thus, the possibility of the number of metroplexes increasing in the future is more than a possibility, it is a likelihood. This would restrict the application of the clustering to a single level of traffic volume. The second major downside to such algorithms is that they are stochastic in nature; there is no guarantee that when the clustering algorithm is applied to the same dataset, the same clusters will arise. Since the goal of this clustering is to produce a static grouping of airports for each period in time, we will require a different type of clustering algorithm. We would like to deterministically compare the same airports using the same data source over several yaers.

In 1999, such an algorithm was created. This algorithm is called Quality Threshold (QT) Clustering, and was first applied to the study of genetic material [34]. While this algorithm is more computationally restrictive than K-Means, it provides all of the required features that the K-Means lacks. It provides a deterministic set of clusters with no a priori knowledge of the number of clusters required. The only necessary piece of knowledge to apply QT clustering, is to define a threshold around which to group the data points. While this number is arbitrary and will only provide consistent clusters when the same dataset is used for the traffic volumes, in the future it will allow us to apply the same threshold to a traffic volume dataset over time to study how each metroplex changes with time, and even to study the creation of new metroplexes as the air traffic in a specific region grows.

The QT clustering algorithm is shown in figure 18. Where G is the set of airports to cluster, d is the threshold with which to use when clustering, i is the current center airport, A_i is the temporary cluster centered around airport i, j is the candidate airport to enter cluster A_i, and C is the cluster that has the most airports of all A_i. This algorithm works by generating a candidate cluster for each airport that is currently not already in a cluster. This first airport is defined as the "center" of its cluster. Each of the candidate clusters is

```
1: Procedure QT_Clust(G, d)
2: if |G| ≤ 1 then
3:    return G
4: else
5:    for all i ∈ G do
6:       flag = TRUE
7:       A_i = i        /* A_i is the cluster started by i */
8:       while (flag = TRUE) and (A_i ≠ G) do
9:          find j ∈ (G − A_i) s.t. diameter(A_i ∪ {j}) is minimum
10:         if diameter(A_i ∪ {j}) > d then
11:            flag = FALSE
12:         else
13:            A_i = A_i ∪ {j}    /* Add j to cluster A_i */
14:         end if
15:      end while
16:   end for
17:   identify set C ∈ {A_1, A_2, ..., A_|G|} with maximum cardinality
18:   return C
19:   call QT_Clust(G − C, d)
20: end if
```

Figure 18: Quality Threshold Clustering [34].

created by placing every airport whose metric (calculated with the "center" airport as the second airport) falls below the threshold. The largest of these candidate clusters is chosen as the next cluster. All of the airports in this cluster are defined as being in a cluster and the calculation recurses until there are no airports that have not been assigned to a cluster.

Due to the nature of our metric increasing as interaction grows, it does not directly map to a distance. Instead, we will slightly modify the existing QT Clustering algorithm to account for this difference and allow our notion of increasing interaction to map to the increasing metric. This change is made by redefining the *diameter* to be defined as the area where the metric is above our threshold rather than the area where the distance is below the threshold. Alternatively, we could invert our metric. This would make it function more as distance, allowing a more natural definition of diameter, but would reduce the idea of using the metric as a measure of airspace complexity. As the interaction increased, our inverted metric would decrease. While both options are viable, we chose the former over the latter to keep the direct mapping between airspace interaction and our metric.

3.5 Results

3.5.1 Annual Traffic Volume Selection

Annual traffic volume at an airport contains flight operations to and from the airport of interest for an entire year. Airport operations can be categorized into two categories: itinerant operations and local operations. Depending on the purpose of the operations, each

category is further divided into user classes, such as air carrier operations, air taxi operations, general aviation operations, and military operations. An itinerant airport operation indicated a flight has either a departure or an arrival operation at the airport of interest while a local airport operation indicates that both ends (departure and arrival) of a flight are at the airport of interest. For our analysis, itinerant air carrier operation, itinerant air taxi operations, and itinerant general aviation operations are included; military operations and all local operations are excluded.

The benefit of using annual traffic volume for cluster analysis is that the annual data does not have day-of-week and seasonality issues. Instead, it provides a traffic volume baseline for our analysis.

The FAA's TAF data, published in January 2009, is used as our data source for determining annual traffic volume. The TAF data records historical traffic data from 1990 to 2007 and projects future traffic data from 2008 to 2025. By selecting calibrating the quality threshold using current traffic volumes and applying the same threshold to past and projected future traffic levels, we can identify the evolution of metroplex composition using the proposed cluster analysis.

3.5.2 Quality Threshold Selection

The metric and clustering calculation was implemented in Fortran and distributed over a compute cluster. The first result we need to explore is that of the threshold. The quality threshold that should be chosen to return a set of clusters that will closely represent our current understanding of metroplexes is a subjective choice. A study showing the relationship between threshold and number of total clusters can be seen in figure 19. This relationship is not monotonic due to the fact that as the threshold changes, the "center" airport for each cluster could change, thus allowing for more or less airports to be included in each cluster. If fewer airports are included, this opens the possibility of increasing the total number of metroplexes.

With this result, we can calibrate our threshold to determine the total number of clusters. To do this tuning, we will use the FAA's Metropolitan Area set of 15 regions. These regions account for 58 percent of all passenger traffic and 15 percent of aircraft based in the U.S. It is also expected that over the next 20 years that these regions will experience significant growth [17]. With this, we determine that a reasonable number of clusters is 15, giving an average threshold of 23×10^{24}. These metroplexes can be depicted graphically overlaid on a map as shown in figure 22(b). The relative size of the points depict the relative total metric for each metroplex. As mentioned before, the value of this threshold is the only subjective part once the metric has been defined. Several other methods for calibrating the threshold are possible, such as the Gap statistic [59], or many of the other statistical methods used for estimating the number of clusters in a dataset.

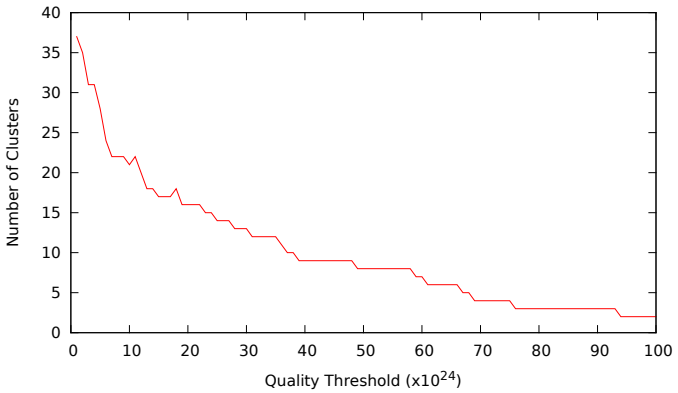

Figure 19: Number of clusters vs. Cluster threshold (2008 TAF data).

A chart of each metroplex sorted by the sum of the metric over the whole cluster is shown in figure 21(b). It can be seen that the Los Angeles metroplex has the most net interaction, with the New York area and Chicago metroplexes in second and third most net interaction. The breakdown of the LA metroplex can be found in figure 20(a), the New York area metroplex in figure 20(b), Chicago metroplex in figure 20(c), and Atlanta metroplex in figure 20(d). The center airport is the airport with 0 metric value on the far right. While the members of these clusters should come as no surprise, one interesting result is that the "center" of the New York metroplex is actually PHL.

These metroplex clusters can be compared against the metropolitain areas as identified by the FAA's OEP initiative as shown in Table 7 [17, 25].

3.5.3 Trending Over Time

Once the metric has been chosen for current day operations, we can use the same value to determine how metroplexes change over time. Table 8 shows the total number of metroplexes for each year studied using the 15 metroplex calibration for 2008. As expected, the number of metroplexes is proportional to the total traffic for the years. Figure 21 depicts the center airport for each metroplex over the years, as well as the total metric for each cluster. These figures tell an interesting story. While the LAX metroplex was almost twice as strong as the New York metroplex in 1990, the New York metroplex grows dramatically by 2008 and is even projected to become stronger than the LAX metroplex in 2014. Figure 22 shows the location of each metroplex and their relative strength.

3.6 Conclusion

We have developed a framework for metroplex identification and a rough ranking system based on our chosen metric. These computational results match our expected metroplex

Metropolitan Area	Airport Code	Airport Name
Atlanta	ATL	Hartsfield-Jackson Atlanta International
Charlotte	CLT	Charlotte Douglas International
Chicago	GYY	Gary Chicago International
	MDW	Midway International
	MKE	General Mitchell International
	ORD	OHare International
	RFD	Chicago Rockford International
Houston	HOU	William P. Hobby
	IAH	George Bush Intercontinental
Los Angeles	BUR	Bob Hope
	LGB	Long Beach-Daugherty Field
	LAX	Los Angeles International
	ONT	Ontario International
	PSP	Palm Springs International
	SNA	John Wayne-Orange County
Las Vegas	LAS	McCarren International
Minneapolis-St. Paul	MSP	Minneapolis-St. Paul International
New York	EWR	Newark Liberty International
	ISP	Long Island MacArthur International
	JFK	John F. Kennedy International
	LGA	LaGuardia
Philadelphia	PHL	Philadelphia International
Phoenix	PHX	Phoenix Sky Harbor International
San Diego	SAN	San Diego International
San Francisco	OAK	Metropolitan Oakland International
	SFO	an Francisco International
	SJC	ineta San Jos International
Seattle	SEA	Seattle-Tacoma International
South Florida	FLL	Fort Lauderdale-Hollywood International
	MIA	Miami International
	PBI	Palm Beach International
Washington-Baltimore	BWI	Baltimore/Washington International Thurgood Marshall
	DCA	Ronald Reagan Washington National
	IAD	Washington Dulles International

Table 7: OEP 15 Metropolitan Areas

Table 8: Number of metroplexes over time

Year:	1990	2008	2014	2018	2020	2025
Number of Metroplexes:	13	15	15	16	16	18
Percent of 2008 Traffic:	93	100	103	108	111	119

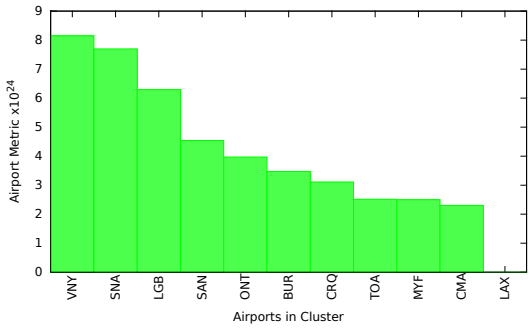

(a) LA

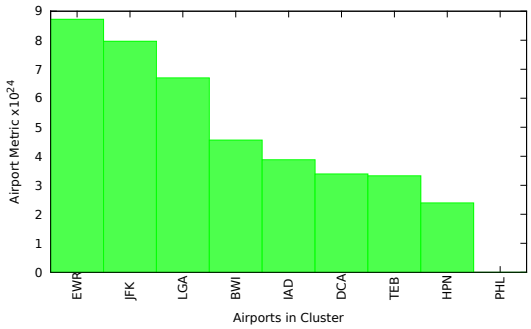

(b) New York

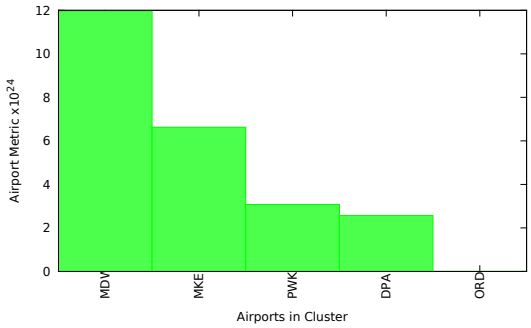

(c) Chicago

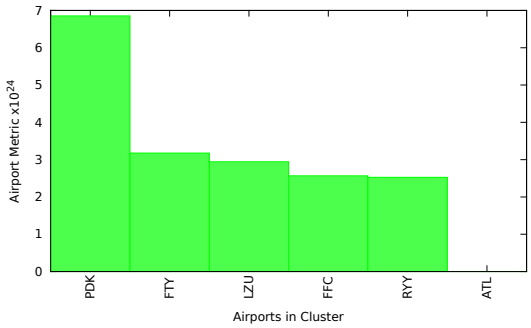

(d) Atlanta

Figure 20: Airports in top 4 metroplexes (2008)

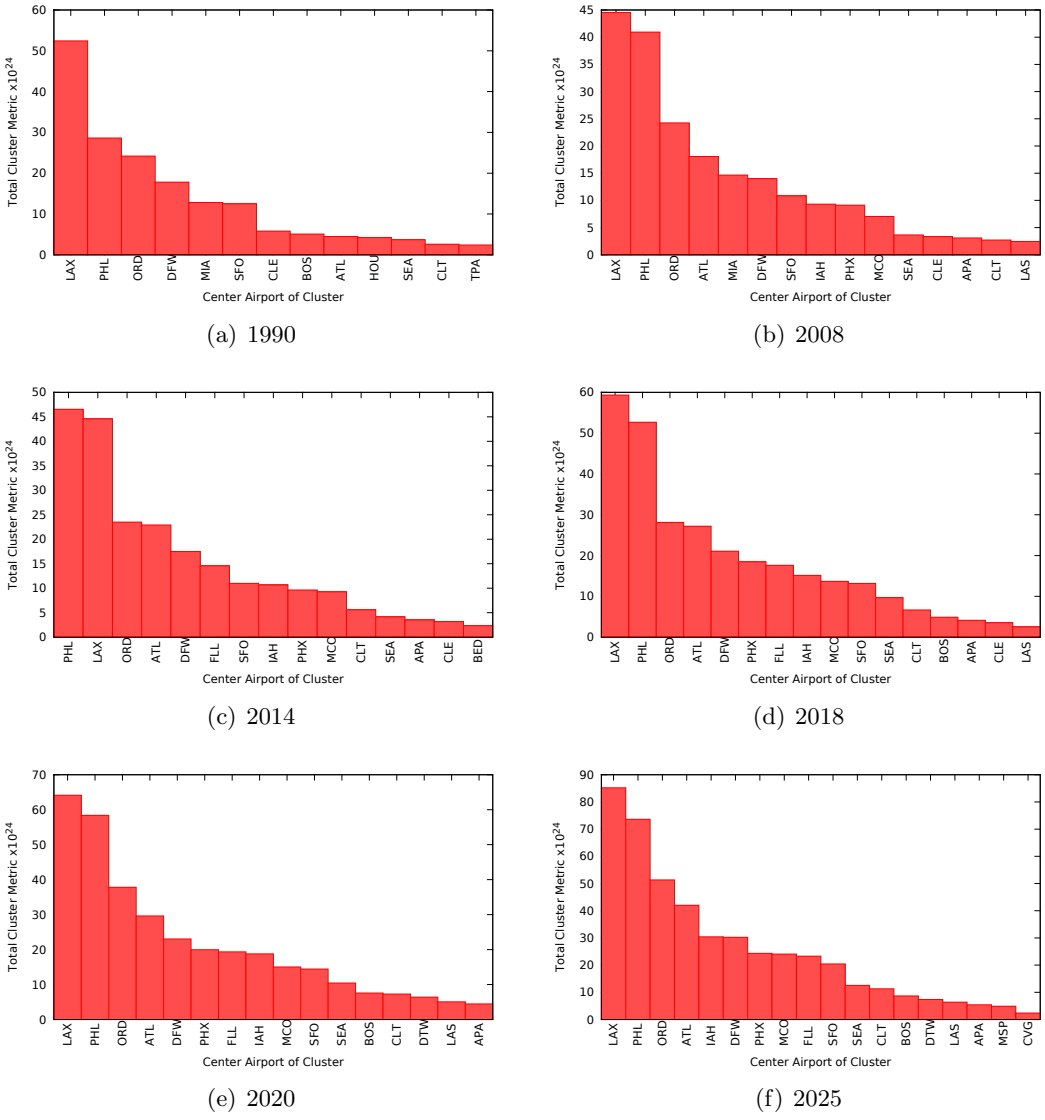

(a) 1990 (b) 2008

(c) 2014 (d) 2018

(e) 2020 (f) 2025

Figure 21: Sorted metroplexes for several years.

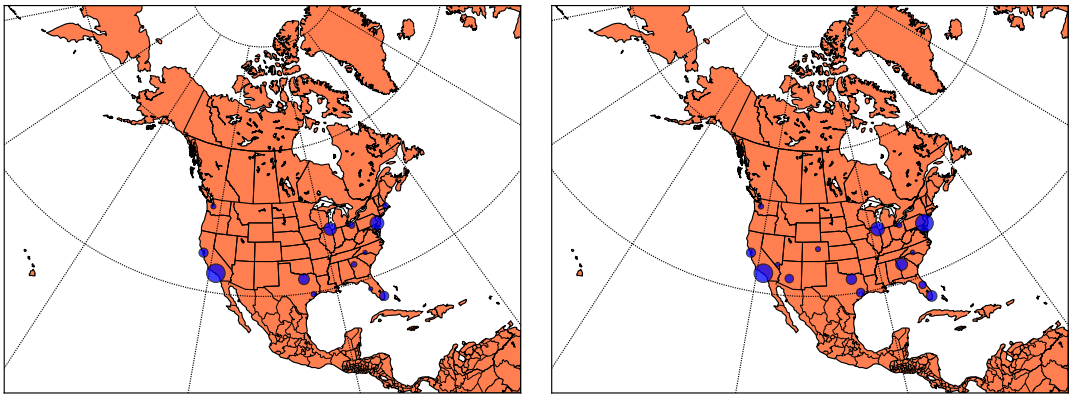

(a) 1990

(b) 2008

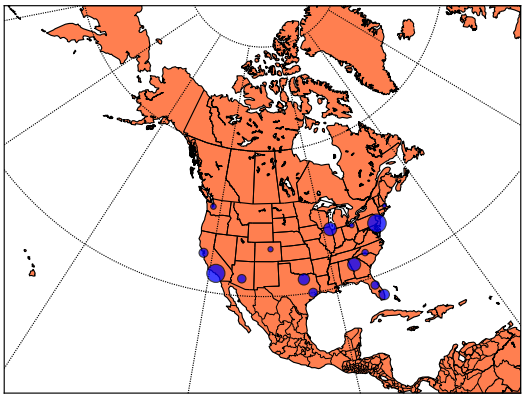

(c) 2014

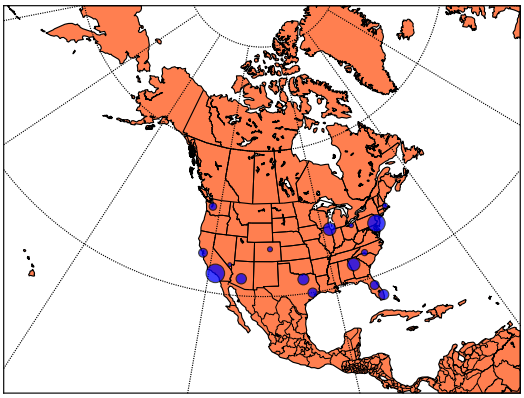

(d) 2018

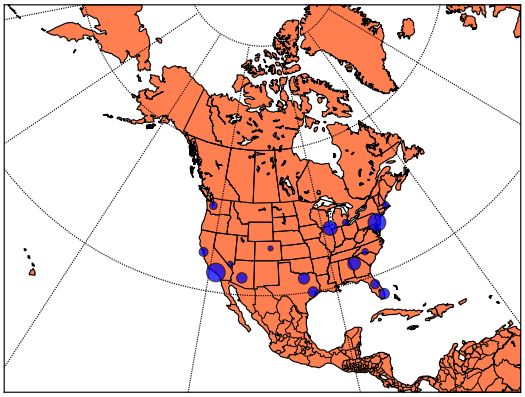

(e) 2020

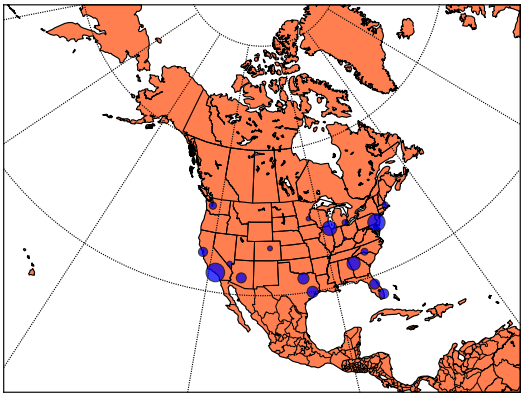

(f) 2025

Figure 22: Geographic location of clusters.

clusters, and these results could be improved with a more thoroughly tuned threshold.

The main focus for future work is to determine a more defensible threshold for the QT Clustering. Exploring different datasets, as well as a more thorough literature review would strengthen a choice of threshold. A good method would be to use the Gap statistic [59], as well as the other metrics presented (Clinski & Harabasz, Krzanowski & Lai, Hartigan, and Silhouette).

Finally, several of the assumptions could be relaxed to provide an optimal approach with restrictions. These restrictions could include things like removing special use airspace, military airspace, or other restricted airspace. Another possible restriction to relax is that of uniform distribution of air traffic. This could be incorporated using air traffic data for the airports and producing a density map that can be used to weight the metric. While there are many benefits, removing these assumptions greatly increase the required knowledge of each airport, which would greatly reduce the practicality of studying the entire NAS as a whole as was done here.

CHAPTER IV

METROPLEX EVALUATION

4.1 Introduction

This chapter builds the tools for studying several classes of generic airspace configurations to determine the qualities that a good airspace configuration would have. Two major factors can contribute to the reduced delay in metroplex operations: properly scheduling arrivals, and minimizing shared resources between airports in the metroplex. While four such configurations were developed, only two of them will be closely examined here. Queuing models will be generated and studied here. The use of queueing models for air transportation problems is fairly common [35, 39, 12, 36, 40] and is used by many commercial tools to study airspace capacity and throughput. Queueing models can also be used to estimate newer trajectory-based operations [45].

The four geometries can be seen in Figure 23. Each of these geometries has a series of entry fixes (marked in red) and departure fixes (marked in blue). There are two airports, airport A and B, and each entry fix has a defined procedure going to either one airport or the other or a procedure for each airport. The two geometries we are going to compare are geometry 1 and geometry 3. These two geometries are similar but differ by having two parallel entry fixes in geometry 3 compared to sharing an entry fix between airport A and airport B. This paper will discus and try to quantify the advantages of limiting the amount of shared resources in a metroplex environment.

Geometry 1 is characterized by four entry fixes at 45, 135, 225, and 315 degree headings. Every entry fix has an arrival procedure for each airport in the metroplex. This shared entry fix configuration closely resembles the old Atlanta airspace configuration. Geometry 3 has eight entry fixes at 40, 50, 130, 140, 220, 230, 310, and 320 degree headings. Half of these fixes have a procedure going to airport A while the other half has procedures to airport B. This allows for each airport to act almost independently of the other. The current ATL airspace configuration closely resembles this geometry. All entry fixes are located on a 40 NM ring from the center of the metroplex. Airport A is located 10 NM north of the center of the metroplex and airport B is located 10 NM south of the center giving a distance of 20 NM between the two airports. This second airport is supposed to approximate PDK.

4.2 Generic Metroplex Configurations

To evaluate algorithms and other hypotheses, several generic metroplex configurations were developed by Dr. Liling Ren, Carolyn Cross, and Anwesha as part of several NASA funded

research projects. These minimal configurations were chosen to demonstrate simple two interdependent airport configurations with varying levels of interaction. The basic configurations consist of combinations of various airport locations and arrival fix distributions. A simple metroplex geometry was used to evaluate several metroplex constraint issues. This geometry consisted of a traditional four corner post configuration that shared the fixes between two airports. This configuration can be seen in Figure 23

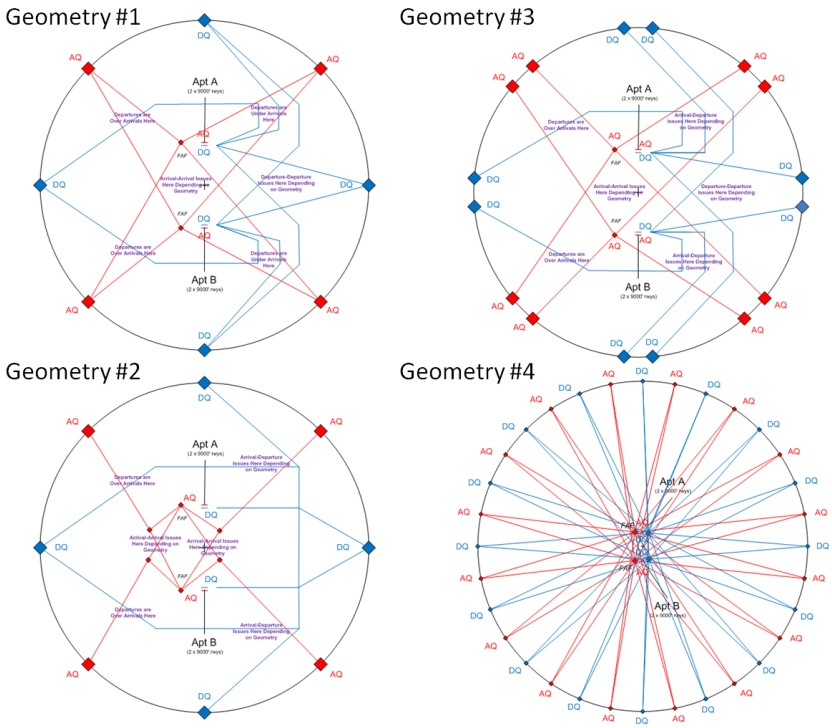

Figure 23: Generic Metroplex Geometry

4.3 Metroplex Demand Scenarios

To accurately compare the two different geometries, the same scheduled demand must be used for both configurations. Metroplex demand generation is the process for creating a traffic demand set (set of scheduled arrivals and departures) for Generic Metroplex airports to support simulation-based evaluation of hypo- thetical terminal airspace configurations. Demand generation process inputs comprise a current-day traffic demand set, a user-specified NAS airport after which to model traffic demand to a particular metroplex airport, and an hourly capacity value and target 24-hour demand-to-16 hour capacity ratio for the airport. The demand generation process comprises the following computational steps:

- The traffic demand set is processed using AvDemand to grow the traffic to a specified volume and to estimate gate arrival times for each flight.

- Those flights to/from the specified NAS airport are captured.
- A portion of the flights of interest are removed to achieve the specified demand-to-capacity ratio as per the specified generic airport hourly capacity.
- The remaining flights–i.e., the arrival flights to and departure flights from the generic airport–are assigned to a peripheral source/sink airport at a specified radius beyond the terminal airspace.
- Each metroplex airport arrival and departure flight is assigned to an arrival or departure fix on the hypothetical terminal airspace boundary with the en-route airspace.
- Update each flights terminal and en-route transit times to reflect the airspace geometry.
- Once transit times are computed, assigns distinct, randomly generated gate departure times to all the generic airport flights in order to eliminate coincident scheduled takeoffs.

Finally, the generated schedule of generic airport arrivals and departures is written to a simulation input file of the appropriate format. The following input parameters are used to generate traffic demand sets for airports A and B in the Generic Metroplex assessments. The seed traffic data set is an Enhanced Traffic Management System (ETMS) derived record of (Instrument Flight Rule) IFR flights for September 26, 2006.

The seed traffic data set was "grown" using AvDemand to 3 times the total traffic volume in accordance with 2008 TAF forecasts. From the grown traffic demand set, ATL traffic is used to create traffic demand sets for both Generic Metroplex airports A and B. Arrival and departure traffic volumes for Generic Metroplex airports A and B are in accordance with each airports capacity of 60 arrivals/hour and 60 departures/hour (each airport has two operationally independent parallel runways) and their respective demand/capacity ratios: 0.7 for airport A and 0.35 for airport B. Figure 24 depicts the generated traffic demand profile with total capacity for Generic Metroplex airports A and B.

The metroplex demand generation process is effective in preserving the directional distribution of sched- uled traffic to the specified reference NAS airport. The directional traffic distribution determines the relative loading of the metroplex arrival and departure fixes, in turn impacting controller workload and possibly re- quiring airspace configurations and traffic management strategies to accommodate it. Figure 25 depicts the directional distributions of of Generic Metroplex airport A and B from the metroplex demand generation process. The heavy ATL scheduled demands in the 45-60 degree and 15-165 degree ranges are preserved in the Generic Metroplex demand set.

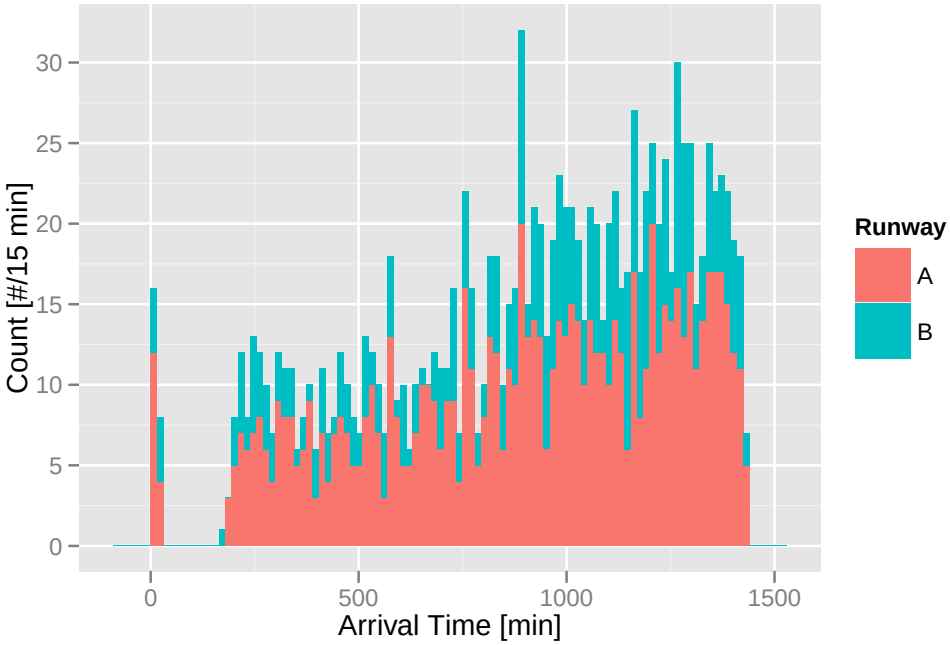

Figure 24: Arrival distribution as a function of time.

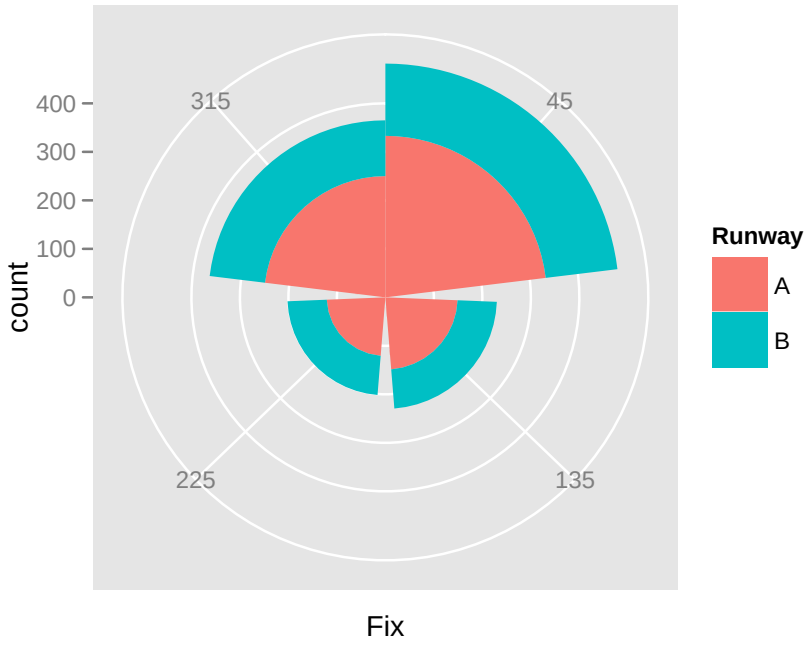

Figure 25: Arrival distribution as a function of fix.

4.4 Linked-List Metroplex Simulation Framework

To thoroughly evaluate the impact of future metroplex concepts, and identify the most promising concepts, a linked node queueing process based simulation was created to determine the delay of arrival operations. In this simulation study, the intention was to vary each parameter to span the range of all the NextGen capabilities as well as technologies that have been conceptualized by the GaTech Team. Details of the linked node queueing process model and the associated assumptions are presented in the next subsection. The parameters tested and their ranges of variation, the test conditions, and specific test cases are described in Sections 4.2 and 4.3. Results from each test case are presented as a separation subsequent subsection.

4.4.1 Linked Node Queueing Process Model

Due to limited time available for this project, only arrival operations were studies. As illustrated in Figure 26, two types of shared resources are model in the linked nodes queueing process: entry fixes and runways at metroplex airports. Theoretically, points where traffic flows merge or cross (at the same altitude) could also be modeled but are omitted for the sake of simplicity. The model is reconfigurable to have any number of entry fixes and any number of runways. Each entry fix is modeled as a single server FIFO queue with infinite capacity. The service time is a random variable corresponding to minimum required separation at the arrival fix (i.e. 5 NM), due to the random fix crossing speed. If an aircraft arrives at the entry fix when the queue is empty and no aircraft is being served (meaning the spacing from the previous aircraft is greater than the minimum required separation), it will be released to enter the metroplex terminal area immediately, thus no queueing delay will be incurred. When another aircraft is being served, regardless of queue length, the aircraft will have to wait until the serve is free. The waiting time in the entry fix queueing is referred to as the entry delay.

Each runway at a metroplex airport is also modeled as a single server FIFO queue with infinite capacity. Note that the runway queue capacity is physically limited due to the limited volume of airspace within the terminal area. When runway queue is full, holding may be implemented at the entry fixes. Assuming an infinite runway queue capacity simplifies the coding of the simulation; it also allows schematic trend analysis as the arrival rate approaches very large values. The service time is a random variable corresponding to minimum required separations at the runway threshold (i.e. wake vortex separation as a function of aircraft weight class) and the random final approach speed. Similar to entry fixes, queueing delays may incur at the runway threshold. This delay is referred to as the runway delay. In the real world, the this delay may be incurred any where between the entry fix and the runway through path stretching or speed adjustment. Based on the temporal-spatial displacement concept, the delay is assumed to incur at the runway threshold without losing

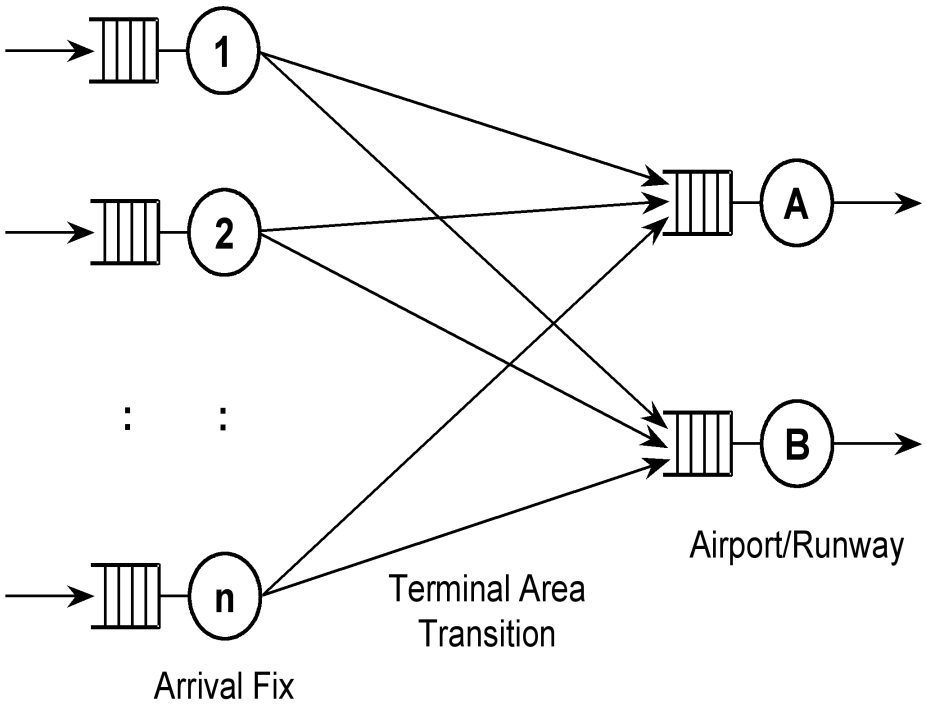

Figure 26: The linked node queuing process model

generality. Potential ground infrastructure limitations are ignored in the model assuming that no other runway delays will incur except the queueing delays due to the required wake vortex separation.

Inputs to the linked node queueing process model are aircraft arriving at entry fixes and destined to predefined runways. For each aircraft, the aircraft type is specified. The arrival aircraft sequence at an entry fix can either be specified by an arrival rate with a specified inter-arrival time distribution, or by a sequence of arrivals (normally one day worth of traffic) with the fix arrival time for each aircraft specified.

The links between the entry fix nodes and the runway thresholds are reconfigurable, ranging from each entry fix linked to a specific runway (fully segregated traffic flows) to every entry fix linked to every runway (fully shared entry fixes, e.g. Generic Metroplex Geometry 1). The link between an entry fix and a runway threshold is a terminal area arrival transition assuming CDA type vertical profile and speed profile, overlaid on the lateral path given in the Generic Metroplex airspace design. A large pool of CDA trajectories were simulated for different aircraft types using TASAT [50] with uncertainty factors such as random aircraft weight, short-terms wind variations, and random pilot action delays. For a specific aircraft, a trajectory is randomly sampled from the pool. As such, the transition time from an entry fix to a runway threshold is a random variable. The arrival time at the runway queue is thus a random variable determined by the release time at the entry fix and the random

terminal area arrival transition time.

The linked node queueing process model is implemented as a discrete-event simulation in SimPy – an object-oriented, process-based discrete-event simulation language based on standard Python [44]. The output of the simulation is a log of events associated with each aircraft including: aircraft identification, entry fix, entry delay, entry fix crossing time, runway, runway delay, and runway threshold crossing time. The system performance can then be measured by entry delay, runway delay, and total delay at per aircraft bases or as cumulative system wide total.

4.5 Simulation Results

4.5.1 Impact of Arrival Scheduling

For the given demand generated for the Generic Metroplex model, simulation was first done without applying any scheduling algorithm to the arrival traffic and then with a simple FCFS scheduling algorithm applied to precondition the schedules. To compare system performance of each airspace geometry design, the cumulative delay is plotted against cumulative aircraft count for the entire day of traffic as shown in Figure 27, Figure 28, Figure 29, and Figure 30. In these plots, the instantaneous slope at each point indicates the throughput per unit delay; the shallower the slope, the better the system performance. The overall position of the curve indicates system performance over time; the lower the curve, the better the performance. As shown in the figure, both entry delays and runway delays were significantly reduced by arrival scheduling. In terms of cumulative total delay, a 75% reduction was achieved. Similar delay reductions results were observed for both Geometry 1 and Geometry 3.

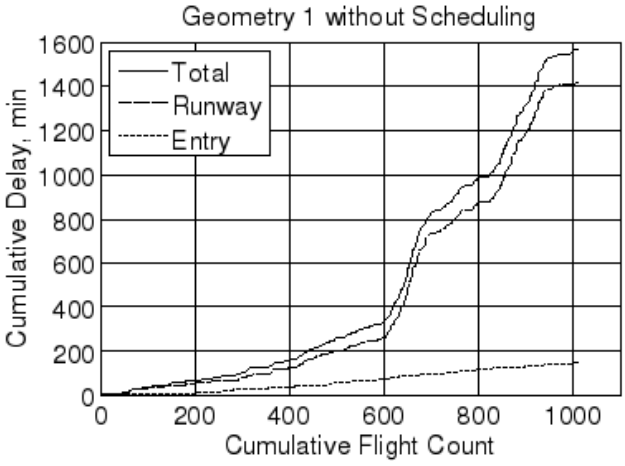

Figure 27: Geometry 1, Unconditioned

Another interesting observation from these Figures is that, without preconditioning the schedule the cumulative entry delay was slightly lower for Geometry 3 than Geometry 1,

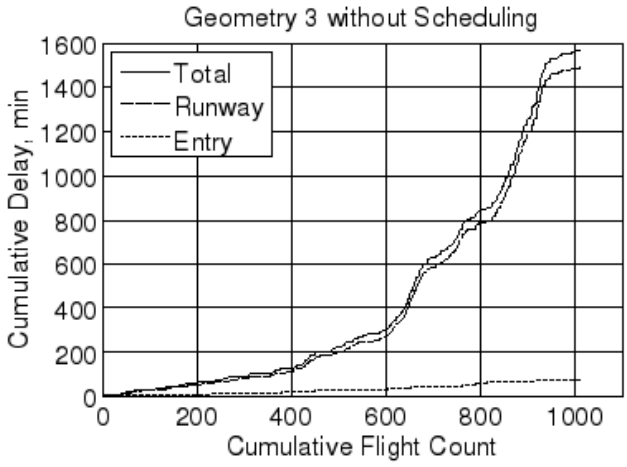

Figure 28: Geometry 3, Unconditioned

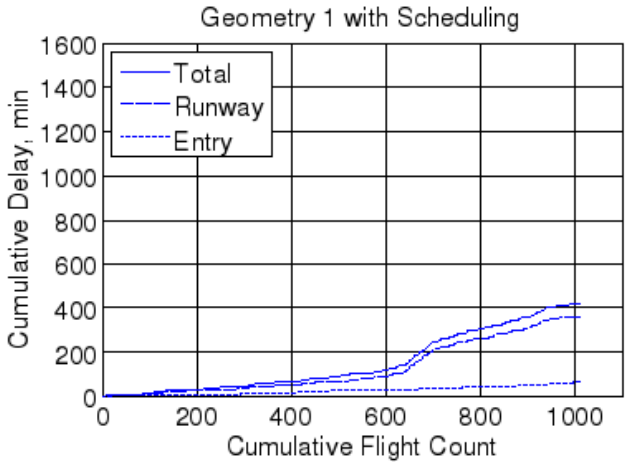

Figure 29: Geometry 1, Conditioned

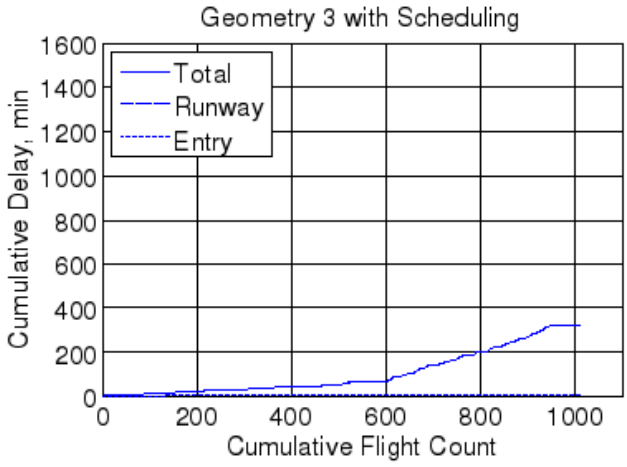

Figure 30: Geometry 3, Conditioned

apparently due to the increased number of entry fixes available. However, the cumulative runway delay was slightly higher for Geometry 3 than Geometry 1. Because traffic flows at entry fixes were less constrained in Geometry 3, the runway thus had to absorb more delays than the runway in Geometry 1. The cumulative total delay, however, remained roughly the same. With scheduling, the cumulative total delay was much lower for Geometry 3 than Geometry 1, indicating improvements bring in by the combination of temporal control and spatial control.

It is also seen in that, regardless of Generic Metroplex geometry and scheduling, the cumulative runway delay was always much higher than the cumulative entry delay. In the initial Generic Metroplex design, there were only two airports each had only one arrival runway. The demand capacity ratio of 0.7 at Airport A was actually relatively high, close to the demand capacity ratio of ATL[48]. This setup determined that runways were choke points in the system and consequently the majority of delays were incurred at runways. The high delay reductions from arrival scheduling reflect the necessity of scheduling for managing critical shared resources. In addition to segregating traffic flows from and to different airports, the increased number of entry fixes increases the total entry fix capacity. As the number of airports increases, the capacity at entry fixes may become more critical, and consequently entry delay will increase. The benefits of airspace geometries with more entry fixes, such as Geometry 3, would be higher.

The comparison of total delay per aircraft between Geometry 1 and Geometry 3 with and without scheduling is shown in Figure 31. As can be seen, without scheduling, on average, a total delay of 1.55 min per aircraft was incurred in both Geometry 1 and Geometry 3. With scheduling, the average total delay per aircraft was reduced to 0.42 min in Geometry 1 and 0.32 min in Geometry 3, corresponding to reductions of 73% and 79% respectively. While without scheduling the average total delay per aircraft was roughly the same in both Geometries, with scheduling, the delay was 23% lower in Geometry 3 than Geometry 1.

The comparison of total delay per aircraft between Airport A and Airport B with and without scheduling is shown in Figure 32. As can be seen, without scheduling, on average, a total delay of 2.16 min per aircraft was incurred for flights destined to Airport A, in both Geometry 1 and Geometry 3. The average total delay per aircraft was 0.34 min for flights destined to Airport B, in both Geometry 1 and Geometry 3. The difference between Airport A and Airport B was mostly due to the difference in traffic demand at these two airports. While the traffic volume at Airport B was about 50% of Airport A, the average total delay per aircraft was 84% lower at Airport B. This nonlinear relationship is typical of queueing systems. This observation suggests that, when airport runways are chock points, moving some operations from busy airports to less busy secondary airport may reduce metroplex system wide delays, because when demand is approaching capacity at busy airports, queueing delays tend to diverge.

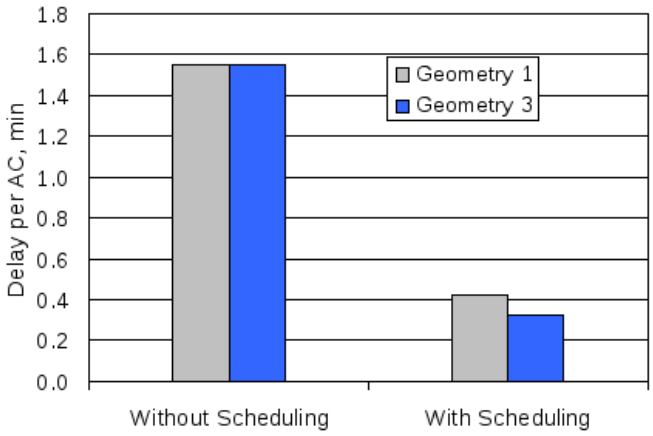

Figure 31: Comparison of total delay per aircraft between geometries, with and without schedule preconditioning

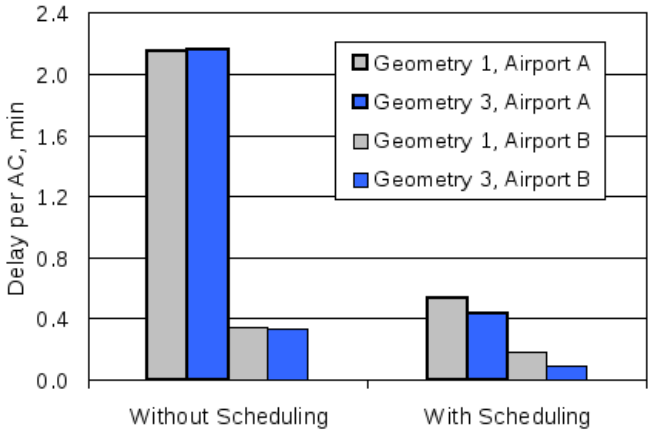

Figure 32: Comparison of total delay per aircraft between geometries, with and without scheduling

4.6 Impact of Temporal Control Accuracy

Figures 33-36 shows cumulative delay versus cumulative aircraft count for the entire day of traffic under three metering accuracy values: $\sigma = 0$ sec, $\sigma = 24$ sec, and $\sigma = 54$ sec. Arrivals without scheduling are shown for Geometry 1 and Geometry 3 in Figure 33 and Figure 34, and with a preconditioned schedule in Figure 35 and Figure 36. It is seen in these figures that in all cases, there was a trend of increase in delays as the metering accuracy decreases (larger σ values). However, in the cases of arrivals with scheduling, the trend was more consistent throughout the day. With scheduling, flights were planned to cross entry fixes at target times to reduce potential conflicts. Lower metering accuracy means less target time compliance, thus negate some of the scheduling benefits. By comparing results without scheduling on the left and results with scheduling on the right, it is seen that even for values comparable or larger than current operational performance, the majority of the scheduling benefits could still be retained.

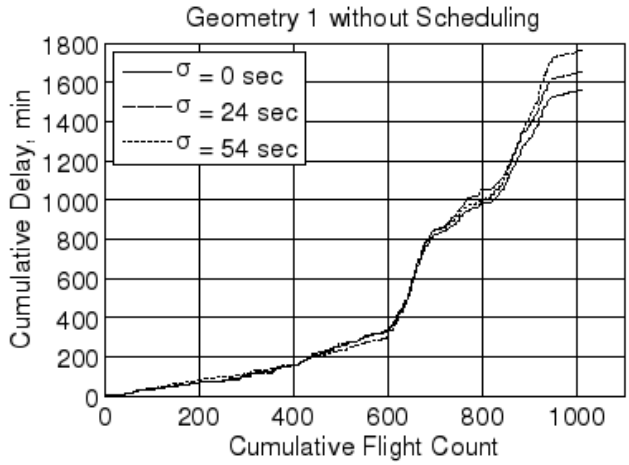

Figure 33: Geometry 1, Unconditioned at various metering accuracy values

4.7 Conclusions

With the developed linked node queueing process model, three simulation studies were conducted: sensi- tivity analysis of delay vs. arrival rate, the impact of arrival scheduling, and the impact of temporal control accuracy. For arrivals, the entry fixes at the boundary of the metroplex terminal area and the runways at metroplex airports are two sets of flow check points.

The arrival rate sensitivity analysis revealed that when runways are the chock points (capacity limits), increasing the number of entry fixes to segregate traffic to different airports would not necessarily help reducing delays. In this case, the entry fixes serve as regulators to limit the number of flights to runway queues thus limit terminal area delays. Without

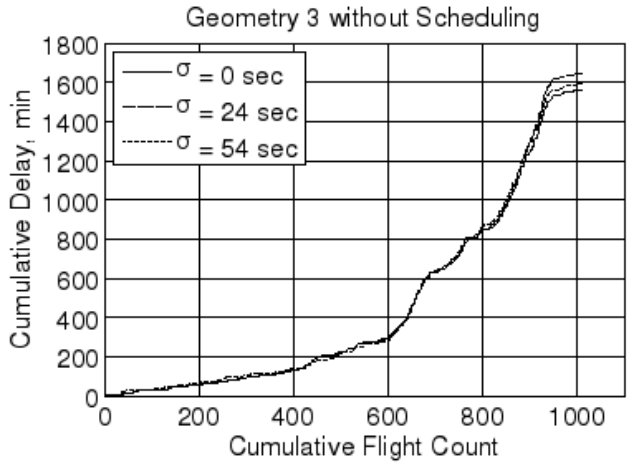

Figure 34: Geometry 3, Unconditioned at various metering accuracy values

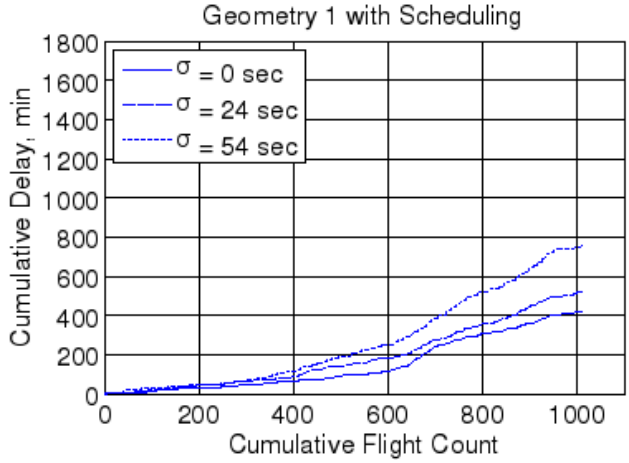

Figure 35: Geometry 1, Conditioned at various metering accuracy values

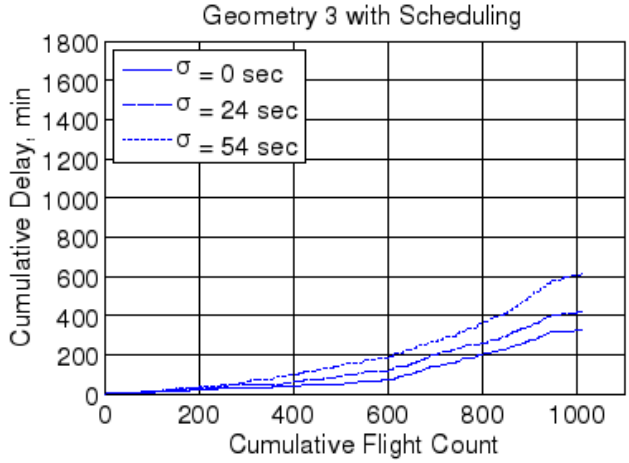

Figure 36: Geometry 3, Conditioned at various metering accuracy values

arrival scheduling, at high traffic volumes, the average delay per aircraft remained roughly the same for the Generic Metroplex Geometry 1 (4 shared entry fixes), Geometry 3 (8 fixes, segregated routes). Actually, delays incurred within terminal area tended to be higher as the number of entry fixes increased, thus would have higher fuel burn costs. It is expected that to realize the benefits of more direct routing and decoupled traffic flows from increased number of entry fixes, some mechanism to regulate arrival traffic should in be in place. It is also expected that for metroplexes with multiple large hub airports, entry fixes may become major choke points, and consequently, increased number of entry fixes would improve system wide throughput.

The simulation revealed that arrival scheduling greatly reduced both entry delays and runway delays were significantly reduced by arrival scheduling. Under the given simulation conditions, total delays for the entire day were reduced by roughly 75%. Although delays were similar for Geometry 1 and Geometry 3 when no scheduling was applied, with scheduling, the decoupling of traffic flows in Geometry 3 provided additional delay reductions. The simulation also revealed that the delay reductions brought in by scheduling were most significant at busy airports. On average, delay per aircraft was reduced by roughly 1.5 min from over 2 min to the order of 0.5 min for Airport A, the busy airport in the Generic Metroplex.

The temporal control accuracy, or metering accuracy, had an impact on delays regardless if scheduling was applied or not. The impact is more evident when scheduling was applied. Because the lower metering accuracy reduced the compliance to target fix-crossing times, some delay reduction benefits would be negated. However, even with the worse possible metering accuracy, two thirds of the delay reductions from the perfect metering still could be retained. This suggests that even without the temporal control accuracy that is expected for future 4DT operations, scheduling would still bring in revolutionary delay reductions.

CHAPTER V

METROPLEX OPTIMIZATION

5.1 Introduction

The consensus amongst government, industry, and academic stakeholders is that there will be a significant increase in air traffic demand within the National Airspace System (NAS) by the time the Next Generation Air Transportation System (NextGen) is operational [27, 11]. Much of the projected demand growth will be in the form of traffic to and from major metropolitan areas, as history has shown that they are the nucleus for both population and economic growth. Thus, even if additional airports are built to accommodate the increased traffic, the airspace above major metropolitan areas will be far more crowded than they are today, and the interactions between traffic flows will be more frequent and more consequential.

To successfully schedule this growing demand more efficient algorithms are required to optimally solve such a complicated problem. This scheduling optimization program is a mixed integer program, which is in general a NP hard problem. While the advantages of using such formal optimization methods in solving airline scheduling problems has been done before [1], due to the computational complexity these solution methods have only been tested in small problems. In this paper we will demonstrate the advantages of a Benders' decomposition scheme to solve these problems in high density traffic for an entire day's worth of traffic under reasonable solution times.

5.2 Mixed Integer Program for Scheduling Metroplex Arrivals

Application of a scheduling algorithm that does not fully account for the interactions between traffic flows can result in a rapid buildup of delay that gets pushed back into the en route airspace. Thus, if a scheduling algorithm is to be used in dense operations, we must first make sure that any savings in time or fuel that are gained within the metroplex are not negated by the added cost of the delay that is pushed back into the NAS as a whole (by way of en route delays).

5.2.1 Objective

The multiplexer algorithm is formulated as a mixed integer linear program for the scheduling of aircraft arrivals and departures. This schedule format is in terms of arrival and departure fix crossing times which allows for future changes in the objective to be minimized (fuel burn, etc.) with minimal changes to the scheduling program.

The current primary objective of the set of programs that have been developed is to minimize the change between the estimated times of arrival and departures with the computed times within the metroplex. The arrival changes are between the reported ETA to an arrival fix and the computed arrival time at the fix while the departure changes are changes to the estimated time to the departure fix and the computed time to the fix. This objective can be written as Equation 4 and rewritten as Equation 5 since the sum of ETAs will be constant.

$$\min \sum_{i \in \text{Flights}} \text{sta}_i - \text{eta}_i + \text{d}_i \tag{4}$$

$$\min \sum_{i \in \text{Flights}} \text{sta}_i + \text{d}_i \tag{5}$$

Where eta_i is the estimated time arrival (program input) for the i^{th}, sta_i is the scheduled time of arrival (program output) and d_i is the delay each aircraft would be required to accumulate inside the TRACON.

The goal for this set of optimization programs is to minimize the difference in the expected estimated time of each aircraft and the scheduled time producing an RTA such that the delays inside the metroplex could be reduced while not drastically increasing the delay absorbed en route.

5.2.2 Problem Formulation

The solution to the scheduling problem that minimizes the objective given in Equation 4 must meet several constraints to be a feasible schedule.

5.2.2.1 Required Minimum Separation Criteria

We assumed that the minimum required separation at the TRACON boundary fix (arrival fix) would be five nautical miles. Assumptions about the aircraft ground speeds while crossing the TRACON boundary fix are necessary for converting this distance-based separation criterion into a time separation for use in the Time-based scheduling algorithms. Our assumptions for arrival- fix crossing ground speeds are shown in Table 9. As shown in the table, when converting the distance-based separation criterion into a time separation, the minimum arrival-fix crossing speed between leading and trailing aircraft was used for the conversion. The resulting time separations for the different aircraft pairs are shown in Table 10.

The runway minimum required separation criteria were assumed to be dependent on the weight classes of the leading and trailing aircraft, as shown in Table11. The runway landing speed assumptions are shown in Table 12. These values were used to convert the

		Leader		
		H	L	S
Trailer	H	290	265	205
	L	265	265	205
	S	205	205	205

Table 9: Arrival-fix Crossing Speeds in Knots

		Leader		
		H	L	S
Trailer	H	62.1	67.9	87.8
	L	67.9	67.9	87.8
	S	87.8	87.8	87.8

Table 10: Arrival-fix Required Crossing Time Separation in Seconds

distance-separations into time separations. The resulting time separation criteria are shown in Table 13.

Since the separation requirements shown in Table 13 are not symmetrical. This implies that the arrival sequence will determine the total time the runway resource is used, thus the requirement that swapping be considered in the problem. This fact forces the problem from being a relatively simple problem to one that is NP-hard. By taking advantage of these asymmetric separation requirements, mathematical models for arrival scheduling can generate efficient schedules, which will lead to lead to increased capacity and reduced delay for the aircraft travelling to the metroplex.

A problem that is devoted to this subject is called Airport Runway Scheduling, and has been the topic of much research over the past 30 years but very few methods resulting from this research have been implemented and fewer still have been put into practice for several reasons:

- Since the problem is NP hard, the solution time required to solve complete problems is computationally infeasible.
- While generating the optimal RTAs required to optimally schedule the system, the problem of actually sending these times to the aircraft is much more difficult and regulated.

The research presented here acknowledges these issues but while the decomposition scheme used here does provide significant speedups, the implementation details will require more study.

		Leader		
		H	L	S
Trailer	H	4	3	3
	L	5	3	3
	S	5	3	3

Table 11: Minimum Required Runway Distance Separation Criteria in NM

		Leader		
		H	L	S
Trailer	H	140.0	136.8	102.7
	L	136.8	136.8	102.7
	S	102.7	102.7	102.7

Table 12: Runway Minimum Landing Speeds in Knots

5.2.2.2 Arrival Fix Constraints

For a schedule to be feasible, the inter-arrival separation must not be violated. To achieve this in an optimization program, the case where the order of flights is swapped must be considered for the sequence to be truly optimal. To allow for swapping, a binary variable is used to determine the order as shown in Equation 6. This variable is used in a Big-M formulation to ensure the separation constraint is not violated as shown in Equation 7. Because this introduces binary variables, there are several computational complexities introduced [2, 3].

$$\text{ent}_{i,j} + \text{ent}_{j,i} = 1 \qquad \forall i \neq j, \quad \text{ent}_{i,j} \in \{0, 1\} \tag{6}$$

$$\text{sta}_j - \text{sta}_i - M \cdot \text{ent}_{i,j} \geq \text{sep}_{i,j} - M \qquad \forall i \neq j \tag{7}$$

Where $\text{sep}_{i,j}$ is the required arrival fix crossing time shown in Table 10.

5.2.2.3 Runway Threshold Constraints

In a similar manner, the runway constraints must also be constructed using a binary decision variable for schedule order, and a constraint to ensure separation. This order variable is constrained in Equation 8 and is used in Equation 9.

		Leader		
		H	L	S
Trailer	H	102.9	78.9	105.2
	L	131.6	78.9	105.2
	S	175.3	105.2	105.2

Table 13: Required Runway Time Separation in Seconds

$$\text{rwy}_{i,j} + \text{rwy}_{j,i} = 1 \qquad \forall i \neq j, \quad \text{rwy}_{i,j} \in \{0,1\} \tag{8}$$

$$\text{sta}_j - \text{sta}_i - M \cdot \text{rwy}_{i,j} + d_j - d_i \geq \text{sep}_{i,j} - M - t_j + t_i \qquad \forall i \neq j \tag{9}$$

Where d_i is the delay that is absorbed by aircraft i while inside the TRACON, and t_i is the optimal transit time (transit time with no external delays). Here, the separation between aircraft i and j is found in Table 13.

5.3 Review of Benders' Algorithm

Benders' decomposition is a well-known algorithm that can be used to solve problems that show a block structure [7]. For this section, we will use the following model for discussion, shown in Equation 10.

$$\begin{aligned} z = \min cy + \textstyle\sum_i f_i x_i & \\ s.t. \quad Ay &= b \\ B_i y + F_i x_i &= d_i \quad \forall i \in 1,k \\ x, y &\geq 0 \\ y &\in \mathbb{Z} \end{aligned} \tag{10}$$

Benders' method will decompose this model such that it can be iteratively solved in a sequence of integer and linear programs. We will call this original model P.

The first step is to assume our integer vector y is fixed. We can then rewrite P as PX as shown in Equation 11 which is one of the k subproblems in our example.

$$\begin{aligned} z_i\left(y^*\right) = \min f_i x_i & \\ s.t. \quad F_i x_i &= d_i - B_i y^* \\ x_i &\geq 0 \end{aligned} \tag{11}$$

The dual of this problem can be found with dual variable u as shown in Equation 12 which we will call PD.

$$\begin{aligned} w_j\left(y^*\right) = \max u_j\left(d_j - B_j y^*\right) & \\ s.t. \quad u_j F_j &\geq f_j \\ u_j &\geq 0 \end{aligned} \tag{12}$$

We will assume that this dual problem is feasible (that $uA_1 \geq c_1$ is non-empty). We will let Π denote the set of all dual extreme points of this polyhedron. The vector y is known as the linking variable, and the x vector is known as the local or subproblem variables for each subproblem PX. With these definitions, the Benders' decomposition algorithm will reformulate P as a master problem of the $n + k$ variables:

- n original linking variables y.
- k continuous variables η_i, one for each subproblem, equal to the dual objective of each subproblem.

$$\eta_i = \min u_i \left(b - A_2^i y^*\right)$$

For each step in the Benders' decomposition algorithm, a candidate solution is generated from the master problem, y^*. Since solving the entire master problem with all of the dual polyhedra is usually computationally infeasible, the Benders' algorithm relies on adding cuts to a restricted master problem where the cuts are appended if the dual solution to a subproblem is shown to be suboptimal. Each iterative solution to the restricted master problem y^* may result in the subproblems being suboptimal or infeasible, but after each such iteration a new inequality is added in such a way as to cut off such infeasible or suboptimal solutions in the next iteration. If a solution (y^*, η^*) from the master problem leads to dual optimal values for each subproblem, then y^* and each x^* is optimal. Otherwise, the process will continue. The following process is followed when solving a MIP with Benders' algorithm:

- A feasible solution to the reduced master problem is given.
- Assume the initial feasible solution is not optimal, and while the problem is not optimal loop:
- Solve the reduced master problem for the linking variables.
- For each subproblem, solve the dual subproblem using the current values for the linking variables.
- If the dual objective is finite, add a constraint to the master problem using the dual variables for each subproblem.
- If the dual objective is infinite, add a constraint to the master problem using the unbounded direction of the objective ray.
- Resolve the master problem with the new constraints until the dual objective of the subproblems and the objective of the master problem converge.

This approach is a row generation method, in which new constraints are added to the reduced master problem. An alternative approach discussed elsewhere [5] is a column generation method that can also be used to solve very large integer programs.

5.4 Application of Benders' Decomposition

To apply Benders' decomposition to this problem, it must first be broken down into a master, or linking, problem, and a set of subproblems. The natural separation which proves to be useful is to use the arrival and entry order constraints as the master problem and treat each runway threshold and arrival fix separation constraints as a subproblem.

5.4.1 Master Problem

The initial master problem is simply given by minimizing some z given the order constraints:

$$\begin{aligned} rwy_{i,j} + rwy_{j,i} &= 1 \quad \forall i,j \in R_1 \\ &\vdots \\ rwy_{i,j} + rwy_{j,i} &= 1 \quad \forall i,j \in R_n \\ ent_{i,j} + ent_{j,i} &= 1 \quad \forall i,j \in A_1 \\ &\vdots \\ ent_{i,j} + ent_{j,i} &= 1 \quad \forall i,j \in A_m \end{aligned}$$

where R_i is each set of aircraft that go through runway i and A_j is the set of aircraft that go through fix j. The constraints on z will be added through Benders' cuts.

5.4.2 Subproblems

The continuous variables are reformulated into a subproblem dependent on the binary order variables that will be passed down from the master problem. The objective of these subproblems is the same as that of the original problem, as given in Equation 5.

The constraints of these sub problems are simply rewritten to treat the binary order variables as constants, as shown in:

$$\mathrm{sta}_j - \mathrm{sta}_i \geq \mathrm{sep}_{i,j} + M \cdot \hat{\mathrm{ent}}_{i,j} - M \qquad \forall i \neq j \tag{13}$$

$$\mathrm{sta}_j - \mathrm{sta}_i + d_j - d_i \geq \mathrm{sep}_{i,j} + M \cdot \hat{\mathrm{rwy}}_{i,j} - M - t_j + t_i \qquad \forall i \neq j \tag{14}$$

5.4.3 Optimality Cuts

Due to the type of problem each subproblem is composed of, there can be no infeasible solutions to the primal (or unbounded rays for the dual), so of the two types of Benders' cuts, only optimality cuts are applicable here. The proof of this fact can be explained physically. For any sequence of arrivals, there exists a scheduled arrival time that can achieve the separation constraints. Furthermore, we can bound the result from above by examining the worst case scenario. In the worst possible case, the last arrival in the ETA list would be the first in the scheduled arrival, followed by the first arrival in the sorted

list of ETAs. This would create a sequence as follows: $[n, 1, n-1, 2, n-2, \dots]$. Assuming the difference between the ETAs of the last and first aircraft is greater than the separation requirement, the upper bound would be given by Equation 15.

$$\sum_{i=0}^{n/2} ETA_{n-i} - ETA_{1+i} + n \max sep \tag{15}$$

where $\max sep$ is the maximum separation between aircraft.

To add the cuts, we simply solve each subproblem and add the constraint shown in Equation 16.

$$z - \pi_k \left(sep_{i,j} - tt_j + tt_i \right) \cdot rwy_{i,j} - \pi_{k+1} \left(\cdots \right) - \cdots \geq 0 \tag{16}$$

Where π_i is the positive dual variable corresponding to the i^{th} constraint in the subproblem.

The master problem is then re-solved with this new constraint, and the new binary order variables are passed down to the subproblem which is also re-solved. This process iterates until the subproblem objective does not significantly decrease when compared to the previous iteration.

5.5 TMA Algorithm as a Baseline for Scheduled Operations

While comparing the mixed integer programming delay values to the delay accumulated by an unscheduled arrival stream is useful, it would not reflect realistic gains over the current air transportation system since there are currently arrival scheduling tools such as the Traffic Management Advisor (TMA) which is in place in most ARTCCs. Many controllers will also have complex models that are built off of years of working in each sector that allow them to accurately predict and even optimize the schedules unassisted by decision support tools. Due to the infeasibility of testing algorithms against mental models that actual controllers use, the TMA algorithm will be used as a baseline to directly compare against the mixed integer programming formulation presented in this thesis. An effort lead by Dr. Saraf of the Saab Sensis Corporation was undertaken to develop a TMA Scheduling Emulation (TMA-SE) algorithm to model this approach.

5.5.1 TMA-SE Description

The TMA-SE mimics the scheduling process outlined in the previous section. Since the purpose is to develop a TMA-like scheduler for multi-airport systems, the TMA SE expands the stream-class concept as follows – all flights using the same arrival-fix and having similar operational characteristics (i.e., the same engine type) are classified into the same stream-class. The scheduling and Order of Consideration algorithms are also slightly adapted to apply to multi-airport systems. The full description of the algorithm is in Aditya Saraf's paper [53] and comprises of the following steps:

1. Start with estimated ETAs at the meter fix and de-conflict in the FCFS order. This gives the initial meter fix STAs.

2. Pick the flight with the earliest meter fix STA from each stream-class.

3. Among these stream-class leader flights, the flight having the earliest runway ETA at its respective metroplex airport runway is chosen as the next flight in the order of consideration. (If there are 'n' airports there would ideally be 'n' different flights that have the earliest ETA to their respective runways. But, in this step we only pick one flight, which is earliest to its runway among all these).

4. Runway and FAF STAs are computed for the chosen flights. Any delay required (to provide minimum required spacing behind the previous flight on the runway) over and above the Allowed Mean Delay Threshold (AMDT) is fed back to the meter fix STA.

5. If delay is required to be fed back to the meter-fix, then all flights in the same stream-class are pushed back (if required) to maintain minimum separation at the arrival-fix

6. Meter-fix and runway STAs for the chosen flights are finalized.

7. The scheduled flights are removed from the processing list.

8. This process is repeated until all flights have been scheduled to the runway.

5.6 Results

To evaluate the computational efficiency and accuracy of this Benders' scheme, a full MILP formulation was also written. A real scenario was used as a case study to determine computational feasibility. The simple metroplex geometry presented in Chapter 4 was used to evaluate the effectiveness of this solution method. This geometry consisted of a traditional four corner post configuration that shared the fixes between two airports. This configuration can be seen in Figure 23, and the demand set is presented in Figures 24 and 25.

5.6.1 Comparison of Benders' Scheme to Entire MIP

To demonstrate the gains found by solving through this Benders' decomposition method, we can compare the solution times of this decomposition against the solution times when solving the entire set of constraints at once. Two different programs were written in C++ using IBM's ILOG CPLEX optimizer, version 12.3. The first program simply solves the entire MIP by building the entire model while the second program decomposes the problem into the master and sub-problem as defined above. A table containing the window size in minutes (with the corresponding average number of aircraft in each window) and the runtimes for each program can be found in Table 14.

Table 14: Runtime in seconds of full MIP and Benders' decomposition method to solve a full day of traffic.

Window [min]	Average #/Window	MIP [sec]	Benders' [sec]
3	2.665	18.335	14.297
4	3.553	65.110	11.714
5	4.440	657.71	11.611
10	8.880	*	6.205
30	26.646	*	4.804
60	53.292	*	6.721
120	106.583	*	16.034
180	159.875	*	19.850
240	213.167	*	34.162
360	319.750	*	125.240
480	426.333	*	208.770

While these results seem too good to be true, similar results have been noted in solving large problems [33]. While the MIP solver is largely CPU bound while solving huge branch and bound trees due to the large number of integer variables, the Benders' program can solve these problems very quickly by solving a much easier binary problem (and efficiently resolving after each constraint) and several very easy LPs. The end result is that the Benders' decomposition program can solve problems that are constrained by the system memory without timing out.

The increase in the solution time for very small problems when solved using the Benders' decomposition scheme is due to the iterative nature of this method. While smaller windows take less time to solve, there are more problems to build. The overhead required to build each master and sub-problem is the driving factor behind the longer runtimes for the smaller windows.

5.6.2 Towards a Fuel Optimal Objective

While minimizing the total delay in the system is a fairly good proxy for fuel burn since additional delay requires aircraft to burn more fuel. However, all delay is not equal. Delay while the aircraft is on the ground before takeoff or while the aircraft is enroute is not nearly as costly as delay while an aircraft is arriving and is flying low altitude patterns in a TRACON. In "Fuel Consumption and Operational Performance," [52] Ryerson, Hansen, and Bonn states that a minute of delay is not the same a a minute of schedule padding. The difference is between 50-60 lbs of fuel for delay vs. a smaller 4.5-12 lbs per minute of schedule padding. For this comparison, a conservative value of 50 lbs for TRACON delay and 12 lbs per minute of enroute or scheduled delay was chosen. This ratio changes the objective shown in Equation 4 to Equation 17.

Table 15: Results for a Delay vs. Fuel Optimal Objective

Objective	Enroute Delay	TRACON Delay
Delay	270.91	234.68
Fuel	513.50	0.34

$$\min \sum_{i \in \text{Flights}} \frac{12}{62} (\text{sta}_i - \text{eta}_i) + \frac{50}{62} \text{d}_i \tag{17}$$

To show how this change in objective modifies the solution, complete optimization output for the MIA-FLL, geometry 3, low demand scenario are shown in Appendix A in Tables 29 and 30. The total enroute delay and TRACON delay are summarized in Table 15. This shows that the change in the weight for enroute/scheduled delay vs the TRACON delay will push more delay out to the more fuel efficient portions of the flight and while it increases the overall delay, it will reduce the fuel usage. The way air traffic controller would primarily absorb such delay is through speed control [19]. While the details of how this delay would be handled by the system is not studied here, knowing how the delay is handled could very well change the weighting of the objective function as shown here. Studies that consider non-convex fuel objectives could also be used and have been studied elsewhere [61]. These changes to the objective, while important for exact results, are not needed to show that a fuel optimal schedule can be considerably different from a schedule that minimizes system delay. Since airlines usually incorporate a cost index that optimizes to minimize airline cost by weighting the fuel based costs and the time based costs, a cost index approach to minimize each airlines cost could be implemented.

This was done using a range of TRACON/Enroute fuel weighting ratios and is plotted in Figure 37. It should be noted that for the range of feasible costs, the TRACON delay should be practically zero, while all of the schedule delay should be absorbed while enroute due to the reduced cost. This fuel optimal objective does result in 10 minutes of added delay which is due to many very small losses in throughput.

Take two flights, for example. FlightNum 1194 and 1198 (see Appendix A). These flights are going to the same runway but are flying through different arrival fixes. Here flight 1194 is delayed an extra 1.316 minutes enroute, and flight 1198 is delayed an extra 0.183 minutes enroute, but flight 1198 is not delayed the 1.498 minutes in the TRACON that it would have been if a delay optimal objective was used. This type of difference adds up over thousands of instances to give a small difference in total throughput.

5.6.3 Comparison Between Benders' MIP and TMA-SE

The results are tabulated as follows: Each metroplex configuration was tabulated individually with three columns of results for all three traffic levels. The three simulation output values are the Enroute Delay, TRACON Delay, and Total Delay. The Enroute Delay is

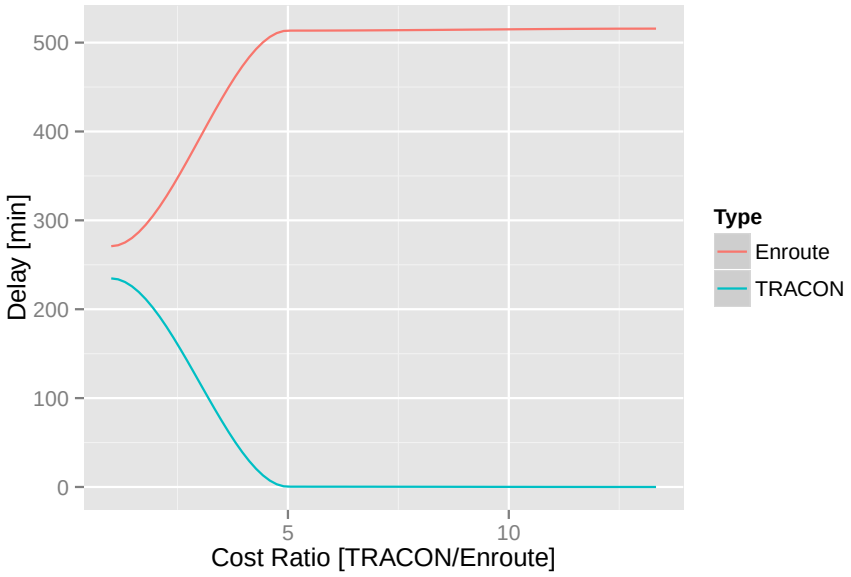

Figure 37: Enroute and TRACON delay as a fuction of fuel-based objective ratio

measured as the difference between the ETA to the arrival fix (which was the input value for the scheduling algorithms) and the time at which the aircraft could leave the arrival fix queue without violating any separation constraints. Implicitly, this value includes the difference between ETA and STA as well as any added delay that would be required to achieve the required 5 NM separation at the arrival fix. Similarly, the TRACON delay was computed by delaying each aircraft that is in queue for the runway long enough to achieve the required wake vortex separation requirements. Table 16 and Table 17 present the average results for the MIA-FLL metroplex configuration with both shared arrival fix airspace configurations and decoupled airspace configurations. This indicates that the MILP Multiplexer algorithm greatly outperforms the standard TMA algorithm when only the interactions considered within these algorithms are simulated. Comparing these two tables also would indicate that decoupling the airspace leads to some savings for both algorithms, but the difference between algorithms is much greater than the difference between airspace configurations. Table 22 and Table 23 present the cumulative results for the same simulations. Similarly, Table 18 and Table 19 present the average results for the SFO-SJC generic metroplex case while Table 24 and Table 25 tabulate the cumulative results. The average results for ORD-MDW are found in Table 20 and Table 21, while the cumulative results are contained in Table 26 and Table 27. These results also support our initial conclusions that while decoupling the airspace interactions will decrease delay, implementing optimal scheduling algorithms that consider all airspace interactions will provide a much greater impact in overall delay as traffic density increases. While the MILP showed little to no improvement over TMA for the low traffic density cases (even showing slightly worse

Table 16: MIA-FLL Average Delay for Shared Airspace [min]

Density	Algorithm	Enroute Delay	TRACON Delay	Total Delay
Low	TMA	0.24	0.37	0.58
Low	MILP	0.17	0.01	0.18
Medium	TMA	11.99	0.58	12.57
Medium	MILP	0.77	0.01	0.78
High	TMA	31.47	0.63	32.10
High	MILP	1.34	0.02	1.36

Table 17: MIA-FLL Average Delay for Decoupled Airspace [min]

Density	Algorithm	Enroute Delay	TRACON Delay	Total Delay
Low	TMA	0.06	0.40	0.46
Low	MILP	0.15	0.00	0.15
Medium	TMA	6.82	0.34	7.16
Medium	MILP	0.59	0.010	0.60
High	TMA	18.61	0.49	19.09
High	MILP	1.10	0.02	1.12

performance in two cases), the MILP Multiplexer formulation shows greater than 10x improvement for all medium density cases and initial results for the high density cases show more than 20x reduction in total delay when compared to the high density TMA results.

5.7 Handling Uncertainty: A Stochastic Formulation

Because the national air system is so complex, and winds play such a big role, uncertainty is a big issue for all such scheduling problems and there is active work to reduce such uncertainty and error [43]. Winds aren't the only source of uncertainty, pop-up flights can enter the schedule with little warning and differences in airline procedures and even pilot reaction times can cause uncertainty. However, to solve such scheduling problems, our Benders decomposition method will have to be resolved multiple times for each iteration. To reduce computational restrictions, our deterministic formulation will be solved and windows will be placed around the Benders' solution.

Table 18: SFO-SJC Average Delay for Shared Airspace [min]

Density	Algorithm	Enroute Delay	TRACON Delay	Total Delay
Low	TMA	0.25	0.08	0.33
Low	MILP	0.17	0.01	0.18
Medium	TMA	11.92	0.11	12.02
Medium	MILP	0.81	0.01	0.82
High	TMA	30.03	0.12	30.15
High	MILP	1.41	0.02	1.43

Table 19: SFO-SJC Average Delay for Decoupled Airspace [min]

Density	Algorithm	Enroute Delay	TRACON Delay	Total Delay
Low	TMA	0.05	0.10	0.15
Low	MILP	0.15	0.00	0.15
Medium	TMA	7.06	0.08	7.14
Medium	MILP	0.56	0.01	0.57
High	TMA	18.49	0.08	18.57
High	MILP	1.07	0.02	1.09

Table 20: ORD-MDW Average Delay for Shared Airspace [min]

Density	Algorithm	Enroute Delay	TRACON Delay	Total Delay
Low	TMA	0.26	0.10	0.36
Low	MILP	0.20	0.00	0.21
Medium	TMA	12.00	0.10	12.11
Medium	MILP	0.84	0.01	0.86
High	TMA	29.93	0.11	30.04
High	MILP	x.xx	x.xx	x.xx

Table 21: ORD-MDW Average Delay for Decoupled Airspace [min]

Density	Algorithm	Enroute Delay	TRACON Delay	Total Delay
Low	TMA	0.06	0.09	0.15
Low	MILP	0.18	0.00	0.19
Medium	TMA	7.04	0.08	7.13
Medium	MILP	0.55	0.01	0.56
High	TMA	18.64	0.08	18.72
High	MILP	1.08	0.01	1.09

Table 22: MIA-FLL Cumulative Delay for Shared Airspace [min]

Density	Algorithm	Enroute Delay	TRACON Delay	Total Delay
Low	TMA	138.00	237.42	375.42
Low	MILP	110.08	3.84	113.92
Medium	TMA	11950.74	576.23	12526.97
Medium	MILP	765.39	10.41	775.80
High	TMA	40248.79	805.18	41053.97
High	MILP	1716.61	24.90	1741.52

Table 23: MIA-FLL Cumulative Delay for Decoupled Airspace [min]

Density	Algorithm	Enroute Delay	TRACON Delay	Total Delay
Low	TMA	36.23	260.12	296.35
Low	MILP	97.72	1.00	98.72
Medium	TMA	6803.02	342.39	7145.41
Medium	MILP	584.10	9.93	594.03
High	TMA	23814.77	624.92	24439.69
High	MILP	1410.70	20.53	1431.23

Table 24: SFO-SJC Cumulative Delay for Shared Airspace [min]

Density	Algorithm	Enroute Delay	TRACON Delay	Total Delay
Low	TMA	158.43	53.84	212.27
Low	MILP	110.87	2.70	113.57
Medium	TMA	11884.01	104.35	11988.36
Medium	MILP	805.55	7.11	812.66
High	TMA	38406.62	150.43	38557.05
High	MILP	1809.09	25.72	1834.81

Table 25: SFO-SJC Cumulative Delay for Decoupled Airspace [min]

Density	Algorithm	Enroute Delay	TRACON Delay	Total Delay
Low	TMA	33.87	61.68	95.55
Low	MILP	94.81	1.61	96.42
Medium	TMA	7046.84	77.35	7124.19
Medium	MILP	557.10	11.94	569.04
High	TMA	23669.25	105.72	23774.98
High	MILP	1372.18	25.51	1397.69

Table 26: ORD-MDW Cumulative Delay for Shared Airspace [min]

Density	Algorithm	Enroute Delay	TRACON Delay	Total Delay
Low	TMA	169.08	63.97	233.06
Low	MILP	130.75	2.57	133.32
Medium	TMA	11965.63	103.52	12069.15
Medium	MILP	841.19	11.77	852.96
High	TMA	38283.05	141.36	38424.41
High	MILP	x.xx	x.xx	x.xx

Table 27: ORD-MDW Cumulative Delay for Decoupled Airspace [min]

Density	Algorithm	Enroute Delay	TRACON Delay	Total Delay
Low	TMA	36.02	60.99	97.01
Low	MILP	118.24	1.32	119.55
Medium	TMA	7021.76	83.48	7105.23
Medium	MILP	548.73	8.06	556.79
High	TMA	23862.89	98.43	23961.32
High	MILP	1377.46	18.44	1395.91

5.7.1 Review of Stochastic Programs

While traditional deterministic optimization models consider the input data to be completely known, stochastic models do not need to know exactly what the input values are but depends on the data following some distribution. A Stochastic Program is an optimization model that seeks to minimize or maximize an objective given the input parameters have known probability distributions. These types of problems are most commonly phrased as a recourse model. In a general recourse model the decisions are made in several stages. The first set of decisions are made before the uncertainty in the input variables have been realized, and subsequent corrections (or recourses) are made to correct for the uncertainty. The most common of these recourse models is the two-stage model. In these stochastic programs, a first stage decision is mode, the uncertainty is realized using the probability distributions, and a single recourse decision is made to correct. The problem is formulated to minimized the cost of the first stage decision and the expected cost of all possible second stage recourse decisions.

5.7.1.1 Two-Stage Stochastic Model

The general two-stage stochastic linear program is shown in Equation 18

$$\begin{aligned} \min_{x\in\mathbb{R}^n} \quad & c^T x + \mathbb{E}_z\left[Q(x,z)\right] \\ \text{s.t.} \quad & Ax = b \\ & x \geq 0 \end{aligned} \tag{18}$$

where x is the vector of first stage decision variables and $z = (q, T, W, h)$ is the input data to the second stage model. The function $Q(x, z)$ is defined as the solution to the second stage problem shown in Equation 19.

$$\begin{aligned} Q(x,z) = \quad \min_{y\in\mathbb{R}^m} \quad & q^T y \\ \text{s.t.} \quad & Tx + Wy = h \\ & y \geq 0 \end{aligned} \tag{19}$$

If the probability distribution of z has a finite number of outcomes for these uncertain terms the expectation can be expanded to form a large scale linear program. For other distributions, the expectation can be estimated through Monte Carlo methods. Traditional solution methods to these large scale LPs are based on cutting plane algorithms such as the L-shaped method [38]. This is an adaptation of the Benders' decomposition [7] which decomposes the problem into a first stage master problem and the recourse actions into subproblems for each outcome scenario.

5.7.2 Two Stage Stochastic Programming Formulation

Formulate program where local minimization is used for a restricted stage-1 problem.

The idea behind this stochastic formulation is that given an ETA 500 nmi out from the TRACON, a desired RTA will be given to a metering fix 150 nmi from the airport while minimizing delay and taking into account all forms of uncertainty. The two major forms of uncertainty expected here is pop-up flights, which could be understood with a probability of pop-up and a distribution of pop-up schedule given a pop-up flight has occurred. The second major source of uncertainty is the uncertainty in meeting the RTA. We will assume that all of the uncertainty happens between the 500 and 150 nmi rings, so that the deterministic problem is sufficient for the inner (stage 2) problem.

Formally, the stochastic problem can be written as Equation 20.

$$\min \sum_i rta_i^1 - eta_i + \mathbb{E}\left[Q(rta^1 \cup P, T)\right] \tag{20}$$

where Q is the Benders' decomposition formulation with the stage 1 rta as the input "eta," P is the schedule of pop-up flights, and T is the RTA distribution from 500 NM to 200 NM. Here Q will return the optimal stage 2 rta for a given stage 1 rta.

Because these expected values cannot be usually solved exactly, Monte Carlo estimations are used. This will reformulate Equation 20 into Equation 21, where N is chosen to be big enough to properly sample the distributions and small enough to be computationally feasible. A good resource for understanding the theoretical implications is given in Römisch's "Stability of ϵ-approximate solutions to convex stochastic programs" [51]. In general, stochastic programs are still an active area of research and are limited in problem size by computational issues. Many of these issues are known and have been identified [65], but there are still many challenges.

$$\min \sum_i rta_i^1 - eta_i + \frac{1}{N}\sum_{i=1}^{N}\left[Q(rta^1 \cup p_i \in P, t_i \in T)\right] \tag{21}$$

The proposed solution method that will be applied here is to further approximate Equation 20 through the following algorithm:

- Solve the deterministic problem from 500 nmi out to generate deterministic RTA values using mean values for ETA distributions.
- Place small bounds of ± 1 minutes around the deterministic RTAs to limit the search space.
- Since we are now solving on a local scale, we can use gradient descent based local optimization methods.
- Compute gradient by sampling once in all n directions. ($n \cdot N$ Benders' decomposition problems where there are n flights in our schedule window and N samples to approximate our expected value)

ID	ETA	Clas
1	0:00	L
2	0:45	L
3	1:30	L
4	2:15	L
5	3:00	L

Table 28: Sample Scenario

- Follow gradient by a small step δ.
- Iterate until the solution does not change more than $10n$ (average change is under 10 seconds per aircraft).

5.7.3 Application to Example Problem

For a sample problem we can take a simple case of five aircraft with ETAs that is densely packed as given in Table 28. We can now consider a case where a single popup flight will always occur, but the time is uniformly distributed between the existing flights. Solving the stochastic program spreads the expected required extra space between the five flights, but the way extra space will be distributed will be entirely dependent on the distribution of the time at which the popup will occur. While the added delay due to the expectation of the popup increases the delay over solving the deterministic problem, but once the popup flight is realized the resulting delay will most likely be greater. Due to the fact that the stochastic solutions will only be as good as the distributions of the input data, this approach should not be attempted until a significant data mining exercise has been performed on the typical operations of the area in question to build a statistically significant sample for the distributions. Otherwise, the statistical model will only add CPU runtime and could easily produce sub-optimal solutions that add extra spacing where a popup flight is unlikely. The deterministic solution to the sample problem only gives 4.96 minutes of total delay, while the stochastic problem that has a 50% probability of introducing a popup flight that is uniformly distributed between 0 and 3 minutes ETA estimates a delay of 6.77 minutes. If the popup flight does not occurr, the extra 2 minutes of delay will be lost capacity, but if the popup flight does occur, the simulated deterministic schedule will have arond 10.12 mintes of total delay while the stochastic program will only require 7.93 minutes of total delay. In situations where the likelyhood of certain events if very probable, a stochastic program will prove it's usefulness, but significant data analysis is required.

A second scenario representing morning arrivals (10 to 11 AM) in a low demand scenario for our generic metroplex with popup flights following a triangular disribution with a mode at 10:30, and lower and upper bounds at 10 and 11 AM was performed. This analysis was done with bounds of 1 minute around the schedule's deterministic solution and was solved

with 10 Monte-Carlo estimations of the expected value and used SciPy's BFGS-B gradient based optimization routine. Due to the low density schedule, the difference between the stochastic solution and the deterministic solution was under a second for all 19 flights. This implies that if the schedule is not dense or that if the stochastic disturbances are not strong enough that the deterministic solution should be reasonable and much more computationally viable. Even with local optimization techniques, many thousand function calls to the optimization program were performed which greatly increased the solution time.

5.8 Conclusion

While others have shown significant gains in the solution of aircraft scheduling in metroplex scenarios through the use of mixed integer programming techniques, the complexity of solving such optimization problems has limited the use of these techniques to small scheduling problems with only a few aircraft. To enable the use of these formal optimization techniques, we have demonstrated that a Benders' decomposition scheme can be successfully used to drastically reduce the time required to solve these scheduling problem. We have used this decomposition to solve a full day of traffic using a rolling horizon method. This type of method can be applied to many different types of problems [41]. The two stage stochastic formulation presented here shows some promise, but for a more realistic understanding of the possible gains when moving to a stochastic program, the distribution of uncertainties in a realistic airspace and schedule as was done for the deterministic problem previously discussed.

CHAPTER VI

CONCLUSIONS AND FUTURE WORK

In this thesis, several areas of metroplex operations were studied. Firstly, a site survey of several TRACONs was performed to compare the operations for several complex airspace configurations. The major metroplex facility comparison shown in Table 3 can be used to compare these TRACONs, but the core metroplex problem can be distilled to the case where more than one airport share the same airspace resources. Usually these resources are arrival or departure fixes, but in many cases a good portion of a STAR can be shared between airports when there is a common arrival path.

A quantitative metroplex identification method was also presented. This method demonstrated how a clustering algorithm can be used to automatically categorize airports into metroplexes using the metric shown in Equation 2. While the computational results matches intuition, the fact that all of the north east is considered to be part of one large metroplex cenetered around PHL including New York and Washington D.C. as members of the metroplex does not follow the OEP Metropolitan Areas which separates these three areas into their own metropolitan areas. One of the real benefits of using this method was that as traffic demand changes, the analysis can easily be rerun using the new demand levels to analyze the change in the number of airports and total interaction metric in each metroplex cluster.

Using the information gathered in the site survey and once a metroplex has been identified, the queuing model developed here can be used to study how a specific demand can be simulated to measure queuing delay or other metrics. This model was used to study throughput analysis and to examine how uncertainty in arrival times will impact the delay in the system. Several generic metroplex configurations were studied to understand the parameters identified through the site visits and this tool also served as a framework for evaluating the TMA-like scheduling algorithm and the mixed integer programs that were developed.

The mixed integer program presented to optimize the metroplex demand schedule was shown to have large gains over the TMA-like algorithm in extremely dense operations. However, solving the unmodified mixed integer program proved to be computationally infeasible for realistically sized problems. To mitigate this computational constraint, a Benders' decomposition scheme was presented to solve this problem which provided a very good speedup and allowed for larger problems to be solved on commodity hardware. The first steps towards optimizing for fuel burn was done through a small change in the objective function weighting the time-based delay values to reflect changes in fuel burn. Finally, a

simple stochastic framework was developed to allow for pop-up flights and uncertainty in the ability for aircraft to hit the RTAs.

This work suggest that the gains that can be made with the advancement of operational scheduling algorithms can offer significantly greater reductions in delay and fuel burn when compared to desegregating airways.

6.1 Future Work

There are several areas of possible future work. In the metroplex identification section, the metric can be made more complex to more accurately represent the actual traffic patterns. This could be done by weighting the traffic around the cone or through restructuring the volume to more accurately reflect the actual traffic patterns. A final area of improvement would be to tune the clustering algorithm. Either to tune the threshold of the existing algorithm or to perform a more complete evaluation of the possible clustering algorithms.

There are many possible areas of research that would advance the optimization work presented here. Methods to further speed up the computation would allow dense schedules to be solved with less hardware. Extending the stochastic framework would also be possible of the mixed integer program could be solved considerably faster as well. However, to evaluate the real world gains that would be possible when using a stochastic framework a more complete understanding of the distribution of pop-up flights and uncertainties would be necessary. Since stochastic solutions are dependent on the distribution of the input parameters, a more flexible stochastic program that could easily be configured to different airspace scenarios with various distributions of pop-up flights that could be dependent on time of day, and many other values. Application of more modern methods to solve stochastic programs could also be applied to allow the stochastic models to be solved in a reasonable amount of time since the simplistic formulation presented here is not computationally feasible for large problems which would be necessary to be applicable to large metroplex problems.

A second possible area of future work would be to consider airline cost index values to provide "fair" schedules that would minimize each airlines cost. Fairness in airline scheduling algorithms is a topic of current interest, and is an active area of research [62].

APPENDIX A

MINIMIZING FUEL VS. MINIMIZING DELAY OUTPUT

To support the results, the output of the optimization program Table 29 and Table 30 are presented below to show the difference between optimizing for minimum delay vs. optimizing for a minimum fuel type objective. In these tables, Class is the weight class for the aircraft, Fix is the arrival fix, Rwy is the assigned runway, FixETA is the time (in minutes from local midnight) that is the input ETA to the optimization tool, TranT is the transit time (in minutes) from the arrival fix to the runway threshold, TermDelay is the optimal TRACON delay for the two objectives for each aircraft, SchDelay is the enroute delay for each objective, and RwyETA or RwySTA are the original ETA for the aircraft to hit the runway threshold while the RwySTA is the new scheduled time at which the aircraft will be at the runway.

Table 29: MIA-FLL Low Output: Minimize for Delay

FlightNum	Class	Fix	Rwy	FixETA	FixSTA	TermDelay
1429	L	135	A	2.53333	2.53333	0
1423	L	315	A	3.45	4.182	0
1426	L	45	A	3.5	3.5	0.332333
1428	L	45	A	11.1833	11.1833	0
1419	L	225	A	17.0333	17.0333	0
1432	L	135	A	17.1333	17.1333	0
1431	L	225	A	18.85	18.85	0
1433	L	225	A	22.75	22.75	0
1001	L	315	A	170.417	170.417	0
1006	L	135	A	199.65	199.65	0
1004	L	45	A	199.7	199.7	1.249
1002	L	315	A	203.3	203.3	2.048
1003	L	135	A	211.933	211.933	0
1005	L	315	A	215.433	215.433	0.882333
1008	L	135	A	216.3	216.3	0
1007	L	45	A	221.65	221.65	0
1009	L	45	A	224.05	224.05	0
1010	L	225	A	237.4	237.4	0
1015	L	315	A	238.133	238.133	0.565667
1013	L	315	A	244.1	244.1	0
1019	L	315	A	245.45	245.45	0

Continued on next page

Table 29 – *Continued from previous page*

1012	L	45	A	245.8	245.8	0
1011	L	135	A	246.033	247.132	0
1016	L	45	A	247.25	247.25	1.18133
1018	L	45	A	249.817	249.817	0
1021	L	135	A	261.45	261.45	0
1022	L	45	A	261.8	261.8	0.949
1014	L	225	A	266.3	266.3	0.864667
1023	L	45	A	268.117	268.117	0
1020	H	45	A	270.75	270.75	0.098
1024	L	315	A	271.783	272.516	0
1017	L	45	A	276.017	276.017	0
1026	L	225	A	284.217	284.217	0
1028	S	45	A	290.15	290.15	0
1029	L	315	A	290.2	290.2	0
1025	L	45	A	290.917	291.613	0.572667
1030	L	135	A	304.867	304.867	0
1027	L	225	A	305.183	305.183	0
1036	L	225	A	314.117	314.117	0
1034	L	45	A	319.667	319.667	0
1031	L	45	A	319.767	320.799	0.183667
1032	L	45	A	322.383	322.383	0
1037	L	45	A	336.55	336.55	0
1035	S	315	A	337.667	337.667	2.5971e-06
1033	L	45	A	344.75	344.75	0
1038	L	315	A	357.083	357.083	0
1039	L	315	A	364.517	364.517	0
1041	H	135	A	374.967	374.967	0
1040	S	135	A	376	376.43	1.09117
1042	L	225	A	390.417	390.417	0
1045	L	45	A	393.083	393.083	0
1044	L	45	A	404.917	404.917	0
1043	L	45	A	405.183	406.049	0.183667
1048	L	45	A	412.05	412.299	0
1049	L	45	A	412.8	413.431	0.183667
1047	L	315	A	419.433	419.433	0
1053	L	45	A	432.267	433.132	0
1046	L	135	A	432.383	434.465	0
1052	L	315	A	434.9	434.9	0
1051	L	45	A	444.983	444.983	0
1050	L	315	A	452.467	452.467	0
1054	L	45	A	453.667	453.667	0

Continued on next page

Table 29 – *Continued from previous page*

1059	L	225	A	454.717	454.717	0
1055	L	225	A	461.217	461.217	0
1056	L	225	A	475.667	475.667	0
1057	L	315	A	478	478	0
1058	L	45	A	478.483	478.483	0
1062	L	225	A	485.367	485.367	0
1061	L	225	A	492.95	492.95	0
1060	L	225	A	493.867	494.082	0.183667
1065	L	45	A	500.983	500.983	0
1063	L	315	A	504.417	504.417	0.965667
1067	L	135	A	511.817	511.817	0.382333
1068	L	225	A	513.967	513.967	0
1069	L	45	A	519.633	519.633	0
1066	L	315	A	521.233	521.233	0
1070	L	135	A	522.333	522.333	0
1064	L	225	A	535.867	535.867	0
1073	H	135	A	537.8	537.8	0
1071	L	225	A	540.6	540.6	0
1074	L	135	A	547.417	547.417	0
1075	L	135	A	553.917	553.917	0
1072	L	135	A	558.183	558.183	0
1078	L	45	A	562.983	562.983	0.232333
1080	L	225	A	565	565	6.66599e-13
1081	L	45	A	565.1	565.1	0
1076	L	45	A	573.3	573.3	0
1082	L	45	A	573.617	574.432	0.183667
1079	L	225	A	577.933	577.933	1.098
1083	L	225	A	581.933	581.933	0
1086	L	225	A	584.6	584.6	0
1084	L	315	A	592.683	593.365	0
1077	L	315	A	600.05	600.05	0
1087	L	135	A	603.433	603.433	0
1089	L	135	A	604.7	604.7	0.049
1085	L	315	A	604.817	604.817	0
1090	L	315	A	612.267	612.267	0
1091	L	135	A	616.583	616.583	0
1092	L	135	A	631.167	631.167	0
1088	H	45	A	632.467	632.467	0.099
1093	L	315	A	641.067	641.067	0
1095	L	135	A	656.733	656.733	0
1094	H	315	A	677.533	677.533	0

Continued on next page

Table 29 – *Continued from previous page*

1097	L	225	A	679	679	0.609333
1096	L	135	A	685.983	685.983	0
1098	L	135	A	693.567	693.567	0
1099	L	45	A	695.1	695.1	0
1101	L	135	A	696.917	696.917	0
1102	S	135	A	703.1	703.1	0
1104	S	135	A	704.383	704.563	0.289333
1103	L	45	A	715.65	715.65	0
1107	L	45	A	716.867	716.867	0.099
1108	L	315	A	720.967	720.967	0
1100	L	315	A	721.067	722.282	0
1106	L	45	A	721.417	721.417	0
1105	L	45	A	722.7	722.7	0.0323333
1109	L	45	A	726.783	726.783	0
1112	L	135	A	731.633	732.897	0
1110	L	225	A	734.517	734.517	0
1114	L	315	A	737.75	737.75	0
1111	L	315	A	738.617	739.066	0
1113	L	315	A	745.467	745.467	0
1115	L	225	A	758.833	758.833	0
1120	L	135	A	760.317	760.317	0
1124	L	45	A	761.533	761.533	0.0823333
1117	L	315	A	761.75	761.75	0
1118	L	45	A	763.017	763.017	1.23033
1122	L	315	A	764.883	764.883	1.13133
1116	L	315	A	771.733	771.733	0
1121	L	315	A	772.333	773.049	0
1126	L	45	A	772.533	773.099	0
1123	L	45	A	773.65	774.414	0
1125	L	315	A	774.783	774.783	0
1119	L	45	A	781.583	781.583	0
1127	L	315	A	782.217	782.217	0
1134	L	225	A	802	802	0
1128	L	225	A	805.8	805.8	0
1138	L	135	A	812.6	812.6	0
1130	L	45	A	813.767	813.767	0.132333
1129	L	135	A	816.317	816.317	0
1135	L	45	A	820.967	821.697	0
1133	L	45	A	822.467	823.013	0
1141	L	45	A	825.1	825.1	1.01567
1139	L	45	A	826.4	826.4	1.03133

Continued on next page

Table 29 – *Continued from previous page*

1136	L	135	A	827.267	827.267	1.497
1144	L	225	A	827.9	827.9	0
1131	L	45	A	828.4	828.4	1.66267
1132	L	45	A	836.1	836.1	0
1142	L	135	A	840.433	840.433	0
1140	L	135	A	847.033	847.033	0
1137	H	135	A	847.533	850.082	0
1143	L	45	A	848.667	848.667	0
1148	L	315	A	860.667	860.667	0
1147	L	135	A	860.733	860.733	0
1145	L	315	A	864.767	865.116	0
1149	L	315	A	865.767	866.431	0
1155	L	315	A	872.5	872.5	0
1153	L	315	A	874.467	875.365	0
1146	L	45	A	874.783	875.032	0
1152	L	315	A	876.8	876.8	0
1150	L	315	A	879.467	879.467	0
1154	L	45	A	884	884	0
1160	L	45	A	885.583	885.583	0
1158	H	135	A	886.367	886.999	0
1159	L	45	A	889.4	889.4	1.00733
1161	L	45	A	889.733	891.723	0
1163	L	135	A	890.833	893.055	0
1156	L	45	A	891.683	894.354	0
1157	L	225	A	891.833	892.192	0
1164	L	45	A	892.783	895.67	0
1167	L	45	A	894.95	899.617	0
1151	L	225	A	896.917	897.153	2.933
1170	L	225	A	898.2	898.285	3.11667
1165	L	45	A	898.9	900.933	0
1162	L	315	A	905.4	905.4	0
1168	L	315	A	909.5	909.5	0
1171	L	45	A	915.9	915.9	0
1175	L	45	A	916.033	918.531	0
1173	L	135	A	916.05	917.232	0
1172	L	45	A	917.05	917.399	2.44767
1166	L	315	A	920.833	922.649	1.59733
1174	L	315	A	922.483	925.562	0
1169	L	45	A	928.983	928.983	0
1176	L	315	A	934.733	934.733	0
1180	L	315	A	935.45	935.865	1.49933

Continued on next page

Table 29 – *Continued from previous page*

1181	L	225	A	935.783	936.066	0
1179	L	45	A	939.4	939.4	0
1177	L	315	A	940.383	940.383	0
1178	L	45	A	941.417	941.417	0
1182	L	135	A	942.1	942.749	0
1187	L	315	A	949.067	949.067	0
1184	L	45	A	949.317	949.317	0.865667
1191	L	135	A	950.6	950.6	0.914667
1189	L	315	A	951.95	951.95	0
1190	L	315	A	954.067	954.067	1.83033
1186	L	225	A	958.05	958.05	0
1192	L	315	A	959.167	959.167	0.182333
1196	L	225	A	960.617	960.617	0
1183	L	225	A	961.967	961.967	0
1188	H	135	A	962.367	964.615	0
1202	L	315	A	964.967	964.967	0
1195	L	225	A	965.75	965.75	0.549
1204	L	315	A	971.583	971.583	0
1185	L	45	A	971.65	971.65	0
1194	L	135	A	972.467	972.982	0
1198	L	225	A	975.883	975.883	1.498
1200	L	45	A	975.883	975.883	0
1201	L	45	A	981.917	981.917	5.36633
1210	S	315	A	984.45	984.45	0
1203	L	315	A	984.55	985.913	3.13733
1206	L	225	A	984.55	986.436	0
1207	L	225	A	985.733	987.752	0
1197	L	45	A	987.8	987.8	0.798667
1199	L	45	A	989.633	989.633	1.59667
1212	L	315	A	991.633	992.998	0
1209	L	315	A	991.683	998.26	0
1205	L	315	A	992.317	995.629	0
1213	L	315	A	994.933	996.945	0
1215	L	315	A	997.65	1000.89	0
1208	L	225	A	997.667	999.593	0
1193	L	135	A	998.667	999.141	0
1218	L	45	A	999.317	1000.44	0
1214	L	135	A	1005.03	1005.03	0
1221	L	225	A	1006.67	1006.67	0
1211	L	45	A	1008.52	1008.53	0
1216	L	135	A	1010.95	1010.95	0

Continued on next page

Table 29 – *Continued from previous page*

1217	L	45	A	1013.38	1013.38	0
1220	L	45	A	1019.7	1019.7	0
1219	L	45	A	1021.52	1021.96	0
1222	L	45	A	1022.58	1024.23	1.24433
1224	H	135	A	1022.98	1022.98	0.396333
1225	L	45	A	1024.93	1026.55	0.239333
1223	L	225	A	1033.4	1033.4	0
1229	L	135	A	1037.4	1037.4	0
1228	L	45	A	1038.1	1038.1	0.599
1227	L	225	A	1041.03	1041.03	2.08133
1238	L	315	A	1047.15	1047.15	0
1231	L	135	A	1051.93	1051.93	0
1234	L	45	A	1055.23	1056.4	0
1235	L	315	A	1058.17	1058.17	0
1226	L	135	A	1058.63	1060.46	0.183667
1236	L	135	A	1059.07	1059.33	0
1230	L	45	A	1064.7	1065.78	0
1239	L	45	A	1064.95	1066.91	0.183667
1237	L	225	A	1065.07	1065.07	0
1233	L	45	A	1067.02	1068.05	0.367333
1245	L	45	A	1069.6	1070.31	0
1244	L	135	A	1070.5	1070.5	1.14233
1240	L	135	A	1072.97	1072.97	0
1241	L	45	A	1074.92	1074.92	0
1243	L	45	A	1075.17	1076.23	0
1232	L	45	A	1077.47	1077.47	0.0813333
1250	L	315	A	1091.62	1091.62	0
1246	L	45	A	1094.8	1094.8	0
1251	L	45	A	1095.67	1095.93	0.183667
1255	L	135	A	1097	1097	0.448
1248	H	135	A	1100.1	1101.58	6.478
1247	L	135	A	1101.07	1102.71	0
1252	L	315	A	1101.22	1101.83	0
1242	L	225	A	1102.25	1103.16	0
1249	L	135	A	1102.82	1105.34	0
1256	L	315	A	1103.25	1103.25	1.21167
1254	L	315	A	1106.12	1106.12	0.976333
1257	L	45	A	1106.28	1106.28	0.357667
1261	L	45	A	1112.4	1112.4	0
1259	L	45	A	1116.23	1116.23	0
1264	L	225	A	1117.5	1117.5	0

Continued on next page

Table 29 – *Continued from previous page*

1262	L	45	A	1117.55	1117.55	0
1253	L	45	A	1118.12	1121.5	-2.78267e-13
1260	L	225	A	1121.9	1121.97	0
1265	L	315	A	1122.02	1122.02	1.248
1258	L	315	A	1124.43	1124.43	1.46267
1271	L	45	A	1127.78	1127.78	0
1269	L	135	A	1136.38	1137.05	0
1267	L	315	A	1137.48	1137.48	0
1263	L	225	A	1137.67	1138.82	0
1275	L	225	A	1141.55	1141.55	0
1276	H	315	A	1142.75	1142.98	0
1274	L	45	A	1143.67	1143.67	0.0823333
1270	L	225	A	1145.53	1145.53	0
1266	L	45	A	1146.18	1146.18	1.26567
1277	L	45	A	1146.47	1148.68	1.39567
1279	L	315	A	1149.22	1149.22	0
1268	L	45	A	1149.82	1149.82	4.21067
1273	L	315	A	1150.57	1151.85	0
1278	L	315	A	1152.53	1154.48	0
1272	L	315	A	1153.12	1153.12	2.67833
1283	L	45	A	1155.9	1157.15	0
1282	L	225	A	1158.93	1158.93	0
1280	L	135	A	1159.32	1159.8	0
1285	H	225	A	1160.23	1162.65	8.259
1284	L	45	A	1160.32	1162.41	0
1286	L	225	A	1161.52	1161.52	0.048
1288	L	225	A	1161.98	1168.14	0
1281	L	315	A	1162.5	1166.81	0
1287	L	225	A	1163.43	1163.78	0.415333
1292	L	45	A	1165.72	1165.72	0.642
1296	L	315	A	1171.35	1172.95	0
1291	L	225	A	1172.6	1174.28	0
1300	L	315	A	1174.7	1174.7	0.881667
1290	L	135	A	1175.3	1175.3	0
1289	L	45	A	1179.13	1179.13	0
1299	L	225	A	1179.8	1179.8	0
1294	L	45	A	1180.6	1180.6	0
1301	L	135	A	1181.73	1181.93	0
1293	L	135	A	1184.78	1184.78	0
1298	L	135	A	1188.07	1188.07	0
1306	L	135	A	1193.38	1194.66	0

Continued on next page

Table 29 – *Continued from previous page*

1295	L	135	A	1193.68	1195.98	0
1302	L	225	A	1195.12	1195.12	0
1304	L	315	A	1195.57	1196.42	0
1311	L	45	A	1196.73	1196.73	1.86167
1307	L	315	A	1197.13	1200.36	0
1303	H	315	A	1198.62	1207.07	0
1310	L	225	A	1199.23	1203.01	0
1312	L	135	A	1199.65	1201.24	0
1297	L	45	A	1199.83	1199.83	2.70867
1319	L	315	A	1203.97	1208.21	0
1318	L	315	A	1206.28	1210.47	0
1317	L	45	A	1210.65	1210.65	0
1309	L	135	A	1212.08	1212.08	0
1321	L	45	A	1214.48	1214.48	0
1323	L	45	A	1216.83	1216.83	0.732333
1320	L	225	A	1219.35	1219.35	0
1314	L	45	A	1219.77	1221.51	0
1326	L	225	A	1220.15	1220.48	1.49933
1313	L	315	A	1221.08	1221.08	2.19699
1316	L	315	A	1222	1227.23	0
1308	L	315	A	1222.2	1222.2	3.71167
1325	L	45	A	1226.05	1226.05	0
1327	L	45	A	1230.83	1230.83	0.299
1322	L	45	A	1230.87	1231.97	0.482667
1328	L	315	A	1231.12	1231.12	0
1330	L	45	A	1232.68	1234.7	0.378
1305	L	45	A	1232.72	1233.57	0.194333
1324	L	315	A	1232.9	1232.9	0
1329	L	315	A	1239.28	1239.48	0
1331	L	315	A	1239.52	1240.79	0
1315	L	45	A	1240.38	1240.38	0
1333	L	135	A	1248.07	1248.07	0
1334	L	315	A	1252.73	1253.07	0
1339	L	45	A	1256.27	1256.27	0
1337	L	315	A	1260.47	1260.47	0
1335	L	45	A	1261.57	1261.57	0.199
1342	L	225	A	1263.55	1263.55	0
1343	L	45	A	1266.25	1267.11	0
1345	L	225	A	1266.7	1266.7	0
1336	L	135	A	1267.83	1268.44	0
1351	H	315	A	1268.12	1268.13	0

Continued on next page

Table 29 – *Continued from previous page*

1338	L	135	A	1268.45	1269.57	2.815
1352	L	45	A	1269.68	1269.74	0
1344	L	45	A	1269.75	1270.87	0.183667
1346	L	135	A	1271.32	1275.02	0
1340	L	135	A	1271.75	1277.65	0
1349	L	225	A	1271.97	1271.97	4.82
1332	H	315	A	1273.82	1273.97	37.1668
1355	L	315	A	1275.15	1276.13	5.90067
1341	L	45	A	1275.63	1275.75	0.566666
1359	L	45	A	1276.88	1276.88	3.38167
1354	S	45	A	1277.52	1282.75	12.1423
1347	L	315	A	1279.42	1283.12	1.54133
1356	L	45	A	1281.43	1284.21	0
1358	L	225	A	1282.18	1286	0
1348	L	45	A	1283.8	1285.53	0
1350	L	45	A	1286.07	1286.66	2.815
1366	L	225	A	1287.6	1289.94	0
1360	L	315	A	1287.93	1290.51	0.735666
1353	L	135	A	1288.1	1288.1	4.02267
1367	L	135	A	1290.47	1290.47	2.97167
1357	S	315	A	1291.72	1291.97	7.82367
1365	L	315	A	1293.43	1293.43	0.440333
1371	L	135	A	1296.78	1298.7	0
1362	L	225	A	1301.53	1301.62	1.476
1368	L	225	A	1302.48	1302.75	1.65967
1364	L	315	A	1302.88	1304.17	4.17333
1363	L	225	A	1303.88	1303.88	3.159
1370	L	315	A	1305.3	1305.3	0.41
1369	L	135	A	1306.62	1306.62	0
1372	L	225	A	1312.8	1312.8	0.408333
1361	L	225	A	1314.33	1314.33	0.190667
1373	L	315	A	1320.15	1320.27	0
1374	H	135	A	1320.77	1320.77	0
1383	L	45	A	1328.93	1328.93	0
1375	L	45	A	1332.37	1332.38	0
1381	H	315	A	1335.53	1339.55	0
1378	L	225	A	1335.92	1338.05	0.0646667
1377	L	315	A	1336.32	1336.63	0.149
1382	L	225	A	1342.67	1342.67	0
1380	L	225	A	1342.75	1343.8	0.183667
1379	L	45	A	1343.42	1343.45	0

Continued on next page

Table 29 – *Continued from previous page*

1386	L	45	A	1344.45	1344.58	0.183667
1376	L	135	A	1347.72	1347.72	0
1389	L	315	A	1353.78	1353.78	0
1390	L	45	A	1356.47	1356.65	0
1393	L	45	A	1356.67	1357.78	0.183667
1387	L	225	A	1362.5	1362.5	0
1385	L	225	A	1363.02	1363.63	0.183667
1384	L	45	A	1365.8	1365.98	0
1388	L	315	A	1366.32	1366.32	0
1394	L	45	A	1366.47	1367.11	1.49933
1391	L	225	A	1367.77	1367.77	0
1392	L	225	A	1369.13	1369.13	1.26467
1397	L	45	A	1375.83	1375.83	0
1403	L	225	A	1381.5	1381.5	0
1396	L	315	A	1381.77	1382.8	0
1395	L	45	A	1383.68	1383.68	0
1399	L	315	A	1385.15	1385.15	0
1404	L	135	A	1386.98	1386.98	0
1402	L	45	A	1389.83	1389.83	0
1406	L	45	A	1392.87	1392.87	0
1398	L	315	A	1397.45	1397.45	0
1409	L	315	A	1399.58	1399.71	0
1405	L	45	A	1400.9	1400.9	0
1411	L	315	A	1403.1	1405.3	0
1401	L	45	A	1406.18	1406.18	1.18233
1408	L	315	A	1407.47	1407.47	0
1400	L	225	A	1409.15	1409.15	0
1410	L	315	A	1413.03	1413.03	0
1412	L	45	A	1413.12	1413.12	0
1407	L	225	A	1414	1414	0.365667
1417	L	45	A	1418.27	1418.27	0
1414	L	45	A	1419.28	1419.58	0
1416	L	135	A	1423.12	1423.12	2.36467
1415	L	45	A	1423.15	1423.15	0.999
1421	L	315	A	1425.92	1425.92	0
1413	H	135	A	1426.23	1426.23	0.647
216	H	315	B	3.05	3.05	0
212	L	315	B	4.51667	5.314	0
218	L	135	B	5.28333	5.799	0
219	L	45	B	7.88333	7.88333	0
214	L	45	B	9.9	9.9	0

Continued on next page

Table 29 – *Continued from previous page*

217	L	45	B	13.8167	13.8167	0
221	L	45	B	26.1833	26.1833	0
215	L	225	B	27.9833	27.9833	0
220	L	225	B	48.0333	48.0333	0
3	L	135	B	166.617	166.617	0
1	L	225	B	170.467	170.467	0
4	L	135	B	187.367	187.367	0
2	L	225	B	192.767	192.767	0
6	L	135	B	213.217	213.217	0
5	L	45	B	214.45	214.45	0
7	L	225	B	227.7	227.7	0
9	L	315	B	229.35	229.35	0
8	L	45	B	231.333	231.333	0
11	H	45	B	254.483	254.483	0
10	L	225	B	262.683	262.683	0
12	L	45	B	265.767	265.767	0
13	S	135	B	289.85	289.85	0
14	S	315	B	318.1	318.1	0
16	L	45	B	328.95	328.95	0
15	L	225	B	347.017	347.017	0
17	H	135	B	352.1	352.1	0
20	L	225	B	386.083	386.083	0
21	L	225	B	393.467	393.467	0
19	L	135	B	394.933	394.933	1.299
24	L	45	B	400.333	400.333	0
22	L	45	B	407.267	407.267	0
18	L	45	B	411.167	411.167	0
23	L	225	B	417.033	417.033	0
25	L	225	B	429.167	429.167	0
26	L	45	B	440.117	440.117	0
27	L	45	B	449.767	449.767	0
28	L	225	B	503.167	503.167	0
29	L	45	B	503.517	503.517	0
31	H	45	B	517.267	517.267	0
30	L	45	B	519.733	520.765	0
32	L	45	B	522.617	522.617	0
33	L	135	B	525.317	525.317	0
34	L	45	B	550.483	550.483	0
35	L	45	B	560.067	560.067	0
36	L	315	B	592.233	592.233	0
38	L	45	B	600.933	600.933	0

Continued on next page

Table 29 – *Continued from previous page*

39	L	315	B	603.617	603.617	0
37	H	45	B	603.683	603.683	1.51567
40	L	135	B	627.483	627.483	0
42	L	45	B	637.8	637.8	0
41	L	135	B	643.167	643.167	0
43	H	315	B	650.867	650.867	0
46	L	45	B	653.633	653.633	0
44	H	315	B	658.367	658.367	0
45	L	135	B	660.017	660.017	0
50	S	315	B	669.533	669.533	0
47	L	225	B	672.517	672.517	0
51	L	225	B	673.2	673.649	0.183667
49	L	135	B	681.733	682.548	0
48	L	45	B	685.333	685.333	0
53	L	315	B	685.717	685.717	0.749
52	L	135	B	693.733	694.699	0
54	L	45	B	703.267	703.267	0
55	L	45	B	712.083	712.083	0
60	L	45	B	723.033	723.832	0
61	L	315	B	724.7	724.7	0.264333
59	L	225	B	729.933	729.933	0
58	S	135	B	731.433	731.433	0.835
57	L	45	B	734.983	734.983	1.26567
56	S	45	B	738.017	738.017	1.53767
62	L	315	B	741.033	741.033	0.290333
63	L	135	B	743.783	743.783	0
64	L	45	B	750.45	750.45	0.0656667
66	L	45	B	771.967	771.967	0
65	L	135	B	781.883	781.883	0
67	L	45	B	801.917	801.917	0
71	L	45	B	817.083	817.083	0
70	L	315	B	818.967	818.967	0
69	H	45	B	819.433	819.433	2.531
68	L	45	B	820.117	820.565	0
73	L	45	B	838.65	838.65	0
74	L	45	B	839.933	839.933	0.0323333
72	L	45	B	843.183	843.183	0
77	L	135	B	852.35	852.35	0
76	L	45	B	861.167	861.167	0
79	L	45	B	865.483	865.483	0
78	L	225	B	867.05	867.05	0

Continued on next page

Table 29 – *Continued from previous page*

75	L	315	B	868.133	868.133	0
84	L	135	B	873.283	873.283	0
81	L	315	B	874.233	874.233	0
80	L	45	B	877.2	877.2	0
82	L	45	B	884.3	886.715	0
85	L	45	B	889.767	890.532	1.13687e-13
87	L	225	B	899.417	899.417	0
83	L	45	B	901.95	902.065	0
88	L	135	B	904.167	904.167	0
86	L	315	B	921.517	921.517	0
89	L	225	B	927.683	927.683	0
91	L	315	B	932.883	932.883	0.932333
92	L	45	B	936.217	936.217	0
90	L	225	B	940.783	940.783	0
97	L	315	B	943.033	943.033	0
96	L	45	B	947.35	947.35	0
95	L	45	B	951.067	951.067	0
99	H	135	B	952.35	952.35	4.298
93	L	45	B	955.933	955.933	0
102	L	45	B	957.783	957.783	0
101	L	315	B	959.1	960.466	0
94	L	45	B	959.333	959.333	0
98	L	315	B	961.633	961.633	0
105	L	225	B	966.433	966.882	0
100	L	315	B	967.95	967.95	0
103	L	315	B	969.9	969.9	0
104	L	315	B	976.4	976.4	0
106	H	135	B	976.95	976.95	0
109	L	315	B	990.633	990.633	0
108	L	45	B	995.117	995.117	0
107	L	45	B	996.533	996.533	0
110	L	45	B	1007.4	1007.4	0
113	L	45	B	1009.12	1009.66	0
115	L	45	B	1013.78	1014.52	0
114	L	135	B	1015.08	1015.08	0
117	L	225	B	1016.18	1016.82	0
116	L	45	B	1020.18	1020.83	0
118	H	45	B	1022.82	1023.1	0
119	L	45	B	1025.42	1025.42	0
112	L	225	B	1027.92	1027.92	0
123	L	45	B	1028.37	1028.37	0

Continued on next page

Table 29 – *Continued from previous page*

111	L	315	B	1029.77	1029.77	0
120	L	135	B	1039.45	1039.45	0
121	L	135	B	1041.82	1041.82	0
125	H	315	B	1047.02	1051.13	0
126	L	45	B	1048.22	1048.22	0.332333
122	L	135	B	1049	1049	0
124	L	45	B	1049.58	1049.58	0.281333
128	L	135	B	1058.2	1058.2	0
131	H	135	B	1059.93	1061.6	0
132	L	45	B	1064.65	1064.65	0.282333
127	L	45	B	1066.25	1069.18	0
133	L	225	B	1066.85	1066.85	0
129	L	315	B	1073.03	1073.03	0
130	L	135	B	1073.45	1074.1	0
134	L	315	B	1082.95	1082.95	0
135	S	45	B	1083.05	1084.69	0
140	L	315	B	1086.93	1086.93	0
138	L	45	B	1091.47	1091.47	0
139	L	315	B	1095.32	1095.32	0
136	L	225	B	1095.53	1095.53	0
137	L	45	B	1096.95	1097.06	0
142	L	45	B	1098.38	1098.38	0
141	L	135	B	1099.88	1099.88	0
143	S	225	B	1111.08	1111.08	0
145	L	225	B	1112.95	1112.95	0.202667
144	L	45	B	1117.23	1118.68	0.786333
146	L	45	B	1137.47	1137.47	0
147	L	45	B	1153.77	1153.77	0
154	L	135	B	1158.9	1161.16	0
148	L	225	B	1160.07	1160.27	-2.2729e-13
150	L	135	B	1163.42	1163.42	0
153	L	45	B	1163.95	1163.95	0
152	L	315	B	1170.5	1170.5	0
149	L	135	B	1172.13	1172.13	0
157	L	135	B	1172.93	1173.27	0.183667
156	L	135	B	1180.05	1180.05	0
151	L	315	B	1182.2	1182.2	0
155	L	315	B	1183.33	1183.52	0
158	L	45	B	1190.07	1190.07	0
159	L	45	B	1191.22	1191.38	0
163	L	315	B	1194.98	1194.98	0

Continued on next page

Table 29 – *Continued from previous page*

161	L	315	B	1197.95	1197.95	0
160	L	315	B	1206.52	1209.34	0
164	L	315	B	1211.43	1211.6	0
162	L	135	B	1212.95	1213.22	0
166	L	45	B	1214.12	1215.62	0
167	L	225	B	1222.78	1222.78	0
168	L	45	B	1224.03	1224.03	0
170	H	315	B	1225.55	1225.55	9.08031e-06
165	L	45	B	1235.83	1235.83	0
169	L	45	B	1236.22	1237.15	0
171	H	315	B	1251.93	1251.93	0
175	L	45	B	1256.75	1257.4	0
173	L	135	B	1265.33	1265.33	0
174	L	315	B	1266.67	1266.67	0
172	L	45	B	1271.28	1272	0.0620002
177	H	315	B	1275	1275	0
179	L	225	B	1278.22	1278.22	0
176	L	315	B	1278.73	1278.73	0
178	S	315	B	1284.43	1284.59	0
181	L	135	B	1297.15	1297.15	0
182	L	315	B	1302.97	1303.04	0.663
180	L	45	B	1303.55	1306.51	0
185	L	45	B	1303.93	1305.2	0
187	H	135	B	1317.98	1317.98	0
186	H	315	B	1319.13	1319.13	0
184	L	135	B	1329.4	1329.4	0
188	L	45	B	1331.25	1331.25	0
183	L	315	B	1335.5	1335.5	0.449
190	L	225	B	1336.92	1336.92	0
193	L	45	B	1337.47	1337.47	0
191	L	45	B	1338.58	1338.6	0.183667
189	L	45	B	1342.32	1342.32	0.915667
194	L	45	B	1355.52	1355.52	0
192	H	315	B	1357.5	1357.5	0
195	L	225	B	1359	1359	0
197	L	45	B	1360.75	1360.75	0
198	L	315	B	1364.85	1364.85	0.282333
196	L	135	B	1368.18	1368.18	0
200	L	315	B	1375.2	1375.2	0
199	L	315	B	1375.72	1376.33	0.183667
201	L	45	B	1378.9	1378.9	0

Continued on next page

Table 29 – *Continued from previous page*

204	L	315	B	1381.15	1381.15	0
205	L	45	B	1390.5	1390.97	0
203	L	135	B	1395.8	1395.8	0.18
206	L	315	B	1398.27	1398.58	0
202	L	45	B	1399.4	1399.4	0.681
207	L	225	B	1399.78	1399.78	0.376
208	H	315	B	1402.92	1402.92	0
210	L	135	B	1409.48	1409.48	0
209	L	315	B	1410.82	1410.82	0
211	L	225	B	1415.47	1415.47	0

Table 30: MIA-FLL Low Output: Minimize for Fuel

FlightNum	Class	Fix	Rwy	FixETA	FixSTA	TermDelay
1429	L	135	A	2.53333	2.53333	0
1423	L	315	A	3.45	4.182	0
1426	L	45	A	3.5	3.83233	0
1428	L	45	A	11.1833	11.1833	0
1419	L	225	A	17.0333	17.0333	0
1432	L	135	A	17.1333	17.1333	0
1431	L	225	A	18.85	18.85	0
1433	L	225	A	22.75	22.75	0
1001	L	315	A	170.417	170.417	0
1006	L	135	A	199.65	199.65	0
1004	L	45	A	199.7	200.949	0
1002	L	315	A	203.3	205.348	0
1003	L	135	A	211.933	211.933	0
1005	L	315	A	215.433	216.316	0
1008	L	135	A	216.3	216.3	0
1007	L	45	A	221.65	221.65	0
1009	L	45	A	224.05	224.05	0
1010	L	225	A	237.4	237.4	0
1015	L	315	A	238.133	238.699	0
1013	L	315	A	244.1	244.1	0
1019	L	315	A	245.45	245.45	0
1012	L	45	A	245.8	245.8	0
1011	L	135	A	246.033	247.132	0
1016	L	45	A	247.25	248.431	0
1018	L	45	A	249.817	249.817	0
1021	L	135	A	261.45	261.45	0

Continued on next page

Table 30 – *Continued from previous page*

1022	L	45	A	261.8	262.749	0
1014	L	225	A	266.3	267.165	0
1023	L	45	A	268.117	268.117	0
1020	H	45	A	270.75	270.848	0
1024	L	315	A	271.783	272.516	0
1017	L	45	A	276.017	276.017	0
1026	L	225	A	284.217	284.217	0
1028	S	45	A	290.15	290.15	0
1029	L	315	A	290.2	290.2	0
1025	L	45	A	290.917	292.186	0
1030	L	135	A	304.867	304.867	0
1027	L	225	A	305.183	305.183	0
1036	L	225	A	314.117	314.117	0
1034	L	45	A	319.667	319.667	0
1031	L	45	A	319.767	320.982	0
1032	L	45	A	322.383	322.383	0
1037	L	45	A	336.55	336.553	0
1035	S	315	A	337.667	337.667	0
1033	L	45	A	344.75	344.75	0
1038	L	315	A	357.083	357.083	0
1039	L	315	A	364.517	364.517	0
1041	H	135	A	374.967	374.967	0
1040	S	135	A	376	377.521	0
1042	L	225	A	390.417	390.417	0
1045	L	45	A	393.083	393.083	0
1044	L	45	A	404.917	404.917	0
1043	L	45	A	405.183	406.232	0
1048	L	45	A	412.05	412.299	0
1049	L	45	A	412.8	413.614	0
1047	L	315	A	419.433	419.433	0
1053	L	45	A	432.267	433.132	0
1046	L	135	A	432.383	434.465	0
1052	L	315	A	434.9	434.9	0
1051	L	45	A	444.983	444.983	0
1050	L	315	A	452.467	452.467	0
1054	L	45	A	453.667	453.667	0
1059	L	225	A	454.717	454.717	0
1055	L	225	A	461.217	461.217	0
1056	L	225	A	475.667	475.667	0
1057	L	315	A	478	478	0
1058	L	45	A	478.483	478.483	0

Continued on next page

Table 30 – *Continued from previous page*

1062	L	225	A	485.367	485.367	0
1061	L	225	A	492.95	492.95	0
1060	L	225	A	493.867	494.266	0
1065	L	45	A	500.983	500.983	0
1063	L	315	A	504.417	505.382	0
1067	L	135	A	511.817	512.199	0
1068	L	225	A	513.967	513.967	0
1069	L	45	A	519.633	519.633	0
1066	L	315	A	521.233	521.233	0
1070	L	135	A	522.333	522.333	0
1064	L	225	A	535.867	535.867	0
1073	H	135	A	537.8	537.8	0
1071	L	225	A	540.6	540.6	0
1074	L	135	A	547.417	547.417	0
1075	L	135	A	553.917	553.917	0
1072	L	135	A	558.183	558.183	0
1078	L	45	A	562.983	563.216	0
1080	L	225	A	565	565	0
1081	L	45	A	565.1	565.1	0
1076	L	45	A	573.3	573.3	0
1082	L	45	A	573.617	574.616	0
1079	L	225	A	577.933	579.031	0
1083	L	225	A	581.933	581.933	0
1086	L	225	A	584.6	584.6	0
1084	L	315	A	592.683	593.365	0
1077	L	315	A	600.05	600.05	0
1087	L	135	A	603.433	603.433	0
1089	L	135	A	604.7	604.749	0
1085	L	315	A	604.817	604.817	0
1090	L	315	A	612.267	612.267	0
1091	L	135	A	616.583	616.583	0
1092	L	135	A	631.167	631.167	0
1088	H	45	A	632.467	632.566	0
1093	L	315	A	641.067	641.067	0
1095	L	135	A	656.733	656.733	0
1094	H	315	A	677.533	677.533	0
1097	L	225	A	679	679.609	0
1096	L	135	A	685.983	685.983	0
1098	L	135	A	693.567	693.567	0
1099	L	45	A	695.1	695.1	0
1101	L	135	A	696.917	696.917	0

Continued on next page

Table 30 – *Continued from previous page*

1102	S	135	A	703.1	703.1	0
1104	S	135	A	704.383	704.853	0
1103	L	45	A	715.65	715.65	0
1107	L	45	A	716.867	716.966	0
1108	L	315	A	720.967	720.967	0
1100	L	315	A	721.067	722.282	0
1106	L	45	A	721.417	721.417	0
1105	L	45	A	722.7	722.732	0
1109	L	45	A	726.783	726.783	0
1112	L	135	A	731.633	732.749	0
1110	L	225	A	734.517	734.517	0
1114	L	315	A	737.75	737.75	0
1111	L	315	A	738.617	739.066	0
1113	L	315	A	745.467	745.467	0
1115	L	225	A	758.833	758.833	0
1120	L	135	A	760.317	760.317	0
1124	L	45	A	761.533	761.616	0
1117	L	315	A	761.75	761.75	0
1118	L	45	A	763.017	764.247	0
1122	L	315	A	764.883	766.015	0
1116	L	315	A	771.733	771.733	0
1121	L	315	A	772.333	773.049	0
1126	L	45	A	772.533	773.099	0
1123	L	45	A	773.65	774.414	0
1125	L	315	A	774.783	774.783	0
1119	L	45	A	781.583	781.583	0
1127	L	315	A	782.217	782.217	0
1134	L	225	A	802	802	0
1128	L	225	A	805.8	805.8	0
1138	L	135	A	812.6	812.6	0
1130	L	45	A	813.767	813.899	0
1129	L	135	A	816.317	816.317	0
1135	L	45	A	820.967	821.249	0
1133	L	45	A	822.467	823.513	0
1141	L	45	A	825.1	826.144	0
1139	L	45	A	826.4	827.46	0
1136	L	135	A	827.267	828.792	0
1144	L	225	A	827.9	827.928	0
1131	L	45	A	828.4	830.091	0
1132	L	45	A	836.1	836.1	0
1142	L	135	A	840.433	840.433	0

Continued on next page

Table 30 – *Continued from previous page*

1140	L	135	A	847.033	847.033	0
1137	H	135	A	847.533	850.082	0
1143	L	45	A	848.667	848.667	0
1148	L	315	A	860.667	860.667	0
1147	L	135	A	860.733	860.733	0
1145	L	315	A	864.767	865.116	0
1149	L	315	A	865.767	866.431	0
1155	L	315	A	872.5	872.5	0
1153	L	315	A	874.467	875.365	0
1146	L	45	A	874.783	875.032	0
1152	L	315	A	876.8	876.8	0
1150	L	315	A	879.467	879.467	0
1154	L	45	A	884	884	0
1160	L	45	A	885.583	885.583	0
1158	H	135	A	886.367	886.999	0
1159	L	45	A	889.4	890.407	0
1161	L	45	A	889.733	893.039	0
1163	L	135	A	890.833	891.74	0
1156	L	45	A	891.683	895.67	0
1157	L	225	A	891.833	892.192	0
1164	L	45	A	892.783	896.986	0
1167	L	45	A	894.95	899.617	0
1151	L	225	A	896.917	897.454	0
1170	L	225	A	898.2	901.401	0
1165	L	45	A	898.9	900.933	0
1162	L	315	A	905.4	905.4	0
1168	L	315	A	909.5	909.5	0
1171	L	45	A	915.9	915.9	0
1175	L	45	A	916.033	918.531	0
1173	L	135	A	916.05	917.232	0
1172	L	45	A	917.05	921.163	0
1166	L	315	A	920.833	922.93	0
1174	L	315	A	922.483	925.562	0
1169	L	45	A	928.983	928.983	0
1176	L	315	A	934.733	934.948	0
1180	L	315	A	935.45	937.579	0
1181	L	225	A	935.783	936.28	0
1179	L	45	A	939.4	939.4	0
1177	L	315	A	940.383	940.383	0
1178	L	45	A	941.417	941.417	0
1182	L	135	A	942.1	942.749	0

Continued on next page

Table 30 – *Continued from previous page*

1187	L	315	A	949.067	949.067	0
1184	L	45	A	949.317	950.182	0
1191	L	135	A	950.6	951.515	0
1189	L	315	A	951.95	951.95	0
1190	L	315	A	954.067	955.897	0
1186	L	225	A	958.05	958.05	0
1192	L	315	A	959.167	959.349	0
1196	L	225	A	960.617	960.617	0
1183	L	225	A	961.967	961.967	0
1188	H	135	A	962.367	963.299	0
1202	L	315	A	964.967	964.967	0
1195	L	225	A	965.75	968.492	0
1204	L	315	A	971.583	971.583	0
1185	L	45	A	971.65	971.65	0
1194	L	135	A	972.467	974.298	0
1198	L	225	A	975.883	976.066	0
1200	L	45	A	975.883	975.883	0
1201	L	45	A	981.917	985.967	0
1210	S	315	A	984.45	984.45	0
1203	L	315	A	984.55	987.735	0
1206	L	225	A	984.55	986.436	0
1207	L	225	A	985.733	990.383	0
1197	L	45	A	987.8	988.599	0
1199	L	45	A	989.633	989.914	0
1212	L	315	A	991.633	994.313	0
1209	L	315	A	991.683	995.629	0
1205	L	315	A	992.317	996.945	0
1213	L	315	A	994.933	998.26	0
1215	L	315	A	997.65	999.576	0
1208	L	225	A	997.667	1000.91	0
1193	L	135	A	998.667	999.141	0
1218	L	45	A	999.317	1000.44	0
1214	L	135	A	1005.03	1005.03	0
1221	L	225	A	1006.67	1006.67	0
1211	L	45	A	1008.52	1008.53	0
1216	L	135	A	1010.95	1010.95	0
1217	L	45	A	1013.38	1013.38	0
1220	L	45	A	1019.7	1019.7	0
1219	L	45	A	1021.52	1021.96	0
1222	L	45	A	1022.58	1024.23	0
1224	H	135	A	1022.98	1026.96	0

Continued on next page

Table 30 – *Continued from previous page*

1225	L	45	A	1024.93	1025.54	0
1223	L	225	A	1033.4	1033.4	0
1229	L	135	A	1037.4	1037.4	0
1228	L	45	A	1038.1	1040.01	0
1227	L	225	A	1041.03	1041.8	0
1238	L	315	A	1047.15	1047.15	0
1231	L	135	A	1051.93	1051.93	0
1234	L	45	A	1055.23	1056.4	0
1235	L	315	A	1058.17	1058.17	0
1226	L	135	A	1058.63	1060.65	0
1236	L	135	A	1059.07	1059.33	0
1230	L	45	A	1064.7	1064.7	0
1239	L	45	A	1064.95	1066.96	0
1237	L	225	A	1065.07	1065.07	0
1233	L	45	A	1067.02	1068.28	0
1245	L	45	A	1069.6	1069.6	0
1244	L	135	A	1070.5	1070.93	0
1240	L	135	A	1072.97	1072.97	0
1241	L	45	A	1074.92	1074.92	0
1243	L	45	A	1075.17	1076.23	0
1232	L	45	A	1077.47	1077.55	0
1250	L	315	A	1091.62	1091.62	0
1246	L	45	A	1094.8	1094.8	0
1251	L	45	A	1095.67	1096.12	0
1255	L	135	A	1097	1097.45	0
1248	H	135	A	1100.1	1108.06	0
1247	L	135	A	1101.07	1101.4	0
1252	L	315	A	1101.22	1101.83	0
1242	L	225	A	1102.25	1103.16	0
1249	L	135	A	1102.82	1104.03	0
1256	L	315	A	1103.25	1105.78	0
1254	L	315	A	1106.12	1108.41	0
1257	L	45	A	1106.28	1106.64	0
1261	L	45	A	1112.4	1112.4	0
1259	L	45	A	1116.23	1116.23	0
1264	L	225	A	1117.5	1117.5	0
1262	L	45	A	1117.55	1117.55	0
1253	L	45	A	1118.12	1121.5	0
1260	L	225	A	1121.9	1121.97	0
1265	L	315	A	1122.02	1123.26	0
1258	L	315	A	1124.43	1125.9	0

Continued on next page

Table 30 – *Continued from previous page*

1271	L	45	A	1127.78	1127.78	0
1269	L	135	A	1136.38	1137.05	0
1267	L	315	A	1137.48	1137.48	0
1263	L	225	A	1137.67	1138.82	0
1275	L	225	A	1141.55	1141.55	0
1276	H	315	A	1142.75	1142.98	0
1274	L	45	A	1143.67	1143.75	0
1270	L	225	A	1145.53	1145.53	0
1266	L	45	A	1146.18	1148.76	0
1277	L	45	A	1146.47	1147.45	0
1279	L	315	A	1149.22	1149.22	0
1268	L	45	A	1149.82	1151.4	0
1273	L	315	A	1150.57	1153.16	0
1278	L	315	A	1152.53	1157.11	0
1272	L	315	A	1153.12	1155.8	0
1283	L	45	A	1155.9	1157.15	0
1282	L	225	A	1158.93	1158.93	0
1280	L	135	A	1159.32	1165.06	0
1285	H	225	A	1160.23	1170.91	0
1284	L	45	A	1160.32	1162.41	0
1286	L	225	A	1161.52	1161.56	0
1288	L	225	A	1161.98	1162.88	0
1281	L	315	A	1162.5	1164.18	0
1287	L	225	A	1163.43	1166.83	0
1292	L	45	A	1165.72	1166.36	0
1296	L	315	A	1171.35	1172.95	0
1291	L	225	A	1172.6	1174.28	0
1300	L	315	A	1174.7	1175.58	0
1290	L	135	A	1175.3	1175.3	0
1289	L	45	A	1179.13	1179.13	0
1299	L	225	A	1179.8	1179.8	0
1294	L	45	A	1180.6	1180.6	0
1301	L	135	A	1181.73	1181.93	0
1293	L	135	A	1184.78	1184.78	0
1298	L	135	A	1188.07	1188.07	0
1306	L	135	A	1193.38	1194.66	0
1295	L	135	A	1193.68	1195.98	0
1302	L	225	A	1195.12	1195.12	0
1304	L	315	A	1195.57	1196.42	0
1311	L	45	A	1196.73	1198.59	0
1307	L	315	A	1197.13	1200.36	0

Continued on next page

Table 30 – *Continued from previous page*

1303	H	315	A	1198.62	1207.07	0
1310	L	225	A	1199.23	1203.01	0
1312	L	135	A	1199.65	1201.24	0
1297	L	45	A	1199.83	1202.54	0
1319	L	315	A	1203.97	1208.21	0
1318	L	315	A	1206.28	1210.47	0
1317	L	45	A	1210.65	1210.65	0
1309	L	135	A	1212.08	1212.08	0
1321	L	45	A	1214.48	1214.48	0
1323	L	45	A	1216.83	1217.57	0
1320	L	225	A	1219.35	1219.35	0
1314	L	45	A	1219.77	1222.83	0
1326	L	225	A	1220.15	1224.61	0
1313	L	315	A	1221.08	1221.96	0
1316	L	315	A	1222	1227.23	0
1308	L	315	A	1222.2	1223.28	0
1325	L	45	A	1226.05	1226.05	0
1327	L	45	A	1230.83	1232.45	0
1322	L	45	A	1230.87	1231.13	0
1328	L	315	A	1231.12	1231.12	0
1330	L	45	A	1232.68	1235.08	0
1305	L	45	A	1232.72	1233.76	0
1324	L	315	A	1232.9	1232.9	0
1329	L	315	A	1239.28	1239.48	0
1331	L	315	A	1239.52	1240.79	0
1315	L	45	A	1240.38	1240.38	0
1333	L	135	A	1248.07	1248.07	0
1334	L	315	A	1252.73	1253.07	0
1339	L	45	A	1256.27	1256.27	0
1337	L	315	A	1260.47	1260.47	0
1335	L	45	A	1261.57	1261.77	0
1342	L	225	A	1263.55	1263.55	0
1343	L	45	A	1266.25	1267.11	0
1345	L	225	A	1266.7	1266.7	0
1336	L	135	A	1267.83	1268.44	0
1351	H	315	A	1268.12	1268.13	0
1338	L	135	A	1268.45	1269.76	0
1352	L	45	A	1269.68	1277.63	0
1344	L	45	A	1269.75	1275	0
1346	L	135	A	1271.32	1276.33	0
1340	L	135	A	1271.75	1272.39	0

Continued on next page

Table 30 – *Continued from previous page*

1349	L	225	A	1271.97	1274.16	0
1332	H	315	A	1273.82	1311.13	0
1355	L	315	A	1275.15	1276.77	0
1341	L	45	A	1275.63	1280.26	0
1359	L	45	A	1276.88	1281.58	0
1354	S	45	A	1277.52	1296.64	0
1347	L	315	A	1279.42	1282.03	0
1356	L	45	A	1281.43	1282.9	0
1358	L	225	A	1282.18	1287.31	0
1348	L	45	A	1283.8	1285.53	0
1350	L	45	A	1286.07	1288.16	0
1366	L	225	A	1287.6	1289.94	0
1360	L	315	A	1287.93	1292.56	0
1353	L	135	A	1288.1	1290.81	0
1367	L	135	A	1290.47	1293.44	0
1357	S	315	A	1291.72	1298.04	0
1365	L	315	A	1293.43	1295.19	0
1371	L	135	A	1296.78	1298.7	0
1362	L	225	A	1301.53	1303.1	0
1368	L	225	A	1302.48	1305.73	0
1364	L	315	A	1302.88	1308.34	0
1363	L	225	A	1303.88	1304.41	0
1370	L	315	A	1305.3	1307.03	0
1369	L	135	A	1306.62	1306.62	0
1372	L	225	A	1312.8	1313.21	0
1361	L	225	A	1314.33	1314.52	0
1373	L	315	A	1320.15	1320.27	0
1374	H	135	A	1320.77	1320.77	0
1383	L	45	A	1328.93	1328.93	0
1375	L	45	A	1332.37	1332.38	0
1381	H	315	A	1335.53	1339.55	0
1378	L	225	A	1335.92	1336.8	0
1377	L	315	A	1336.32	1338.1	0
1382	L	225	A	1342.67	1342.67	0
1380	L	225	A	1342.75	1343.98	0
1379	L	45	A	1343.42	1343.45	0
1386	L	45	A	1344.45	1344.76	0
1376	L	135	A	1347.72	1347.72	0
1389	L	315	A	1353.78	1353.78	0
1390	L	45	A	1356.47	1356.65	0
1393	L	45	A	1356.67	1357.96	0

Continued on next page

Table 30 – *Continued from previous page*

1387	L	225	A	1362.5	1362.5	0
1385	L	225	A	1363.02	1363.82	0
1384	L	45	A	1365.8	1365.98	0
1388	L	315	A	1366.32	1366.32	0
1394	L	45	A	1366.47	1367.3	0
1391	L	225	A	1367.77	1367.77	0
1392	L	225	A	1369.13	1371.71	0
1397	L	45	A	1375.83	1375.83	0
1403	L	225	A	1381.5	1381.5	0
1396	L	315	A	1381.77	1382.8	0
1395	L	45	A	1383.68	1383.68	0
1399	L	315	A	1385.15	1385.15	0
1404	L	135	A	1386.98	1386.98	0
1402	L	45	A	1389.83	1389.83	0
1406	L	45	A	1392.87	1392.87	0
1398	L	315	A	1397.45	1397.45	0
1409	L	315	A	1399.58	1399.71	0
1405	L	45	A	1400.9	1402.28	0
1411	L	315	A	1403.1	1404.05	0
1401	L	45	A	1406.18	1407.37	0
1408	L	315	A	1407.47	1407.47	0
1400	L	225	A	1409.15	1409.15	0
1410	L	315	A	1413.03	1413.03	0
1412	L	45	A	1413.12	1413.12	0
1407	L	225	A	1414	1414.37	0
1417	L	45	A	1418.27	1418.27	0
1414	L	45	A	1419.28	1419.58	0
1416	L	135	A	1423.12	1425.48	0
1415	L	45	A	1423.15	1424.15	0
1421	L	315	A	1425.92	1425.92	0
1413	H	135	A	1426.23	1426.88	0
216	H	315	B	3.05	3.05	0
212	L	315	B	4.51667	5.314	0
218	L	135	B	5.28333	5.799	0
219	L	45	B	7.88333	7.88333	0
214	L	45	B	9.9	9.9	0
217	L	45	B	13.8167	13.8167	0
221	L	45	B	26.1833	26.1833	0
215	L	225	B	27.9833	27.9833	0
220	L	225	B	48.0333	48.0333	0
3	L	135	B	166.617	166.617	0

Continued on next page

Table 30 – *Continued from previous page*

1	L	225	B	170.467	170.467	0
4	L	135	B	187.367	187.367	0
2	L	225	B	192.767	192.767	0
6	L	135	B	213.217	213.217	0
5	L	45	B	214.45	214.45	0
7	L	225	B	227.7	227.7	0
9	L	315	B	229.35	229.35	0
8	L	45	B	231.333	231.333	0
11	H	45	B	254.483	254.483	0
10	L	225	B	262.683	262.683	0
12	L	45	B	265.767	265.767	0
13	S	135	B	289.85	289.85	0
14	S	315	B	318.1	318.1	0
16	L	45	B	328.95	328.95	0
15	L	225	B	347.017	347.017	0
17	H	135	B	352.1	352.1	0
20	L	225	B	386.083	386.083	0
21	L	225	B	393.467	393.467	0
19	L	135	B	394.933	396.232	0
24	L	45	B	400.333	400.333	0
22	L	45	B	407.267	407.364	0
18	L	45	B	411.167	411.167	0
23	L	225	B	417.033	417.033	0
25	L	225	B	429.167	429.167	0
26	L	45	B	440.117	440.117	0
27	L	45	B	449.767	449.767	0
28	L	225	B	503.167	503.167	0
29	L	45	B	503.517	503.517	0
31	H	45	B	517.267	517.267	0
30	L	45	B	519.733	520.765	0
32	L	45	B	522.617	522.617	0
33	L	135	B	525.317	525.317	0
34	L	45	B	550.483	550.483	0
35	L	45	B	560.067	560.067	0
36	L	315	B	592.233	592.233	0
38	L	45	B	600.933	600.933	0
39	L	315	B	603.617	603.617	0
37	H	45	B	603.683	605.199	0
40	L	135	B	627.483	627.483	0
42	L	45	B	637.8	637.8	0
41	L	135	B	643.167	643.167	0

Continued on next page

Table 30 – *Continued from previous page*

43	H	315	B	650.867	650.867	0
46	L	45	B	653.633	653.633	0
44	H	315	B	658.367	658.367	0
45	L	135	B	660.017	660.017	0
50	S	315	B	669.533	669.533	0
47	L	225	B	672.517	672.517	0
51	L	225	B	673.2	673.832	0
49	L	135	B	681.733	682.548	0
48	L	45	B	685.333	685.333	0
53	L	315	B	685.717	686.466	0
52	L	135	B	693.733	694.699	0
54	L	45	B	703.267	703.267	0
55	L	45	B	712.083	712.083	0
60	L	45	B	723.033	723.864	0
61	L	315	B	724.7	724.997	0
59	L	225	B	729.933	729.933	0
58	S	135	B	731.433	734.236	0
57	L	45	B	734.983	736.249	0
56	S	45	B	738.017	738.017	0
62	L	315	B	741.033	741.539	0
63	L	135	B	743.783	743.783	0
64	L	45	B	750.45	750.516	0
66	L	45	B	771.967	771.967	0
65	L	135	B	781.883	781.883	0
67	L	45	B	801.917	801.917	0
71	L	45	B	817.083	817.083	0
70	L	315	B	818.967	818.967	0
69	H	45	B	819.433	822.381	0
68	L	45	B	820.117	820.117	0.349
73	L	45	B	838.65	838.65	0
74	L	45	B	839.933	839.966	0
72	L	45	B	843.183	843.183	0
77	L	135	B	852.35	852.35	0
76	L	45	B	861.167	861.167	0
79	L	45	B	865.483	865.483	0
78	L	225	B	867.05	867.05	0
75	L	315	B	868.133	868.133	0
84	L	135	B	873.283	873.283	0
81	L	315	B	874.233	874.233	0
80	L	45	B	877.2	877.2	0
82	L	45	B	884.3	886.715	0

Continued on next page

Table 30 – *Continued from previous page*

85	L	45	B	889.767	891.539	0
87	L	225	B	899.417	899.417	0
83	L	45	B	901.95	902.065	0
88	L	135	B	904.167	904.167	0
86	L	315	B	921.517	921.517	0
89	L	225	B	927.683	927.683	0
91	L	315	B	932.883	933.816	0
92	L	45	B	936.217	936.217	0
90	L	225	B	940.783	940.783	0
97	L	315	B	943.033	943.033	0
96	L	45	B	947.35	947.35	0
95	L	45	B	951.067	951.314	0
99	H	135	B	952.35	956.663	0
93	L	45	B	955.933	955.933	0
102	L	45	B	957.783	957.783	0
101	L	315	B	959.1	960.481	0
94	L	45	B	959.333	959.333	0
98	L	315	B	961.633	961.633	0
105	L	225	B	966.433	966.433	0
100	L	315	B	967.95	967.95	0
103	L	315	B	969.9	969.9	0
104	L	315	B	976.4	976.4	0
106	H	135	B	976.95	976.95	0
109	L	315	B	990.633	990.633	0
108	L	45	B	995.117	995.117	0
107	L	45	B	996.533	996.533	0
110	L	45	B	1007.4	1007.4	0
113	L	45	B	1009.12	1009.66	0
115	L	45	B	1013.78	1014.52	0
114	L	135	B	1015.08	1015.08	0
117	L	225	B	1016.18	1016.82	0
116	L	45	B	1020.18	1020.83	0
118	H	45	B	1022.82	1023.1	0
119	L	45	B	1025.42	1026.68	0
112	L	225	B	1027.92	1027.92	0
123	L	45	B	1028.37	1028.37	0
111	L	315	B	1029.77	1029.77	0
120	L	135	B	1039.45	1039.45	0
121	L	135	B	1041.82	1041.82	0
125	H	315	B	1047.02	1051.13	0
126	L	45	B	1048.22	1048.55	6.65894e-07

Continued on next page

Table 30 – *Continued from previous page*

122	L	135	B	1049	1049	0
124	L	45	B	1049.58	1049.86	0
128	L	135	B	1058.2	1058.2	0
131	H	135	B	1059.93	1061.83	0
132	L	45	B	1064.65	1065.83	0
127	L	45	B	1066.25	1070.73	0
133	L	225	B	1066.85	1067.05	0
129	L	315	B	1073.03	1073.18	0
130	L	135	B	1073.45	1074.1	0
134	L	315	B	1082.95	1082.95	0
135	S	45	B	1083.05	1084.69	0
140	L	315	B	1086.93	1086.93	0
138	L	45	B	1091.47	1091.47	0
139	L	315	B	1095.32	1095.32	0
136	L	225	B	1095.53	1095.53	0
137	L	45	B	1096.95	1097.25	0
142	L	45	B	1098.38	1098.56	0
141	L	135	B	1099.88	1099.88	0
143	S	225	B	1111.08	1111.08	0
145	L	225	B	1112.95	1113.15	0
144	L	45	B	1117.23	1119.47	0
146	L	45	B	1137.47	1137.47	0
147	L	45	B	1153.77	1153.77	0
154	L	135	B	1158.9	1161.16	0
148	L	225	B	1160.07	1160.27	0
150	L	135	B	1163.42	1163.42	0
153	L	45	B	1163.95	1163.95	0
152	L	315	B	1170.5	1170.5	0
149	L	135	B	1172.13	1172.13	0
157	L	135	B	1172.93	1173.45	0
156	L	135	B	1180.05	1180.05	0
151	L	315	B	1182.2	1182.2	0
155	L	315	B	1183.33	1183.52	0
158	L	45	B	1190.07	1190.07	0
159	L	45	B	1191.22	1191.38	0
163	L	315	B	1194.98	1194.98	0
161	L	315	B	1197.95	1197.95	0
160	L	315	B	1206.52	1209.34	0
164	L	315	B	1211.43	1211.6	0
162	L	135	B	1212.95	1213.22	0
166	L	45	B	1214.12	1215.62	0

Continued on next page

Table 30 – *Continued from previous page*

167	L	225	B	1222.78	1222.78	0
168	L	45	B	1224.03	1224.03	0
170	H	315	B	1225.55	1225.55	0
165	L	45	B	1235.83	1236.21	0
169	L	45	B	1236.22	1237.53	0
171	H	315	B	1251.93	1251.93	0
175	L	45	B	1256.75	1257.4	0
173	L	135	B	1265.33	1265.33	0
174	L	315	B	1266.67	1266.67	0
172	L	45	B	1271.28	1272.07	0
177	H	315	B	1275	1275	0
179	L	225	B	1278.22	1278.22	0
176	L	315	B	1278.73	1278.73	0
178	S	315	B	1284.43	1284.59	0
181	L	135	B	1297.15	1297.15	0
182	L	315	B	1302.97	1305.01	0
180	L	45	B	1303.55	1303.88	0
185	L	45	B	1303.93	1306.51	0
187	H	135	B	1317.98	1317.98	0
186	H	315	B	1319.13	1319.13	0
184	L	135	B	1329.4	1329.4	0
188	L	45	B	1331.25	1331.25	0
183	L	315	B	1335.5	1335.95	0
190	L	225	B	1336.92	1338.63	0
193	L	45	B	1337.47	1337.47	0
191	L	45	B	1338.58	1338.78	0
189	L	45	B	1342.32	1342.32	0
194	L	45	B	1355.52	1355.52	0
192	H	315	B	1357.5	1357.5	0
195	L	225	B	1359	1359	0
197	L	45	B	1360.75	1360.75	0
198	L	315	B	1364.85	1365.13	0
196	L	135	B	1368.18	1368.18	0
200	L	315	B	1375.2	1375.2	0
199	L	315	B	1375.72	1376.52	0
201	L	45	B	1378.9	1378.9	0
204	L	315	B	1381.15	1381.15	0
205	L	45	B	1390.5	1390.97	0
203	L	135	B	1395.8	1395.98	0
206	L	315	B	1398.27	1398.58	0
202	L	45	B	1399.4	1400.08	0

Continued on next page

Table 30 – *Continued from previous page*

207	L	225	B	1399.78	1400.16	0
208	H	315	B	1402.92	1402.92	0
210	L	135	B	1409.48	1409.48	0
209	L	315	B	1410.82	1410.82	0
211	L	225	B	1415.47	1415.5	0

REFERENCES

[1] Atkins, S., Capozzi, B., Hinkey, J., Idris, H., and Kaiser, K., "Investigating the nature of and methods for managing metroplex operations," Tech. Rep. CR2011-216413, NASA, 2011.

[2] Balas, E., Ceria, S., and Cornuéjols, G., "Mixed 0-1 programming by lift-and-project in a branch-and-cut framework," *Management Science*, vol. 42, no. 9, pp. 1229–1246, 1996.

[3] Balas, E. and Perregaard, M., "A precise correspondence between lift-and-project cuts, simple disjunctive cuts, and mixed integer gomory cuts for 0-1 programming," *Mathematical Programming*, vol. 94, no. 2, pp. 221–245, 2003.

[4] Ball, M., Barnhart, C., Dresner, M., Hansen, M., Neels, K., Odoni, A., Peterson, E., Sherry, L., Trani, A. A., and Zou, B., "Total delay impact study: a comprehensive assessment of the costs and impacts of flight delay in the united states," 2010.

[5] Barnhart, C., Johnson, E. L., Nemhauser, G. L., Savelsbergh, M. W., and Vance, P. H., "Branch-and-price: Column generation for solving huge integer programs," *Operations Research*, vol. 46, no. 3, pp. 316–329, 1998.

[6] Beasley, J., Krishnamoorthy, M., Sharaiha, Y., and Abramson, D., "Scheduling aircraft landingsthe static case," *Transportation science*, vol. 34, no. 2, pp. 180–197, 2000.

[7] Benders, J. F., "Partitioning procedures for solving mixed-variable programming problems," *Numerische Mathematik*, vol. 4, no. 1, p. 238252, 1962.

[8] Bianco, L., Dell'Olmo, P., and Odoni, A., *Modelling and simulation in air traffic management*. Springer Verlag, 1997.

[9] Bianco, L., Rinaldi, G., and Sassano, A., "A combinatorial optimization approach to aircraft sequencing problem," in *NATO ADVANCED RESEARCH WORKSHOP ON FLOW CONTROL*, 1987.

[10] Bonnefoy, P. and Hansman, R., "Emergence of secondary airports and dynamics of regional airport systems in the united states," tech. rep., MIT International Center for Air Transportation Report, 2006.

[11] Borener, S., Carr, G., Ballard, D., and Hasan, S., "Can NGATS meet the demands of the future?," *Journal of Air Traffic Control*, vol. 48, no. 1, pp. 34–38, 2006.

[12] Chandran, B. G., *Predicting airspace congestion using approximate queueing models*. PhD thesis, 2002.

[13] Chatterji, G. B. and Sridhar, B., "Neural network based air traffic controller workload prediction," in *American Control Conference, 1999. Proceedings of the 1999*, vol. 4, pp. 2620–2624, IEEE, 1999.

[14] Clarke, J.-P. B., Ho, N. T., Ren, L., Brown, J. A., Elmer, K. R., Tong, K.-O., and Wat, J. K., "Continuous descent approach: Design and flight test for louisville international airport," *Journal of Aircraft*, vol. 41, September-October 2004.

[15] Codato, G. and Fischetti, M., "Combinatorial benders' cuts for mixed-integer linear programming," *Operations Research*, vol. 54, no. 4, pp. 756–766, 2006.

[16] Consultants, S., "Seattle-tacoma international airport greenhouse gas emissions inventory-2006," tech. rep., Port of Seattle, 2009.

[17] Corporation, T. M., "Capacity needs in the national airspace system (2007-2025): An analysis of airports and metropolitan area demand and operational capacity in the future," tech. rep., FAA, May 2007.

[18] Dear, R. and of Technology. Flight Transportation Laboratory, M. I., *The Dynamic Scheduling of Aircraft in the Near Terminal Area*. Thesis. 1976. Ph. D, Flight Transportation Laboratory, Massachusetts Institute of Technology, 1976.

[19] Ehrmanntraut, R., "The potential of speed control, in proceedings of the 23rd dasc," *Salt Lake City, Utah, USA*, 2004.

[20] EPA, "The green book nonattainment areas for criteria pollutants," tech. rep., EPA, 2008.

[21] Erzberger, H. and Paielli, R. A., "Concept for next generation air traffic control system.," *Air Traffic Control Quarterly*, vol. 10, no. 4, pp. 355–378, 2002.

[22] Eun, Y., Hwang, I., and Bang, H., "Optimal arrival flight sequencing and scheduling using discrete airborne delays," *Intelligent Transportation Systems, IEEE Transactions on*, vol. 11, pp. 359 –373, june 2010.

[23] FAA, "Aviation & emissions, a primer," tech. rep., FAA, 2005.

[24] FAA, "National plan of integrated airport systems (npias) 2009-2013," tech. rep., FAA, 2008.

[25] FAA, "Operational evolution partnership version 1.0 2007 - 2025, executive overview," tech. rep., FAA, 2008.

[26] FAA, "Air traffic management glossary of terms," tech. rep., FAA, 2009.

[27] FAA, "FAA aerospace forecast – fiscal years 2009-2025," tech. rep., FAA, 2009.

[28] FAA, "Nas architecture 6," tech. rep., FAA, 2009.

[29] FAA and MITRE, "Airport capacity benchmark report 2004," tech. rep., FAA, September 2004.

[30] Font, R. and Schleicher, D., "Virtual airspace modeling and simulation system-wide concept report," tech. rep., NASA, June 2006.

[31] Gary, M. and Johnson, D., "Computers and intractability: A guide to the theory of np-completeness," 1979.

[32] Hartigan, J. A., *Clustering Algorithms*. New York: Wiley, 1975.

[33] Heinz, S. and Beck, C., "Solving resource allocation/scheduling problems with constraint integer programming," Tech. Rep. 11-14, ZIB, Takustr.7, 14195 Berlin, 2011.

[34] Heyer, L. J., Kruglyak, S., and Yooseph, S., "Exploring expression data: Identification and analysis of coexpressed genes," *Genome Research*, vol. 5, 1999.

[35] Ho, Y.-C., *Discrete event dynamic systems: analyzing complexity and performance in the modern world*. IEEE, 1992.

[36] Horangic, B. R., *Some queueing models of airport delays*. PhD thesis, Massachusetts Institute of Technology, 1990.

[37] JPDO, "Concept of operations for the next generation air transportation system," Tech. Rep. 2, JPDO, 2007.

[38] Laporte, G. and Louveaux, F. V., "The integer l-shaped method for stochastic integer programs with complete recourse," *Operations research letters*, vol. 13, no. 3, pp. 133–142, 1993.

[39] Long, D., Lee, D., Johnson, J., Gaier, E., and Kostiuk, P., "Modeling air traffic management technologies with a queuing network model of the national airspace system," tech. rep., National Aeronautics and Space Administration, Langley Research Center, 1999.

[40] McClain, E., Clarke, J.-P., and Timar, S., "Generic metroplex airspace comparison for shared resource configurations," in *AIAA Aviation, Technology, Integration, and Operations Conference*, 2010.

[41] Michalska, H. and Mayne, D. Q., "Robust receding horizon control of constrained nonlinear systems," *Automatic Control, IEEE Transactions on*, vol. 38, no. 11, pp. 1623–1633, 1993.

[42] Mogford, R. H., Guttman, J., Morrow, S., and Kopardekar, P., "The complexity construct in air traffic control: A review and synthesis of the literature.," tech. rep., DTIC Document, 1995.

[43] Mondoloni, S., Paglione, M., and Green, S., "Trajectory modeling accuracy for air traffic management decision support tools," in *ICAS 2002 Congress*, 2002.

[44] Müller, K. and Vignaux, T., "Simpy: Simulating systems in python," Feb. 2003.

[45] Nikoleris, T. and Hansen, M., "Queueing models for trajectory-based aircraft operations," *Transportation Science*, 2012.

[46] Perry, T. S., "In search of the future of air traffic control," *Spectrum, IEEE*, vol. 34, no. 8, pp. 18–35, 1997.

[47] Planning, J., "Development office: Concept of operations for the next generation air transportation system," *Draft Version 0.2 (July 24, 2006)*, 2007.

[48] Ren, L., Clarke, J.-P., Schleicher, D., Timar, S., Saraf, A., Crisp, D., Gutterud, R., Lewis, T., and Thompson, T., "Atlanta large tracon (a80) site survey report," tech. rep., NASA, 2009.

[49] Ren, L., Clarke, J.-P., Schleicher, D., Timar, S., Saraf, A., Crisp, D., Gutterud, R., Lewis, T., and Thompson, T., "Contrast and comparison of metroplex operations: An air traffic management study of atlanta, los angeles,new york, and miami," Sep 2009.

[50] Ren, L. and John-Paul, "Flight-test evaluation of the tool for analysis of separation and throughput," *Journal of Aircraft*, vol. 45, no. 1, pp. 323–332, 2008.

[51] Römisch, W. and Wets, R., "Stability of ε-approximate solutions to convex stochastic programs," *SIAM Journal on Optimization*, vol. 18, no. 3, pp. 961–979, 2007.

[52] Ryerson, M. S., Hansen, M., and Bonn, J., "Fuel consumption and operational performance," *Transportation Research Part D*, vol. 15, pp. 305–314, 2010.

[53] Saraf, A., Clarke, J.-P., Schleicher, D., and Timar, S., ch. Modeling of Traffic Management Advisor as a Baseline for the Assessment of Metroplex Time-based Scheduling Concepts. Aviation Technology, Integration, and Operations (ATIO) Conferences, American Institute of Aeronautics and Astronautics, Sep 2011. 0.

[54] Schleicher, D., Lewis, T., Gutterud, R., Wong, L., Clarke, J.-P., Crisp, D., Thompson, T., Saraf, A., and Sliney, B., "Sct site survey report," tech. rep., NASA, 2009.

[55] Schleicher, D., Ren, L., Gutterud, R., Timar, S., Crisp, D., Lewis, T., Clarke, J.-P., and Saraf, A., "Miami site survey report," tech. rep., NASA, 2009.

[56] Schleicher, D., Wendel, E., and Huang, A., "Demand loading analysis for a 3x nextgen future," in *Proceedings of the 7th Aviation Technology, Integration, and Operations Conference*, 2007.

[57] Sölveling, G., Solak, S., Clarke, J., and Johnson, E., "Scheduling of runway operations for reduced environmental impact," *Transportation Research Part D: Transport and Environment*, vol. 16, no. 2, pp. 110–120, 2011.

[58] Soomer, M. and Franx, G., "Scheduling aircraft landings using airlines' preferences," *European Journal of Operational Research*, vol. 190, pp. 277–291, October 2008.

[59] Tibshirani, R., Walther, G., and Hastie, T., "Estimating the number of clusters in a dataset via the gap statistic," *Journal of the Royal Statistical Society: Series B (Statistical Methodology)*, vol. 63, pp. 411–423, 2000.

[60] Timar, S., Lewis, T., Gutterud, R., Ren, L., Crisp, D., Saraf, A., Levy, B., Rappaport, D., Stefanidis, K., Clarke, J.-P., Thompson, T., and Schleicher, D., "New york site survey report," tech. rep., NASA, 2009.

[61] Vela, A. E., Solak, S., Clarke, J., Singhose, W. E., Barnes, E. R., and Johnson, E. L., "Near real-time fuel-optimal en route conflict resolution," *Intelligent Transportation Systems, IEEE Transactions on*, vol. 11, no. 4, pp. 826–837, 2010.

[62] Wang, Y., Wang, F., Wang, D., Gong, Z., and Liu, J., "Revisit the fairness issues in flight landing scheduling," in *Intelligent Transportation Systems (ITSC), 2012 15th International IEEE Conference on*, pp. 1435 –1440, sept. 2012.

[63] Wanke, C., "Using air-ground data link to improve air traffic management decision support system performance," in *USA-Europe ATM R&D Seminar*, 1997.

[64] Welch, J. D. and Lloyd, R. T., "Estimating airport system delay performance," in *Proc., 4th USA/Europe Air Traffic Management R&D Seminar*, pp. 11–11, 2001.

[65] Wets, R., "Challenges in stochastic programming," *Mathematical Programming*, vol. 75, no. 2, pp. 115–135, 1996.

[66] Yousefi, A. and Donohue, G. L., "Temporal and spatial distribution of airspace complexity for air traffic controller workload-based sectorization," in *AIAA 4th Aviation Technology, Integration and Operations (ATIO) Forum, Chicago, Illinois*, 2004.